

**DRIFT STABILITY AND GROUND SUPPORT
PERFORMANCE UNDER THERMAL AND
DYNAMIC LOAD IN FRACTURED ROCK MASS
AT YUCCA MOUNTAIN, NEVADA**

Prepared for

**Nuclear Regulatory Commission
Contract NRC-02-97-009**

Prepared by

**Center for Nuclear Waste Regulatory Analyses
San Antonio, Texas**

July 2000



**DRIFT STABILITY AND GROUND SUPPORT
PERFORMANCE UNDER THERMAL AND
DYNAMIC LOAD IN FRACTURED ROCK MASS
AT YUCCA MOUNTAIN, NEVADA**

Prepared for

**Nuclear Regulatory Commission
Contract NRC-02-97-009**

Prepared by

Rui Chen

**Center for Nuclear Waste Regulatory Analyses
San Antonio, Texas**

July 2000

ABSTRACT

The mechanical environment at the proposed geological repository for permanent disposal of high-level nuclear waste at Yucca Mountain (YM), Nevada, has three major characteristics that make it unique: high thermal stress, fractured rock mass, and seismic ground motion. These environmental characteristics directly affect the design of stable excavations and effective ground support. Currently, the design of underground excavation and ground support is based on methodologies developed for, and experience gained from, underground mining and tunneling under ambient thermal conditions. It is not obvious if these methodologies and experience can be applied to the design of emplacement drift and ground support under heated conditions at YM.

The overall objective of this study is to understand rock mass behavior, drift stability, and ground support performance under heated conditions. Emphasis is placed on those aspects of rock mass deformation that distinguish a thermal-stress controlled problem from conventional mining and tunneling problems under ambient conditions. The study also examines the effects of rock mass properties, fracture network characteristics, and ground motion parameters on drift stability and ground support performance. Modeling results show that thermal load changes the orientation of the maximum principal stress from approximately vertical to approximately horizontal near the repository horizon and shifts the location of the concentration of maximum principal stress from drift sidewalls to roof and floor areas. Consequently, fracture displacement is mainly along subvertical fractures in sidewall areas following drift excavation, whereas it occurs mainly along subhorizontal fractures in roof and floor areas after 150 yr of heating. Modeling results also show that thermally induced rock mass deformation is stress controlled and is much greater in a higher quality rock mass because of its higher Young's modulus. As a result, loads acting on ground support systems are greater and support element failure is more extensive in a higher quality rock mass. These results contradict the common belief that a lower quality rock mass would experience greater deformation than a higher quality rock mass under the same loading conditions and indicate that a higher quality rock mass may need stronger ground support under the thermal load expected at the proposed YM repository. Drift stability and ground support performance appear to be affected by low-frequency seismic ground motions (< 10 Hz) and ground motion parameters. Such effects, however, may be partly caused by modeling artifacts.

CONTENTS

Section	Page
ACRONYMS	vii
FIGURES	ix
TABLES	xi
ACKNOWLEDGMENTS	xiii
EXECUTIVE SUMMARY	xv
1 INTRODUCTION	1-1
2 MODEL DESCRIPTION	2-1
2.1 MODEL GEOMETRY	2-1
2.2 BOUNDARY AND INITIAL CONDITIONS	2-1
2.3 LOADING CONDITIONS	2-3
2.3.1 Thermal load	2-3
2.3.2 Dynamic load	2-4
2.4 ROCK BLOCK THERMAL-MECHANICAL AND FRACTURE MECHANICAL PROPERTIES	2-8
2.5 FRACTURE NETWORK CHARACTERISTICS	2-10
2.6 GROUND SUPPORT MODELING AND PARAMETERS	2-11
2.6.1 Rock Bolts	2-11
2.6.2 Steel Sets	2-14
2.7 MODELING PROCEDURES	2-15
3 PERFORMANCE OF DRIFT WITHOUT GROUND SUPPORT	3-1
3.1 DRIFT PERFORMANCE UNDER <i>IN SITU</i> AND THERMAL LOAD	3-1
3.1.1 Effect of Rock Mass Properties	3-1
3.1.1.1 Drift Convergence	3-1
3.1.1.2 Fracture Shear Displacement and Yield of Rock Blocks	3-2
3.1.2 Effect of Fracture Pattern	3-7
3.2 DRIFT PERFORMANCE UNDER SEISMIC GROUND MOTION	3-10
4 GROUND SUPPORT PERFORMANCE	4-1
4.1 GROUND SUPPORT PERFORMANCE UNDER <i>IN SITU</i> AND THERMAL LOAD	4-1
4.1.1 Effect of Rock Mass Properties	4-1
4.1.1.1 Rock Bolts	4-1
4.1.1.2 Steel Sets	4-7
4.1.1.3 Effectiveness of Rock Bolts and Steel Sets	4-13
4.1.2 Effect of Fracture Pattern	4-13
4.2 GROUND SUPPORT PERFORMANCE UNDER DYNAMIC LOAD	4-17
4.2.1 Effect of Input Ground Motion Frequency	4-17
4.2.2 Effect of Ground Motion Amplitude, Duration, and Repeated Ground Motions	4-24

CONTENTS (cont'd)

Section	Page
4.2.3 Effect of Design Ground Motion Time History	4-28
4.2.4 General Discussion on Dynamic Modeling Using Universal Distinct Element Code	4-28
5 CONCLUSIONS	5-1
6 REFERENCES	6-1

ACRONYMS

CNWRA	Center for Nuclear Waste Regulatory Analyses
CRWMS M&O	Civilian Radioactive Waste Management System Management and Operating Contractor
DOE	Department of Energy
EDA-II	Enhanced Design Alternative II
ESF	Exploratory Studies Facility
FLAC	Fast Lagrangian Analysis of Continua
LA	License Application
NRC	Nuclear Regulatory Commission
QA	Quality Assurance
RMQ	Rock Mass Quality
SR	Site Recommendations
TM	Thermal-Mechanical
UDEC	Universal Distinct Element Code
WP	Waste Package
YM	Yucca Mountain
YMRP	Yucca Mountain Review Plan
VA	Viability Assessment

FIGURES

Figure	Page	
2-1	A typical drift-scale model geometry showing a regular fracture pattern with fracture spacing scaled up away from the drift: (a) full model, (b) submodel for dynamic analyses	2-2
2-2	Uniform hazard spectrum for horizontal motions at a generic rock outcrop, 1,000-yr return period.	2-5
2-3	Design ground motion velocity time histories at the repository interface	2-6
2-4	Distribution of rock bolts	2-14
3-1	Drift convergences following excavation for RMQ5 and RMQ1 rock masses and for various fracture patterns analyzed in this study	3-3
3-2	Fracture shear displacement for Pattern F. Thickness of the dark lines is proportional to fracture shear displacement: (a) RMQ5 rock mass after drift excavation, (b) RMQ1 rock mass after drift excavation, (c) RMQ5 rock mass after 150 yr of thermal load, and (d) RMQ1 rock mass after 150 yr of thermal load	3-4
3-3	Yielding of rock blocks for Pattern F: (a) RMQ5 rock mass after drift excavation, (b) RMQ1 rock mass after drift excavation, (c) RMQ5 rock mass after 150 yr of thermal load, and (d) RMQ1 rock mass after 150 yr of thermal load	3-5
3-4	Falling key blocks in drift roof area for Pattern E: (a) following excavation and (b) 150 yr after thermal load	3-9
3-5	Simulated rockfall for Pattern E (Using 10 Hz ground motion, with other properties from the basecase; see section 2.5): (a) RMQ5 rock mass and (b) RMQ1 rock mass	3-11
4-1	Comparison of axial force on rock bolts for Pattern E: (a) RMQ5 after excavation, (b) RMQ1 after excavation, (c) RMQ5 after 150 yr of thermal load, and (d) RMQ1 after 150 yr of thermal load	4-2
4-2	Comparison of shear force along rock/grout interfaces for Pattern E: (a) RMQ5 after excavation, (b) RMQ1 after excavation, (c) RMQ5 after 150 yr of thermal load, and (d) RMQ1 after 150 yr of thermal load	4-3
4-3	Comparison of axial strain in rock bolts for Pattern E: (a) RMQ5 after excavation, (b) RMQ1 after excavation, (c) RMQ5 after 150 yr of thermal loading, and (d) RMQ1 after 150 yr of thermal loading	4-4
4-4	Comparison of axial failure on rock bolts for Pattern E: (a) RMQ5 after excavation, (b) RMQ1 after excavation, (c) RMQ5 after 150 yr of thermal load, and (d) RMQ1 after 150 yr of thermal load	4-5
4-5	Comparison of shear failure along grout/rock interfaces for Pattern E: (a) RMQ5 after excavation, (b) RMQ1 after excavation, (c) RMQ5 after 150 yr of thermal load, and (d) RMQ1 after 150 yr of thermal load	4-6
4-6	Comparison of axial force on steel sets for Pattern E: (a) RMQ5 after excavation, (b) RMQ1 after excavation, (c) RMQ5 after 150 yr of thermal load, and (d) RMQ1 after 150 yr of thermal load	4-8
4-7	Comparison of shear force on steel sets for Pattern E: (a) RMQ5 after excavation, (b) RMQ1 after excavation, (c) RMQ5 after 150 yr of thermal load, and (d) RMQ1 after 150 yr of thermal load	4-9

FIGURES (cont'd)

Figure	Page
4-8	Comparison of moment in steel sets for Pattern E: (a) RMQ5 after excavation, (b) RMQ1 after excavation, (c) RMQ5 after 150 yr of thermal load, and (d) RMQ1 after 150 yr of thermal load
4-9	Comparison of axial force along rock mass/steel sets interface for Pattern E: (a) RMQ5 after excavation, (b) RMQ1 after excavation, (c) RMQ5 after 150 yr of thermal load, and (d) RMQ1 after 150 yr of thermal load
4-10	Comparison of shear force on steel sets for Pattern E: (a) RMQ5 after excavation, (b) RMQ1 after excavation, (c) RMQ5 after 150 yr of thermal load, and (d) RMQ1 after 150 yr of thermal load
4-11	Effect of fracture pattern on axial force acting on rock bolts after 150 yr of thermal load in an RMQ5 rock mass
4-12	Effect of fracture pattern on shear force on grout/rock interface after 150 yr of thermal load in an RMQ5 rock mass
4-13	Effect of fracture pattern on axial strain on rock bolt after 150 yr of thermal load in an RMQ5 rock mass
4-14	Axial force in rock bolts after 150 yr of thermal load and a ground motion event with various input frequencies for Pattern E in an RMQ5 rock mass: (a) 10-Hz ground motion, (b) 5-Hz ground motion, and (c) 1-Hz ground motion
4-15	Shear force acting on grout/rock interface after 150 yr of thermal load and a ground motion event with various input frequencies for Pattern E in an RMQ5 rock mass: (a) 10-Hz ground motion, (b) 5-Hz ground motion, and (c) 1-Hz ground motion
4-16	Rock bolt axial strain after 150 yr of thermal load and a ground motion event with various input frequencies for Pattern E in an RMQ5 rock mass: (a) 10-Hz ground motion, (b) 5-Hz ground motion, and (c) 1-Hz ground motion
4-17	Axial force in rock bolts after 150 yr of thermal load and a ground motion event with various input frequencies for Pattern E in an RMQ1 rock mass: (a) 10-Hz ground motion, (b) 5-Hz ground motion, and (c) 1-Hz ground motion
4-18	Shear force on grout/rock interface after 150 yr of thermal load and a ground motion event with various input frequencies for Pattern E in an RMQ1 rock mass: (a) 10-Hz ground motion, (b) 5-Hz ground motion, and (c) 1-Hz ground motion
4-19	Rock bolt axial strain after 150 yr of thermal load and a ground motion event with various input frequencies for Pattern E in an RMQ1 rock mass: (a) 10-Hz ground motion, (b) 5-Hz ground motion, and (c) 1-Hz ground motion
4-20	Axial force along rock bolts subjected to 150 yr of thermal load and a 5-Hz ground motion for Pattern E in an RMQ5 rock mass: (a) basecase, (b) effect of ground motion amplitude, (c) effect of duration, and (d) effect of repeated ground motions
4-21	Shear force on grout/rock interface after subjecting to 150 yr of thermal load and a 5-Hz ground motion for Pattern E in an RMQ5 rock mass: (a) basecase, (b) effect of ground motion amplitude, (c) effect of duration, and (d) effect of repeated ground motions
4-22	Axial force of rock bolts after subjecting to 150 yr of thermal load and a 5-Hz ground motion for Pattern E in an RMQ5 rock mass: (a) basecase, (b) effect of ground motion amplitude, (c) effect of duration, and (d) effect of repeated ground motions

TABLES

Table	Page
2-1 Geothermal gradient at Yucca Mountain	2-3
2-2 Converted velocity and stress wave amplitudes for a 0.4-g cosine wave.....	2-8
2-3 Rock block and fracture mechanical properties	2-9
2-4 Universal Distinct Element Code Version 3.1 parameters used to generate fracture patterns	2-11
2-5 Parameters for rock bolts	2-13
2-6 Parameters for steel sets	2-15
3-1 Summary of drift convergence resulting from <i>in situ</i> and thermal loads	3-2

ACKNOWLEDGMENTS

This report was prepared to document work performed by the Center for Nuclear Waste Regulatory Analyses (CNWRA) for the Nuclear Regulatory Commission (NRC) under Contract No. NRC-02-97-009. The activities reported here were performed on behalf of the NRC Office of Nuclear Material Safety and Safeguards, Division of Waste Management. The report is an independent product of the CNWRA and does not necessarily reflect the views or regulatory position of the NRC.

The author thanks W.C. Patrick and B. Sagar for their reviews of this report. The author also thanks B. Dasgupta for assisting with the analyses and G.I. Ofoegbu and S. Hsiung for their thoughtful discussions. The author is grateful to C. Patton for assisting with the word processing and preparation of the final report and to B. Long and A. Woods for editorial reviews.

QUALITY OF DATA, ANALYSES, AND CODE DEVELOPMENT

DATA: All CNWRA-generated original data contained in this report meet quality assurance (QA) requirements described in the CNWRA QA Manual. Sources for other data should be consulted for determining the level of quality for those data.

ANALYSES AND CODES: The distinct element code UDEC Version 3.1, used for all of the analyses in this study, is controlled under the CNWRA software QA technical operating procedure TOP-018.

EXECUTIVE SUMMARY

The mechanical environment at the proposed geological repository for permanent disposal of high-level nuclear waste at Yucca Mountain (YM), Nevada, has three major characteristics that make it unique: high thermal stress, fractured rock mass, and seismic ground motion. These environmental characteristics directly affect the design of stable excavations and effective ground support. So far, design of underground excavation and ground support has been based on methodologies developed for and experience gained from underground mining and tunneling under ambient thermal conditions. These methodologies can be broadly categorized as empirical and numerical approaches. The Department of Energy (DOE) has proposed to use both kinds of methods, and it appears that emphasis has been placed on empirical approaches. Numerical approaches are used for confirmation purposes. It is not obvious if methodologies, particularly empirical design methodologies based on experience obtained in ambient environments, can be applied to the design of emplacement drift and ground support under heated conditions at YM. Furthermore, the numerical design approaches are challenged by the irregularity and complexity of fracture network characteristics, potential ground motions, and uncertainties in rock mass and fracture properties.

The overall objective of this study is to understand rock mass behavior, drift stability, and ground support performance under heated conditions. Emphasis is placed on those aspects of rock mass deformation that distinguish a thermal-stress controlled problem from a conventional mining and tunneling problem under ambient conditions. Ground support was assumed to be fully grouted rock bolts and steel sets. The study also examines the effects of rock mass properties, fracture network characteristics, and ground motion parameters on drift stability and ground support performance. Modeling results demonstrate the following conclusions:

- Thermal load changes the orientation of the maximum principal stress from approximately vertical to approximately horizontal near the repository horizon and shifts the location of the concentration of maximum principal stress from the drift sidewalls to the roof and floor areas.
- Thermally induced deformation is greater in a higher quality rock mass than in a lower quality rock mass based on observations of drift closure, the distribution and magnitude of fracture shear displacement, and the extent of rock block yield. This result is because a higher quality rock mass has higher Young's modulus. This observation contradicts the common understanding that a lower quality rock mass would experience greater deformation than a higher quality rock mass under the same loading conditions. Such common understanding, however, is based on experiences and observations from underground tunneling and mining under ambient conditions rather than heated conditions.
- Fracture shear displacement following drift excavation is mainly along subvertical fractures and is limited to those subvertical fractures that bound the sidewalls of the emplacement drift. In contrast, fracture shear displacement after thermal load is mainly along subhorizontal fractures and occurs in roof and floor areas.
- Rock mass deformation following drift excavation is controlled by factors such as existing fractures, depth of the drift, drift geometry and dimension, and density of overburden rocks. It is a structure-controlled phenomenon, and the deformation is greater in a lower quality rock mass than in a higher quality rock mass. On the other hand, rock mass deformation after thermal load is controlled by high thermal stresses. It is a stress controlled phenomenon and is greater in a higher quality rock mass.
- Consequently, under the thermal load expected at the proposed YM repository, a higher quality rock

mass would need more ground support than a lower quality rock mass. Because thermally induced rock deformation mainly occurs in roof and floor areas, ground support design should concentrate on stabilizing these areas. Experience on ground support design gained from the exploratory studies facility, and conventional underground mining and tunneling may not be applicable to ground support design under thermal load, particularly not for higher quality rock masses.

- Notable rock-mass deformation, particularly fracture shear displacement along subhorizontal fractures, is observed in interdrift pillars in a higher quality rock mass after thermal load. Although this kind of deformation may not directly affect drift stability, it may alter rock mass hydrological properties and change fluid flow characteristics. A slight increase in rock mass thermal expansion coefficient could significantly increase the extent and magnitude of such deformation.
- Although a higher quality rock mass shows greater deformation under thermal load, a numerical model with more fractures (which, logically, should have lower quality) exhibits more extensive deformation. Consequently, it may not be appropriate to simply factor the effect of fractures into overall rock mass quality in design of drifts and ground support using a numerical approach. Some fractures need to be explicitly modeled, and modeling results need to be appropriately interpreted.
- Thermal load increases the loads acting on ground support (both rock bolts and steel sets) in both a lower quality rock mass and a higher quality rock mass. The increase in loads acting on the ground support system, however, is more significant in a higher quality rock mass. This result is consistent with observations on rock-mass deformation in previous conclusions.
- Fracture patterns affect the distribution and magnitude of loads acting on ground supports. The locations of peak magnitudes of load acting along rock bolts are well correlated with intersecting fractures. In general, the complexity of load distribution in ground-support systems increases as the number of intersecting fractures increases. The more complicated the fracture pattern, the less uniform the loads on ground supports.
- Under seismic ground motion, an unsupported emplacement drift in a lower quality rock mass appears to be less stable and experiences more extensive simulated rockfall. Such simulated rockfall is affected significantly by fracture patterns.
- The performance of a ground support system, measured by ground support loads and failure, does not appear to be affected by high-frequency motion (e.g., 10 Hz), regardless of rock mass quality. At lower-frequency (e.g., less than about 5 Hz), ground support performance is affected by ground motion and input ground motion parameters to various degrees, with the effect of frequency being the most significant. Some observed effects of ground motion parameters, however, may be caused by modeling artifacts.

Results obtained from this study directly contribute to the resolution of preclosure design aspects of the Repository Design and Thermal-Mechanical Effects Key Technical Issue. Knowledge gained and findings obtained from this study have been helpful in developing acceptance criteria and review methods for repository subsurface design for the YM Review Plan and in evaluating DOE design approaches for subsurface facilities, particularly for ground support. Information on fracture displacements also contributes to the evaluation of thermal-mechanical effects on rock mass permeability changes, which may bear some importance in postclosure performance assessment.

1 INTRODUCTION

The mechanical environment at the proposed geological repository for permanent disposal of high-level nuclear waste at Yucca Mountain (YM), Nevada, is unique and complicated for three primary reasons.

- (i) The rock mass surrounding the repository will be heated by radioactive decay of the nuclear wastes. Such heat will put a significant thermal load on both the rock mass and ground support. Previous modeling results show that the thermal load will significantly alter stress distribution around the emplacement drift and may increase the maximum compressive stress up to 70 MPa, depending on repository design configuration, rock mass stiffness, and thermal expansion characteristics (Chen et al., 2000b, in press).
- (ii) The rock mass at YM is highly fractured and contains lithophysae (i.e., voids formed by escaping gas during cooling of the volcanic rock). The fracture network characteristics are complicated and irregular. Fracture network modelers often identify two or three sets of dominant fractures plus an additional set accounting for random fractures. Although fracture set parameters are yet to be finalized, it is obvious there is large variability and uncertainty in these parameters (Civilian Radioactive Waste Management System Management and Operating Contractor, 1999a,b).
- (iii) YM is located in the tectonically active Central Basin and Range Province of the North American Cordillera (Wernicke, 1992). Numerous Quaternary faults, volcanoes, paleoearthquakes, and historic earthquakes are evidence of the tectonic activity of the region. Site-specific seismic hazard analyses (Wong and Stepp, 1998) show that mean horizontal peak ground accelerations at the reference rock outcrop are about 0.55 g and 1.32 g for 10,000-yr and 100,000-yr return period earthquakes, respectively. Such earthquakes may affect the integrity and radiological safety of the proposed repository because of possible disruptions to underground openings.

These environmental factors directly affect whether stable excavations and effective ground support can be designed. So far, design of underground excavation and ground support has been using methodologies based on experience gained from underground mining and tunneling, mostly under ambient conditions rather than heated conditions (Barton et al., 1974). These methodologies can be broadly grouped into two categories: empirical and numerical. These design methodologies have been used by the Department of Energy (DOE) in its ground support design at YM for the Exploratory Studies Facilities (ESF) (Civilian Radioactive Waste Management System Management and Operating Contractor, 1995) and for Viability Assessment (VA) (Civilian Radioactive Waste Management System Management and Operating Contractor, 1998). It appears that emphasis has been placed on the empirical approach based on rock mass classification (Barton et al., 1985) and numerical approaches have been used for confirmatory purposes (Civilian Radioactive Waste Management System Management and Operating Contractor, 1995, 1997a,b, 1998). It is not obvious, however, how well the empirical design approaches are applicable to the heated conditions at the proposed YM repository. Furthermore, numerical design approaches are challenged by the irregularity and complexity of the fracture network, potential ground motions, and uncertainties in rock mass thermal properties and rock mass and fracture mechanical properties (Chen et al., 2000b, in press).

Parametric studies to screen inputs and their effects on drift stability at YM were conducted using the 2^k fractional factorial experimental design approach (Ahola et al., 1996; Chen et al., 2000a, in press). These studies found that thermal load is an important parameter that affects most of the performance measures evaluated. Other input parameters that show significant effects on drift stability include rock mass Young's

modulus and thermal expansion coefficient. The effect of earthquake ground motion on drift stability was modeled dynamically using regular (Ahola, 1997) and irregular (Chen, 1999) fracture patterns and simple input seismic ground motions. These studies found that although seismic ground motion does not have a significant effect on the extent of rock block yielding and fracture shear displacement, it may induce local instability in the form of rockfalls. Such effect, however, largely depends on the fracture patterns used in the numerical models.

Based on these previous studies and additional modeling exercises, an attempt was made to identify important factors that affect drift stability and limitations in modeling drift stability at YM using a discontinuum approach, particularly when a simplified fracture pattern is used (Chen et al., 2000b, in press). The study concluded that explicitly simulating rockfall using discontinuum modeling tools is not a feasible practice at the current stage of technology for three reasons: (i) simulated rockfall depends largely on fracture patterns, (ii) the sharp corners and extreme block aspect ratios in a complicated fracture pattern often trigger numerical instability, and (iii) there is no practical way for a numerical model to incorporate the degree of complexity and irregularity of fracture network characteristics that occur *in situ*, particularly when such numerical models are two-dimensional. Chen et al. (2000b, in press) indicated that although discontinuum modeling is not a practical tool for simulating rockfall explicitly for complicated fracture patterns, it could be an effective tool in understanding mechanisms of rock mass failure, in conducting bounding sensitivity analyses, and in conducting confirmation analyses of rockfall for simple and well defined fracture patterns.

With additional, more systematic analyses, this report further elaborates on understanding failure and deformation mechanisms of different quality rock masses, with emphasis on those aspects of rock mass deformation that distinguish a thermal-stress controlled problem from conventional mining and tunneling problems under ambient conditions. It also examines the performance of ground support under thermal and dynamic load using rock bolts and, to a lesser extent, steel sets as examples. Dynamic analyses included evaluation of the effects of input ground motion parameters on drift stability and ground support performance, including frequency content, amplitude, duration of strong motion, repeated ground motion events, and wave forms. All the analyses were performed using Universal Distinct Element Code (UDEC) Version 3.1, developed by the Itasca Consulting Group, Inc. (2000).

2 MODEL DESCRIPTION

This chapter describes the numerical model used in this study, including (i) model geometry, (ii) boundary and initial conditions, (iii) loading conditions and numerical approaches in considering thermal and dynamic load, (iv) rock block thermal-mechanical (TM) and fracture mechanical properties, and (v) numerical implementation of fracture network characteristics. It also describes numerical approaches and input parameters used for ground support analyses.

2.1 MODEL GEOMETRY

A two-dimensional drift scale model was used assuming plane strain condition. The model included one 5.5-m diameter emplacement drift, centered in the model with vertical boundaries passing through centers of the adjacent pillars (figure 2-1). The drift spacing was 81 m as specified for the Enhanced Design Alternative II (EDA-II) design (TRW Environmental Safety Systems, Inc., 1999). Previous numerical modeling exercises show that the 81-m drift spacing is wide enough to eliminate boundary effects. Consequently, modeling a single drift was sufficient for both static and dynamic analyses (Chen et al., 2000b, in press). Such a model, however, represents a drift in the central portion of the repository emplacement drift panel. The effect of repository edges was not considered. Vertically, the model extended from the ground surface (approximately 320 m above the waste emplacement level) to the ground water table (about 350 m below the waste emplacement level). For dynamic analyses, a submodel extending 50 m above and 50 m below the emplacement horizon was used to reduce the size of the problem (figure 2-1b). To further reduce the size of the problem, a detailed fracture pattern was modeled only in close vicinity of the drift. Beyond this region, fracture spacings were scaled up, but a comparable fracture pattern was maintained (e.g., figure 2-1).

2.2 BOUNDARY AND INITIAL CONDITIONS

The vertical boundaries represented lines of symmetry based on the assumption of multiple parallel drifts. These boundaries were assigned zero heat flux, assuming uniform heat load and homogeneous thermal properties. Other thermal boundary conditions included fixed temperature at the top (ground surface) and base (water table) of the model. Heat generated by the nuclear waste emplaced in the drift was simulated as surface heat flux on the drift wall and applied to the interior boundary of the drift. Mechanical boundary conditions for static analyses included zero horizontal displacement along vertical boundaries, zero stresses on the top (ground surface), and zero vertical displacement on the base of the model. For dynamic analyses, viscous nonreflecting boundary conditions were applied to the top and base of the model. To allow shear waves to propagate vertically, one-dimensional free-field boundary elements were used along the vertical boundaries. Descriptions of free-field boundary elements can be found in Itasca Consulting Group, Inc. (2000). Both shear and compressive seismic waves were applied to the base of the model and propagated vertically through the model. As discussed in section 2.3.2, the viscous boundary condition on the base of the model restricts the form of the input seismic waves to be stress waves. Previous studies show that using a submodel rather than the full model for dynamic analyses produces sufficiently accurate results, provided appropriate dynamic boundary conditions are applied (Chen et al., 2000b, in press).

The initial vertical stress (σ_v) was defined using a vertical stress gradient of 0.022 MPa/m, equivalent to an average overburden rock mass density of 2,210 kg/m³ and gravitational acceleration of 9.81 m/s². The initial horizontal stress (σ_h) was estimated from vertical stress using a horizontal to vertical stress ratio of approximately 0.266 [based on a Poisson's ratio (ν) of 0.21 and $\sigma_h = \sigma_v \nu / (1 - \nu)$]. The resultant stresses at the repository horizon were approximately 7 MPa vertically and 1.9 MPa horizontally.

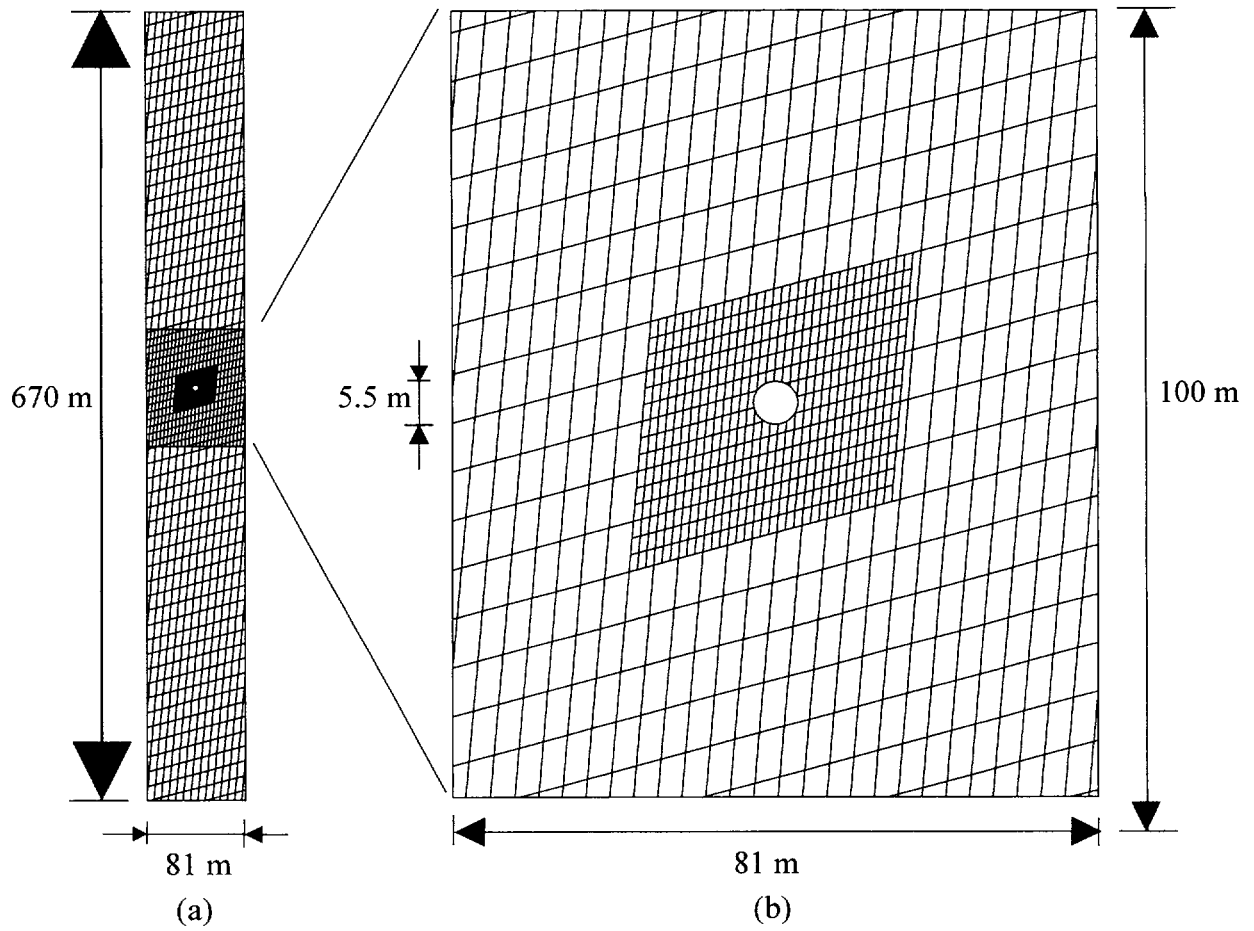


Figure 2-1. A typical drift-scale model geometry showing a regular fracture pattern with fracture spacing scaled up away from the drift: (a) full model and (b) submodel for dynamic analyses

The initial temperature was set to be 18.7 °C at the ground surface (Civilian Radioactive Waste Management System Management and Operating Contractor, 1997c, 1998) and interpolated using the geothermal gradient for the YM site given in table 2-1 (Civilian Radioactive Waste Management System Management and Operating Contractor, 1997c). These data gave a temperature of 34.3 °C at the base of the model and 24.7 °C at the repository horizon.

Table 2-1. Geothermal gradient at Yucca Mountain (Civilian Radioactive Waste Management System Management and Operating Contractor, 1997c)

Depth (m)	Geothermal Gradient (°C/m)
0–150	0.020
150–400	0.018
400–700	0.030
> 700	0.008

2.3 LOADING CONDITIONS

In addition to *in situ* stresses from the overlying rocks, an emplacement drift at the proposed YM repository will be subjected to thermal load generated by radioactive wastes. An emplacement drift may also be subjected to dynamic loading from earthquake ground motions (Wong and Stepp, 1998).

2.3.1 Thermal load

Thermal load depends on the repository design configuration. As mentioned earlier, this study was based on EDA-II configurations (TRW Environmental Safety Systems, Inc., 1999). Although details may continue to evolve, EDA-II is the design that will most likely be submitted by the DOE in its site recommendation (SR) and, eventually, in the license application (LA) (Barrett, 1999). In EDA-II, the thermal load is designed to be an areal mass loading of 60 MTU/acre. This thermal loading translates to approximately 71 W/m² initial heat flux on the drift walls (Chen et al., 2000b, in press) according to the inventory data presented by DOE (i.e., 70,011 MTU total mass and 71,499 kW total heat output, see Civilian Radioactive Waste Management System Management and Operating Contractor, 1997c). The 71 W/m² was applied directly as the initial heat flux on the drift wall in the UDEC model. This initial heat flux was modeled to decrease with time exponentially with a single decay constant (exponent) of -0.0104 (W/m²)/yr. This decay constant was obtained using a curve-fitting procedure following the decay characteristics defined in table V-1 of Civilian Radioactive Waste Management System Management and Operating Contractor (1997c) as described in detail in Chen (1998). The decay constant from curve fitting was further modified (calibrated) through a trial-and-error process. The trial-and-error process compared temperature history at the drift wall from the UDEC model for the first 150 yr following waste emplacement with temperatures from a parallel study using a continuum modeling approach (Ofoegbu, 2000). This approximate modeling approach was selected because UDEC can only use exponential decay with one decay constant. However, it is considered that the approximation has little effect on UDEC modeling results for the first 150 yr following waste emplacement. It should be noted that the EDA-II design includes ventilation, and, if designed successfully,

ventilation could reduce the drift wall temperature significantly. The effects of ventilation were not considered in this study mainly because information required to account for such effects has not been developed by the DOE.

2.3.2 Dynamic load

The proposed YM repository is located in the tectonically active Central Basin and Range Province of the North American Cordillera (Wernicke, 1992). Numerous Quaternary faults, volcanoes, paleoearthquakes, and historic earthquakes are evidence of the tectonic activity of the region. Recent seismic hazard analyses (Wong and Stepp, 1998) show that the mean horizontal peak ground accelerations at the reference rock outcrop are about 0.55 g and 1.32 g for 10,000-yr and 100,000-yr return period earthquakes, respectively. Such earthquakes may affect the integrity and radiological safety of the proposed repository because of possible disruptions to underground openings, particularly because the rock mass surrounding the proposed repository is highly fractured and contains irregular fracture patterns (Brechtel et al., 1995; Lin et al., 1993; Anna, 1998). Drift stability and the performance of rock support during seismic ground motion need to be evaluated in design of subsurface facilities. Also, potential damage to waste packages emplaced in the drifts by direct rockfall due to earthquake ground motion needs to be considered in repository performance assessment.

Design ground motion parameters for the proposed repository are yet to be finalized by DOE. Consequently, this study considered a range of ground motion parameters. The basecase used a simple cosine wave with frequency of 5 Hz and acceleration amplitude of 0.4 g in both vertical and horizontal directions, assuming a single ground motion event. The 0.4 g peak acceleration was selected for the basecase because it bounds the mean peak spectral accelerations in the 1,000-yr return period uniform hazard spectrum at a generic rock outcrop (figure 2-2) (Risk Engineering, Inc., 1998). It is likely that ground motion attenuates with depth so that the peak acceleration will be lower at the waste emplacement level. The attenuation characteristics, however, are yet to be developed by the DOE. In the basecase, the model was subjected to the ground motion for a 1-s simulation time followed by a 2-s simulation period for the model to return to equilibrium. Both shear and compressive waves were applied to the model assuming that the two components have the same amplitude. The effect of frequency content was examined by varying frequency to 1 Hz and 10 Hz from the basecase model (5 Hz). For the 1-Hz cases, duration of the ground motion was increased to 5 s to allow a reasonable number of loading cycles, followed by a 5-s recovery time if no significant rockfall was simulated and numerical stability was maintained. If significant rockfall was simulated, however, UDEC would have difficulty maintaining numerical stability and would drop the time step significantly making it impractical to regain model equilibrium within a reasonable computational time. The effect of ground motion amplitude was studied by doubling the basecase ground motion level (i.e., to 0.8 g). The effect of duration was evaluated by increasing the duration of strong motion from 1 s to 4 s. The effect of repeated ground motion events was analyzed by subjecting the model to the basecase ground motion twice. Finally, the effect of wave form was studied by subjecting the model to the preliminary design ground motion time histories (velocity histories) for YM at the repository level (figure 2-3). This design ground motion was developed by Risk Engineering, Inc. (1998) based on site-specific, probabilistic seismic hazard analyses (Wong and Stepp, 1998). Velocity history was used because UDEC Version 3.1 does not accept acceleration or displacement histories as input. Also, because UDEC Version 3.1 does not perform frequency-domain analyses, only time-domain analyses were conducted. The seismic ground motion was applied at the base of the model in UDEC analyses.

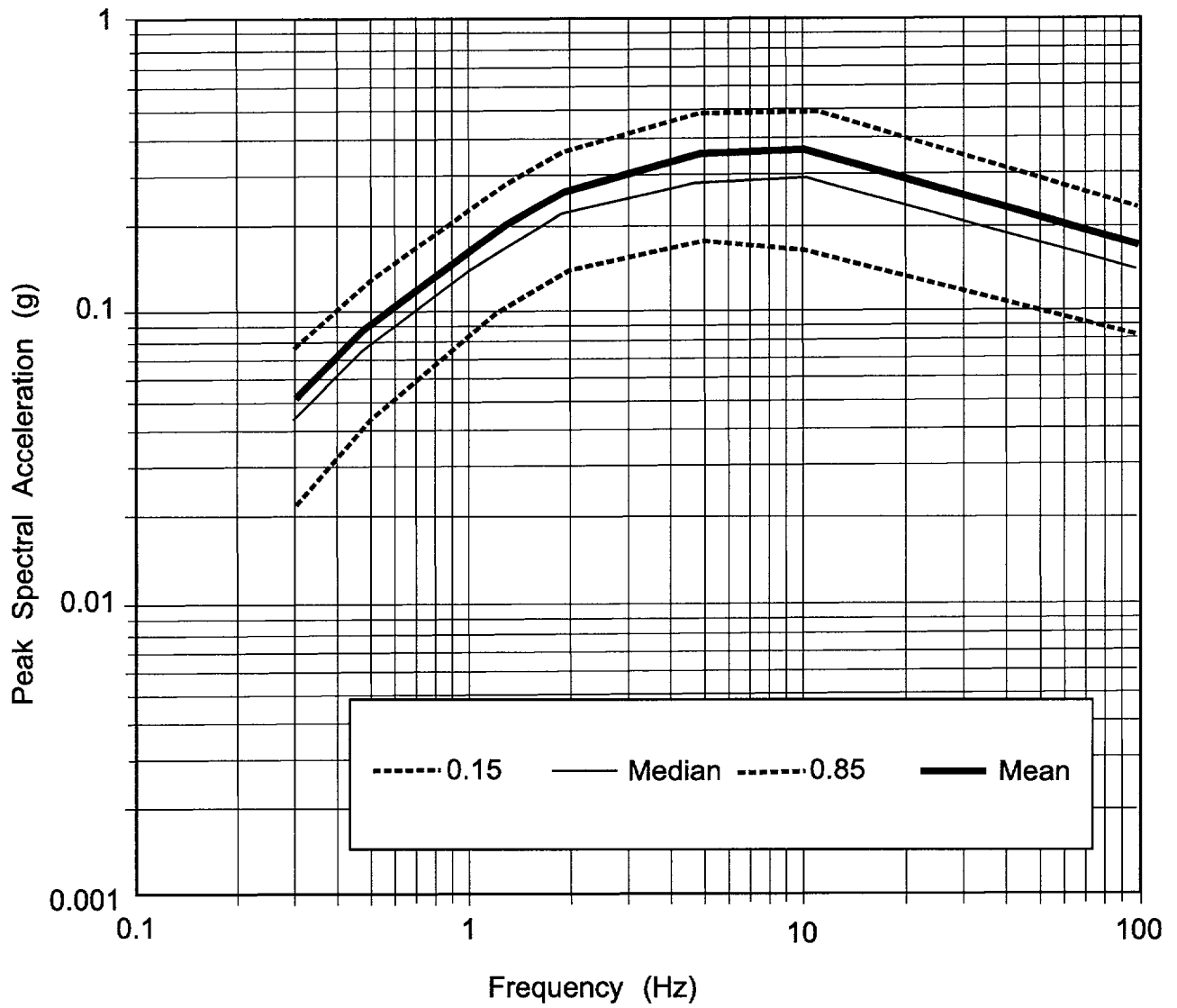
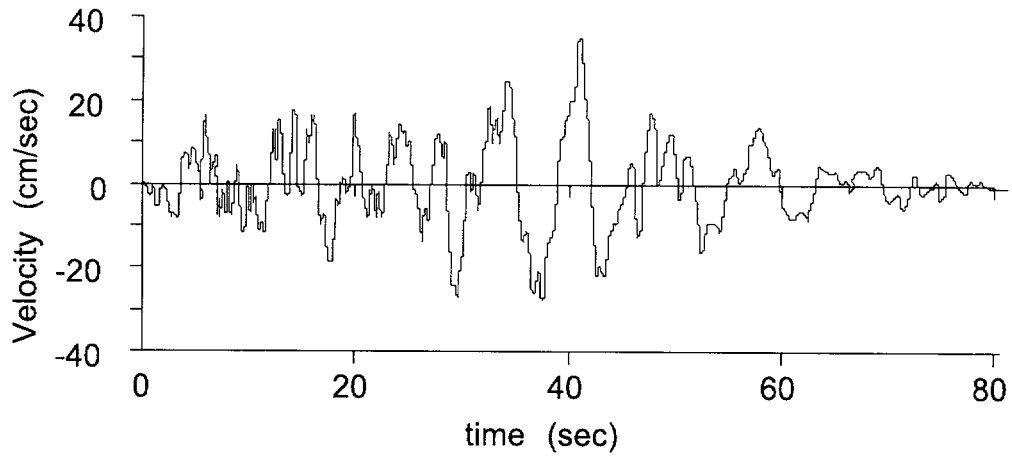
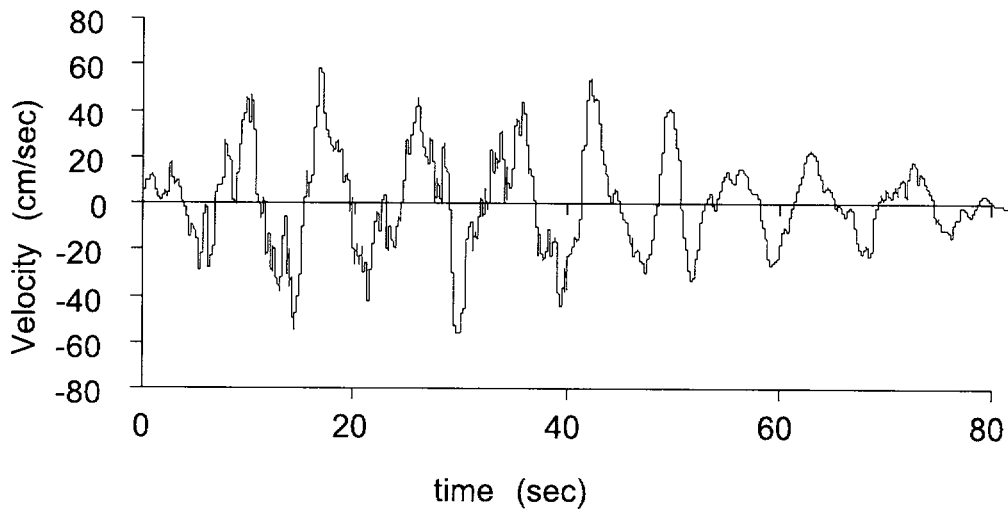


Figure 2-2. Uniform hazard spectrum for horizontal motions at a generic rock outcrop, 1,000-yr return period



(a) Vertical time history



(b) Horizontal time history

Figure 2-3. Design ground motion velocity time histories at the repository interface (Risk Engineering, Inc., 1998)

As mentioned previously, it is necessary to use viscous boundaries at the base of the model for nonrigid boundaries to minimize seismic reflection. In UDEC, the use of viscous boundaries at the base restricts the input ground motion waves to be stress waves rather than velocity waves. Also, UDEC does not take acceleration or displacement as dynamic input. Therefore, acceleration was converted to velocity and, then, to stresses as seismic input for simple cosine waves. For a cosine wave of angular frequency ω and amplitude A , the displacement time history is

$$x(t) = A \cos(\omega t) \quad (2-1)$$

where t is time. Angular frequency ω is equal to $2\pi f$, where f is frequency. The velocity and acceleration are simply

$$\begin{aligned} V(t) &= \frac{dx}{dt} = -A\omega \sin(\omega t) \\ a(t) &= \frac{d^2x}{dt^2} = -A\omega^2 \cos(\omega t) \end{aligned} \quad (2-2)$$

Consequently, the amplitude of the input ground acceleration a in g can be converted to ground velocity V as

$$V = \frac{g}{2\pi f} a \quad (2-3)$$

where g is gravitational acceleration and is equal to 9.81 m/s^2 . Equation (2-3) was used to convert acceleration to velocity. The converted maximum velocity for a 0.4-g cosine wave is given in table 2-2 for the three frequencies considered in this study.

To convert a velocity history to a stress history for UDEC Version 3.1 modeling, the procedure recommended by Itasca Consulting Group, Inc. (2000) was followed:

$$\begin{aligned} \sigma_n &= 2(\rho C_p)V_n \\ \sigma_s &= 2(\rho C_s)V_s \end{aligned} \quad (2-4)$$

where σ_n and σ_s are applied normal and shear stresses; C_p and C_s are rock mass p- and s-wave velocities; V_n and V_s are input normal and shear ground motion velocities; and ρ is rock mass density. C_p and C_s can be estimated from rock mass density and elastic properties as

$$\begin{aligned} C_p &= \sqrt{\frac{K + 4G/3}{\rho}} \\ C_s &= \sqrt{G/\rho} \end{aligned} \quad (2-5)$$

where K is rock mass bulk and shear moduli. These parameters for the proposed YM repository host rock masses are given in section 2.4 for rock mass quality category 5 (RMQ5) and rock mass quality category 1 (RMQ1). Using the rock mass bulk and shear moduli and Eqs. (2-4) and (2-5), the input ground motion velocity histories were converted to stress histories. Table 2-2 shows the converted maximum stress wave amplitudes for a 0.4-g cosine wave and for RMQ5 and RMQ1 rock masses. For the cases that used design ground motion as seismic input, the stress histories were calculated using Eqs. (2-4) and (2-5) directly from velocity histories in figure 2-3.

Table 2-2. Converted velocity and stress wave amplitudes for a 0.4-g cosine wave

Frequency (Hz)	Maximum Velocity (m/s)	Maximum Stress (MPa)			
		RMQ5		RMQ1	
		Normal	Shear	Normal	Shear
10	0.0625	1.13	0.68	0.55	0.33
5	0.1250	2.25	1.37	1.10	0.67
1	0.6250	11.26	6.83	5.49	3.33

2.4 ROCK BLOCK THERMAL-MECHANICAL AND FRACTURE MECHANICAL PROPERTIES

Rock block properties include rock mass density, thermal properties (thermal expansion coefficient, thermal conductivity, and specific heat capacity), elastic properties (Young's modulus and Poisson's ratio), strength properties (cohesion and friction angle), and postfailure properties (dilation angle). The property data used in this study were selected to be consistent with a parallel modeling effort using a continuum approach (Ofoegbu, 2000). The bulk density of 2,210 kg/m³ for the TSw2 lower lithophysal unit was used (see table 4-3 in Civilian Radioactive Waste Management System Management and Operating Contractor, 1998). The thermal expansion coefficient was chosen to be 7.5×10^{-6} per °C. This value is within the range measured by DOE (Civilian Radioactive Waste Management System Management and Operating Contractor, 1997a). Thermal conductivity was chosen to be 2.13 W/m-K and specific heat capacity was chosen as 968.96 J/kg-K (Civilian Radioactive Waste Management System Management and Operating Contractor, 1998). Sensitivity of modeling results to these properties is not discussed in this report, although DOE data show temperature dependency and uncertainties in rock mass thermal conductivity and specific heat capacity (Civilian Radioactive Waste Management System Management and Operating Contractor, 1998). A general discussion on sensitivity of rock mass TM responses to thermal expansion coefficient is given in Chen et al., (2000b, in press). Ofoegbu (2000) further examined rock mass TM responses when constant and temperature-dependent thermal conductivity and specific heat capacity were considered.

Two groups of rock mass mechanical property data were considered (table 2-3). These two sets of properties represent a high quality (RMQ5) rock mass and a low quality (RMQ1) rock mass. The elastic properties for RMQ5 and RMQ1 rock masses were selected based on property values proposed by the DOE for VA (Civilian Radioactive Waste Management System Management and Operating Contractor, 1998). The strength properties, particularly friction angles used in this modeling, were lower than those proposed by the DOE. As detailed in Chen et al. (2000b, in press) and Ofoegbu (2000), the lower friction angles were chosen

for three primary reasons: (i) DOE strength property values are inconsistent with empirical procedures used to determine these values, as well as measured laboratory or field data, (ii) strength property values much lower than those estimated by DOE were obtained based on DOE rock mass quality data (Ofoegbu, 2000), and (iii) strength properties are likely to degrade under sustained thermal load (Ofoegbu, 2000). Dilation for rock blocks was chosen as one half the friction angle. Unconfined compressive strength and uniaxial tensile strength were calculated from cohesion and the friction angle based on the Mohr-Coulomb failure criterion. For comparison, both rock mass mechanical property values used in this study and those used in the DOE VA analyses (Civilian Radioactive Waste Management System Management and Operating Contractor, 1998) are presented in table 2-3. Fracture normal and shear stiffnesses were assumed to be 500 GPa/m. Fracture cohesion was chosen to be 0.07 MPa (Civilian Radioactive Waste Management System Management and Operating Contractor, 1997b) with no dilation. A fracture friction angle of 35° was used rather than the 56° used in most analyses conducted by DOE (e.g., Civilian Radioactive Waste Management System Management and Operating Contractor, 1997b, 1998). This lower fracture friction angle was a median value from independent laboratory testing by Hsiung et al. (1993). Fracture mechanical property data are also given in table 2-3.

Table 2-3. Rock block and fracture mechanical properties

Rock Mass Elastic Properties	RMQ5	RMQ1	VA_RMQ5	VA_RMQ1
Mass Density (kg/m ³)	2210.00	2210.00	2235.00	2235.00
Young's Modulus (GPa)	32.61	7.76	32.61	7.76
Poisson's Ratio	0.21	0.21	0.21	0.21
Bulk Modulus (GPa)	18.74	4.46	18.74	4.46
Shear Modulus (GPa)	13.48	3.21	13.48	3.21
Rock Mass Strength Properties	RMQ5	RMQ1	VA_RMQ5	VA_RMQ1
Cohesion (MPa)	5.08	2.82	5.20	1.50
Friction Angle (degrees)	34.42	27.50	46.00	43.00
Unconf Comp Strength (MPa)	19.28	9.29	26.09	7.08
Dilation Angle	17.21	13.75	0.00	0.00
Tensile Strength (MPa)	5.35	4.42	4.21	1.32
Joint Properties	RMQ5	RMQ1	VA_RMQ5	VA_RMQ1
Cohesion (MPa)	0.07	0.07	0.07	0.07
Friction Angle (degrees)	35.00	35.00	56.00	56.00
Dilation Angle (degrees)	0.00	0.00	0.00	0.00
Tensile Strength (MPa)	0.00	0.00	0.00	0.00
Normal Stiffness (GPa/m)	500.00	500.00	50.00	50.00
Shear Stiffness (GPa/m)	500.00	500.00	50.00	50.00

2.5 FRACTURE NETWORK CHARACTERISTICS

The rock mass of the proposed YM repository is highly fractured. Fracture data have been collected by the DOE through borehole exploration (Brechtel et al., 1995; Lin et al., 1993), surface mapping at YM and the surrounding region (Sweetkind and Williams-Stroud, 1996), and full-periphery geological mapping and detailed line surveys in the ESF (Civilian Radioactive Waste Management System Management and Operating Contractor, 1999a; Anna, 1998). Fracture network characterization and fracture network modeling, however, are open technical issues that remain to be resolved before DOE submits an LA for the proposed YM repository (Nuclear Regulatory Commission, 1999a). Future network modeling at YM needs to determine the number of fracture sets and reasonable ranges and associated uncertainties (statistics) in fracture orientation, spacing, and persistence. Even if fracture network characteristics are well understood and characterized, it is impractical to model explicitly such a complex fracture network using a discontinuum numerical tool such as UDEC. Consequently, much simplified fracture patterns are often used in drift stability and ground support design analyses.

To facilitate discussions in this report, three terms are introduced to describe simplified fracture patterns that are often used in TM modeling at YM: (i) a regular fracture pattern, (ii) an irregular fracture pattern, and (iii) the complexity of a fracture pattern. A regular fracture pattern is defined by infinite fracture length and constant orientation and spacing for each fracture set. An irregular fracture pattern is defined by uniform distributions of fracture orientation, spacing, trace length, and gap length. Complexity of a fracture pattern increases with increasing number of fracture sets, decreasing fracture spacing, and increasing deviations from the mean of fracture parameters.

A regular fracture pattern with two sets of through-going fractures, each having a constant orientation and spacing, has been widely used in drift stability and ground support design analyses for the proposed YM repository (Civilian Radioactive Waste Management System Management and Operating Contractor, 1995, 1998; U.S. Department of Energy, 1997). Nevertheless, previous studies show that fracture patterns appear to have controlling effects on some aspects of drift stability, particularly rockfall (Chen, 1998, 1999; Chen et al., 2000b, in press). For example, these previous studies show that changing fracture set orientation and/or spacing from constant to that of slight variation significantly increases drift instability and, consequently, rockfall.

Three fracture patterns were selected for analyses in this study to further explore the effects of fracture pattern on ground support and drift stability (table 2-4). Patterns C and F are regular fracture patterns. Fracture spacing in Pattern F is about twice that in Pattern C. Pattern E is an irregular fracture pattern, with parameters selected from previous studies (Pattern C in Chen, 1998; Chen 1999). As described in Chen (1998), this fracture pattern was selected with the intention of matching the parameters with those developed in the DOE preliminary statistical analyses of site-specific fracture data¹. However, statistics of fracture parameters had to be simplified to a uniform probability distribution due to limitations in fracture modeling capabilities in UDEC (Chen, 1998).

¹Pye, J.H., D.C. Kicker, and G.H. Nieder-Westermann. Plans for mapping of subsurface facilities. *Notes from U.S. Department of Energy/Nuclear Regulatory Commission Appendix 7 Discussions*. October 16, 1997.

2.6 GROUND SUPPORT MODELING AND PARAMETERS

The analyses conducted in this study are not design analyses. These analyses examine how thermal and dynamic load might affect ground support performance. Consequently, parameters, particularly strength parameters for the ground support, are chosen to avoid significant failure of the support elements under thermal and dynamic load so that ground support performance can be examined based on comparisons of loads acting on support elements.

Table 2-4. Universal Distinct Element Code Version 3.1 parameters used to generate fracture patterns

Pattern	Fracture Set	Angle*		Trace Length		Gap Length		Fracture Spacing	
		Mean	Deviation [†]	Mean	Deviation [†]	Mean	Deviation [†]	Mean	Deviation [†]
C	1st	85	0	Infinite	NA	NA	NA	1.0	0.0
	2nd	15	0	Infinite	NA	NA	NA	2.0	0.0
E	1st	85	10	7.5	1	-0.2	0	0.4	0.1
	2nd	20	5	5.0	1	-0.2	0	0.75	0.1
	3rd	110	10	12.0	4	-0.3	0	1.8	0.5
F	1st	85	0	Infinite	NA	NA	NA	0.5	0.0
	2nd	15	0	Infinite	NA	NA	NA	1.0	0.0

* The angle is measured counter-clockwise from the horizontal axis.
[†] Deviation is the standard deviation from the mean assuming a uniform probability distribution.

2.6.1 Rock Bolts

In UDEC, restraint of rock blocks that may experience inelastic deformation in the failed region surrounding an excavation is simulated using cable elements (Itasca Consulting Group, Inc., 2000). These elements allow modeling shear resistance along element lengths, as provided by the shear resistance (bond) between the grout and either the cable or the host rock mass. The cable is assumed to be divided into several segments with nodal points located at the end of each segment. Shearing resistance is represented by spring/slider connections between the structural nodes and the block zones in which the nodes are located. The axial behavior of the cable elements is assumed to be governed entirely by the reinforcing element itself, usually steel, and may be either a bar or cable. Because such reinforcing elements are slender and offer little bending resistance, they are treated as one-dimensional members subject to uniaxial tension or compression.

Three groups of input parameters are necessary in modeling rock bolts: geometric parameters, parameters of the reinforcing steel bar or cable (bolt parameters), and grout parameters. Geometric parameters include length of the rock bolt, bolt diameter (D), and thickness of the grout (t) or hole diameter ($D + 2t$). In UDEC, bolt length needs to be specified, and D and t are used to estimate grout mechanical and strength parameters.

Grout parameters include grout shear modulus (G) and grout compressive strength (F). However, these parameters are not directly used in UDEC. Instead, grout shear stiffness (K_{bond}) and the maximum bond force per unit length (S_{bond}) are used. (K_{bond}) is estimated from G , t , and D (Itasca Consulting Group, Inc., 2000):

$$K_{\text{bond}} = \frac{2\pi G}{10 \ln\left(1 + \frac{2t}{D}\right)} \quad (2-6)$$

(S_{bond}) is either directly measured by pull-out tests conducted at different confining pressures or estimated from (Itasca Consulting Group, Inc., 2000):

$$S_{\text{bond}} = \pi(D + 2t)\tau_{\text{peak}}$$

$$\tau_{\text{peak}} = \tau_i Q_B \quad (2-7)$$

where τ_i is approximately one-half of the uniaxial compressive strength of the weaker of the rock and grout (usually rock), Q_B is the quality of the bond between the grout and rock ($Q_B = 1$ for perfect bonding).

Bolt parameters include bolt Young's modulus, bolt tensile yield force, bolt density, bolt thermal expansion coefficient, bolt compressive yield force (1.0×10^4 MN is UDEC default), and bolt extensional failure strain (optional, can be unlimited). These parameters are directly input to UDEC.

In this study, length of the rock bolts was assumed to be the same as the radius (2.75 m) of the emplacement drifts. Barton et al. (1974) recommended that the length of rock bolts be estimated as

$$L = 2 + 0.15 \frac{B}{\text{ESR}} \quad (2-8)$$

where L is length in meters, B is span in meters, and ESR is excavation support ratio. For emplacement drifts, $B = 5.5$ m and assuming $\text{ESR} = 1$, the recommended rock bolt length is 2.825 m, which is close to the 2.75 m bolt length used in this modeling. Twelve rock bolts were installed with a uniform spacing in upper spring-line and roof areas (figure 2-4). The rock bolts are numbered sequentially from left to right.

Parameters used in this study are listed in table 2-5. The study began with the first set of parameters. This set of parameters was chosen from the rock bolt design parameters selected by the DOE for the ESF (Civilian Radioactive Waste Management System Management and Operating Contractor, 1995), assuming a bolting pattern based on 1.0-m row spacing in the out-of-plane direction. The bolt type represented by this set of parameters is Williams' hollow continuous threaded steel bar (Williams Form Engineering Corp., 1992). As stated in Eq. (2-7), τ_i is approximately one-half of the uniaxial compressive strength of the weaker of rock and grout. This study assumed that the grout material can be selected so its uniaxial compressive strength is higher than rock mass uniaxial compressive strength. The rock compressive strength (q_u) can be evaluated based on Mohr-Coulomb yield criterion as

$$q_u = 2c \tan(\alpha) \quad (2-9)$$

where c and α are cohesion and friction angle. Based on c and α used in this study for RMQ5 and RMQ1 rock masses (table 2-3) and Eq. (2-7), S_{bond} is calculated to be 1.513 MN/m, for RMQ5 and 0.744 MN/m for RMQ1 rock masses.

Using this set of parameters, however, rock bolts experienced both extensive element axial failure and grout failure under thermal load. To better examine the performance of rock bolts with load built up in the cable element and between cable nodes and host rock mass, the second set of parameters was chosen to increase tensile yielding force for the cable element because most axial failure was tensile failure when the first set of parameters was used. In the model using the second set of parameters, maximum bond force per unit length was also increased to avoid grout failure. Physically, increasing tensile yielding force for the cable reinforcement can be achieved by selecting stronger steels. Increasing maximum bond force per unit length can be achieved by increasing grout thickness [or hole diameter, see Eq. (2-7)]. When grout thickness or hole diameter is increased, K_{bond} will also change [see Eq. (2-6)], which may alter the shear force on the grout/rock interface and, consequently, failure status. Alternatively, a different grout shear modulus may need to be selected to determine a proper value for K_{bond} . These design details are beyond the scope of this study. The second set of parameters for grout in table 2-5 is hypothetical and not directly calculated from the geometrical data of rock bolts. The thermal expansion coefficient for rock bolts is assumed to be the same as the rock mass thermal expansion coefficient to avoid differential expansion between rock mass and reinforcement or bolts. Future studies need to consider differential thermal expansion because it is not likely that the two thermal expansion coefficients are the same. Differential expansion may cause more extensive failure of both the reinforcing and grout elements.

Table 2-5. Parameters for rock bolts

Parameters		Unit	First Set	Second Set
Geometric	Bolt Diameter (D)	cm	0.3	—
	Grout Thickness (t)	m	0.105	—
	Hole Diameter (D + 2t)	m	0.53	—
Bolt	Young's Modulus (E)	MPa	2.0×10^5	2.0×10^5
	Tensile Yield Force	MN	0.267	0.534
	Density	kg/m ³	7875	7875
	Thermal Expansion Coefficient	/°C	7.5×10^{-6}	7.5×10^{-6}
	Compressive Yield Force	MN	1.0×10^4	1.0×10^4
	Extensional Failure Strain	—	no limit	no limit
Grout	Shear Modulus (G)	MPa	8.97×10^3	8.97×10^3
	Compressive Strength	MN	20.685	20.685
	Grout Shear Stiffness (K_{bond})	MN/m/m	16.34×10^3	16.34×10^3
	Maximum Bond Force Per Length (S_{bond})	MN/m	RMQ5: 1.513 RMQ1: 0.744	RMQ5: 3.026 RMQ1: 1.488

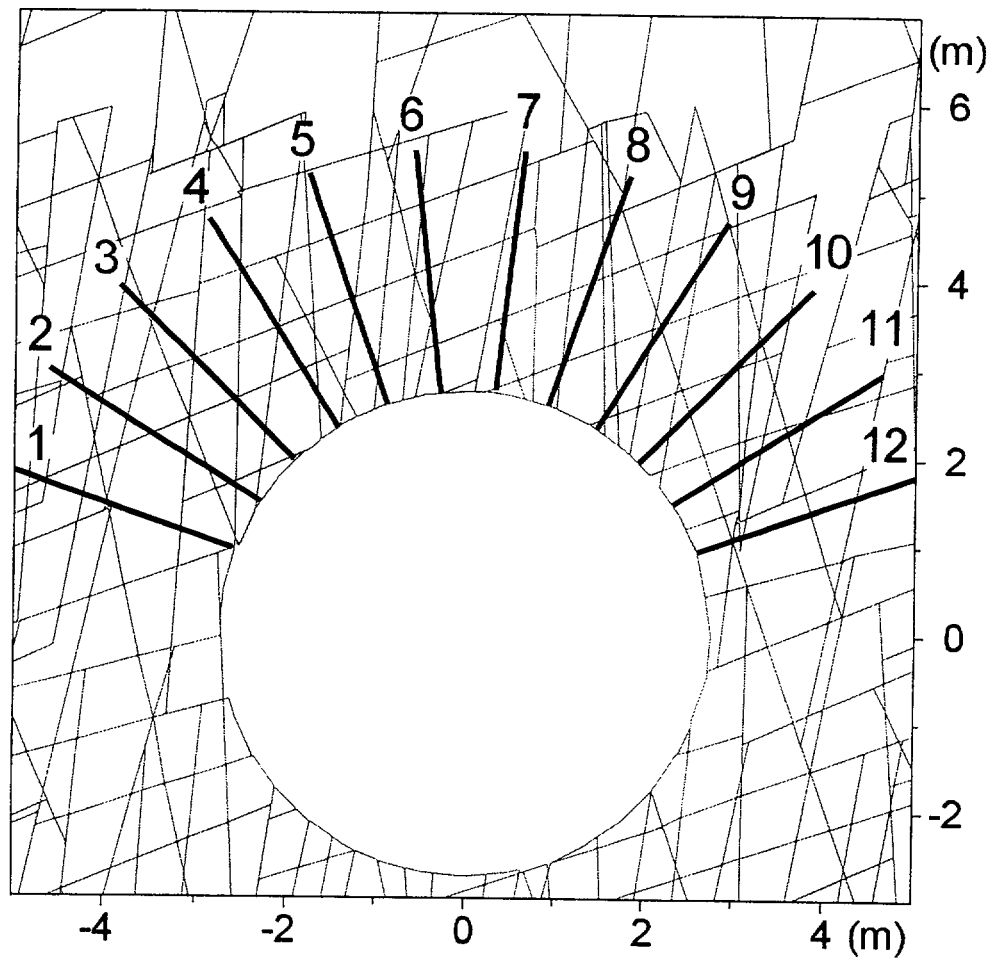


Figure 2-4. Distribution of rock bolts

2.6.2 Steel Sets

Steel sets can be simulated using the two-dimensional structural (beam) elements in UDEC (Itasca Consulting Group, Inc., 2000). Steel sets—like surface linings for tunnels and exposed slopes—are typically thin, and their characteristic response to bending usually cannot be neglected. Beam elements generally provide an effective method to include bending effects. In UDEC, the beam elements are attached to a rock surface via spring connections oriented both radially and tangentially with respect to the support structure. Also in UDEC, the structural element formulation is a plane-stress formulation. Therefore, it can be directly applied in modeling steel sets so long as the elastic modulus of the beam element is scaled to account for the spacing of the steel sets. Therefore, the force and moments in the beam structural element, which are calculated by UDEC, are scaled forces and moments. To simplify the interpretation of the UDEC results, this study assumes that the steel sets have unit spacing (i.e., 1 m) out of plane. Also, it assumes that the steel sets have a rectangular cross section, and the cross-sectional area and moment of inertial are taken as those for the W8 × 30 steel sets described in Civilian Radioactive Waste Management System Management and Operating Contractor (CRWMS M&O) (1995). Pertinent parameters are given in table 2-6. Steel sets

thickness in the radial direction is assumed to be 0.1 m; Young's modulus was taken from CRWMS M&O (1995). Other parameters are assumed, lacking actual property values. Cohesion, friction angle, dilation angle, and tensile strength for the rock/steel sets interface were assumed the same as the host rock mass properties to be conservative (because rock mass is weaker than the steel sets, and UDEC documentation suggests using the weaker of the materials involved). Interface normal stiffness and shear stiffness were taken as rock fracture normal and shear stiffness, respectively.

Table 2-6. Parameters for steel sets

Parameters		Unit	Values
Geometric	Thickness	m	0.1
	Cross Sectional Area	m ³	5.9×10^{-3}
	Moment of Inertia	m ⁴	4.578×10^{-5}
Steel Sets	Young's Modulus	MPa	2.0×10^5
	Tensile Yield Strength	MN	4.0
	Density	kg/m ³	7875
	Thermal Expansion Coefficient	/°C	7.5×10^{-6}
	Compressive Yield Force	MN	1.0×10^4
	Poisson's Ratio	—	0.2

2.7 MODELING PROCEDURES

UDEC simulation started by obtaining an initial model equilibrium under *in situ* stress. After reaching the initial equilibrium, the emplacement drift was "excavated" by deleting the rock blocks within the drift boundary. In cases without ground support, a new equilibrium was obtained after drift excavation before TM analyses. In cases with ground support, a certain amount of initial closure was allowed (see section 4.1.1), then ground support was installed and a new equilibrium obtained. TM analyses started after these initial analyses and were conducted for a simulation period of 150 yr following waste emplacement. This simulation period was chosen to represent the preclosure and earlier postclosure period, assuming potential closure of the repository between 50–150 yr. UDEC uses a time sequential coupling approach in conducting a TM analyses. This approach consists of running the thermal analysis for a period of time during which the nodal or grid-point temperature is updated. The thermal time is then held while mechanical cycling is conducted to update stresses, displacements, and block rotations to reach a new mechanical equilibrium. Dynamic excitation was applied at the end of the TM simulation time (i.e., 150 yr following waste emplacement).

3 PERFORMANCE OF DRIFT WITHOUT GROUND SUPPORT

Modeling results for an emplacement drift without ground support are discussed in this chapter. The effects of rock mass properties are examined in terms of drift convergence, fracture shear displacement, and yielding of rock blocks. Responses of different quality rock masses to thermal load were observed to be different and may be governed by different deformation and failure mechanisms. Consequently, different strategies may need to be applied to support different quality rock mass in ground support design. Most importantly, modeling results show that, under thermal load, higher quality rock mass may need stronger support, particularly in roof and floor areas. The effect of fracture pattern is primarily on local drift instability as loose blocks falling from the roof area, particularly under seismic loading.

3.1 DRIFT PERFORMANCE UNDER *IN SITU* AND THERMAL LOAD

3.1.1 Effect of Rock Mass Properties

Numerical simulation of drift performance largely depends on rock block and fracture mechanical properties. As observed previously (Chen et al., 2000b, in press), when either RMQ1 or RMQ5 property data with the DOE-derived strength property values (Civilian Radioactive Waste Management System Management and Operating Contractor, 1998) were used, little yield of rock blocks or fracture displacement was predicted either under *in situ* stress or thermal load. With reduced friction angle as given in table 2-3, some interesting phenomena were observed. These effects of rock mass properties on drift performance are discussed in the following sections.

3.1.1.1 Drift Convergence

At YM, the convergence curves of an emplacement drift under *in situ* stress are nearly linear elastic, particularly for an RMQ5 rock mass (figure 3-1). As the complexity of fracture patterns increases and rock mass quality decreases, the drift convergence curves become more nonlinear. Also, as shown in table 3-1, the total convergence following drift excavation for an RMQ5 rock mass is about 20 percent of that for an RMQ1 rock mass for the same fracture pattern. This convergence ratio of RMQ5 versus RMQ1 rock masses implies that the *local-mine stiffness* as defined in Hoek and Brown (1980) of an RMQ5 rock mass is about 5 times that of an RMQ1 rock mass.

Drift convergence resulting from thermal load shows a quite different picture. Drift convergence due to thermal load is greater in a higher quality rock mass (RMQ5) than in a lower quality rock mass (RMQ1) for both Patterns C and F (table 3-1). This drift convergence indicates greater thermally induced deformation when the rock mass quality is higher as a consequence of higher thermal stresses caused by higher elastic modulus. Final convergences are not measured for Pattern E due to rockfall in the roof area, which makes the measured convergence difficult to interpret for this case.

Table 3-1. Summary of drift convergence resulting from *in situ* and thermal loads

Pattern	Rock Mass	Convergence resulting from <i>in situ</i> stress (mm)		Convergence resulting from thermal load (mm)	
		Vertical	Horizontal	Vertical	Horizontal
Pattern C	RMQ5	3.8	1.6	4.5	2.6
	RMQ1	15.8	6.8	2.2	2.0
Pattern E	RMQ5	4.7	2.7	—	—
	RMQ1	22.6	14.7	—	—
Pattern F	RMQ5	4.0	1.8	13.7	9.6
	RMQ1	17.3	9.6	4.9	3.3

3.1.1.2 Fracture Shear Displacement and Yield of Rock Blocks

Fracture shear displacement occurs mainly along subvertical fractures following drift excavation and is limited to those subvertical fractures that bound the sidewall of the emplacement drift (figures 3-2a and b). The orientation of the *in situ* stress at the repository horizon is such that the maximum principal stress is near vertical and the minimum principal stress is near horizontal. This stress state favors slip along subvertical fractures. Excavating the drift causes vertical stress to increase and horizontal stress to decrease in the drift sidewalls such that shear stress along subvertical fractures overcomes shear strength, causing the fractures to slip. This kind of fracture shear displacement, therefore, is controlled by factors such as depth of the drift, density of overburden rocks, and drift dimension and geometry. These factors apply prior to thermal loading.

Following drift excavation, no rock block yield was observed in an RMQ5 rock mass, and only limited rock block yield was observed in an RMQ1 rock mass near the drift sidewall (compare figures 3-3a and b), indicating the excavation-induced stress is high enough to satisfy the failure criterion in an RMQ1 rock mass but not in an RMQ5 rock mass that has higher strength values. Similar to fracture shear displacement, yield of rock blocks following drift excavation is controlled by factors that exist prior to thermal loading. Also, differences in fracture shear displacement and rock block yielding between RMQ1 and RMQ5 rock masses are consistent with observations from traditional mining and tunneling in ambient condition. Such observations show that a lower quality rock mass would experience greater deformation than a higher quality rock mass under the same loading conditions.

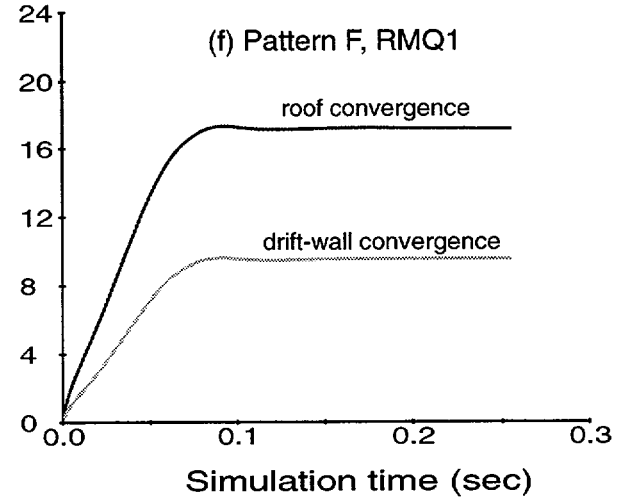
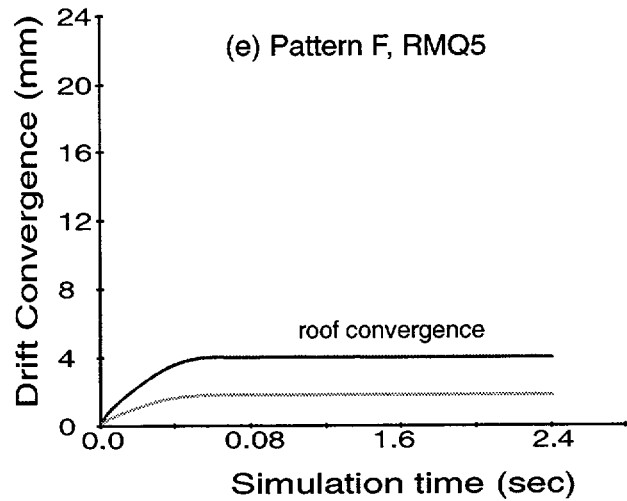
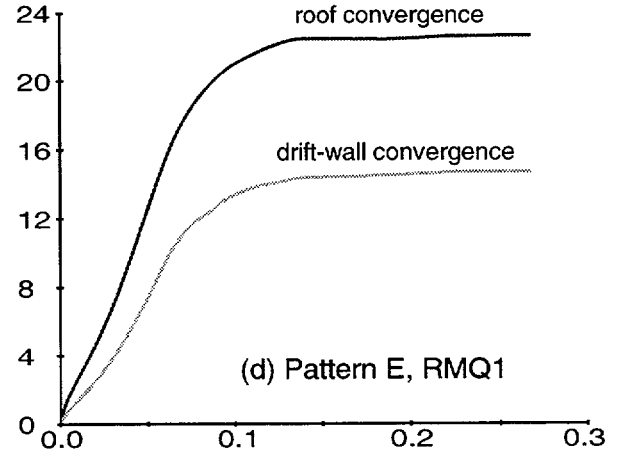
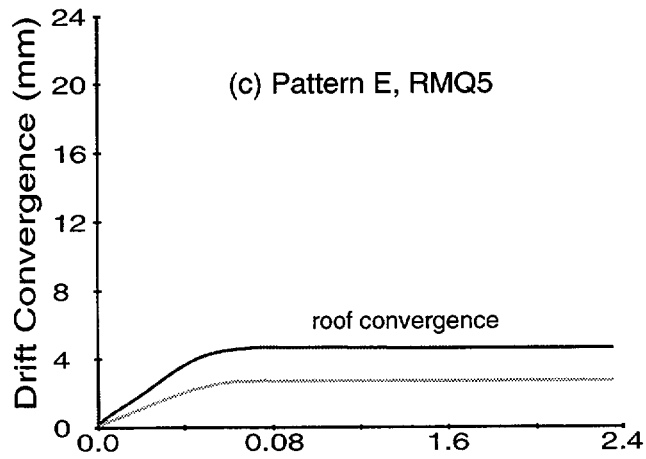
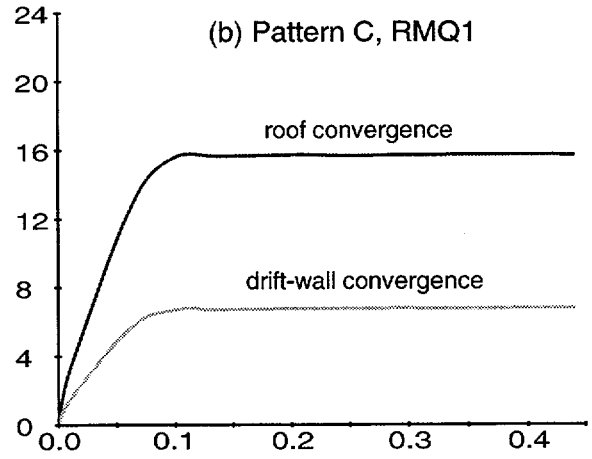
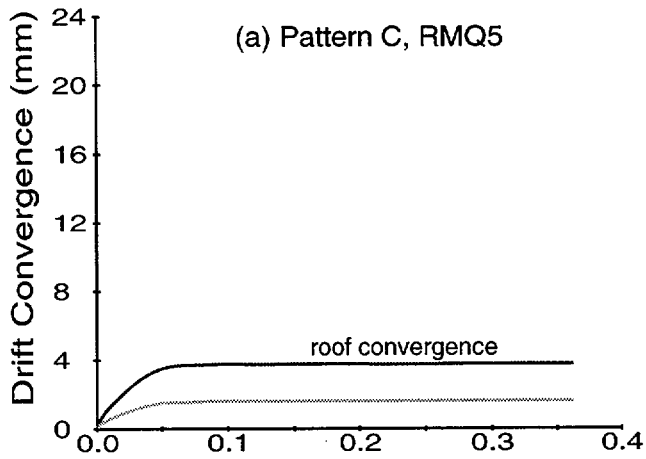


Figure 3-1 Drift convergences following excavation for RMQ5 and RMQ1 rock masses and for various fracture patterns analyzed in this study

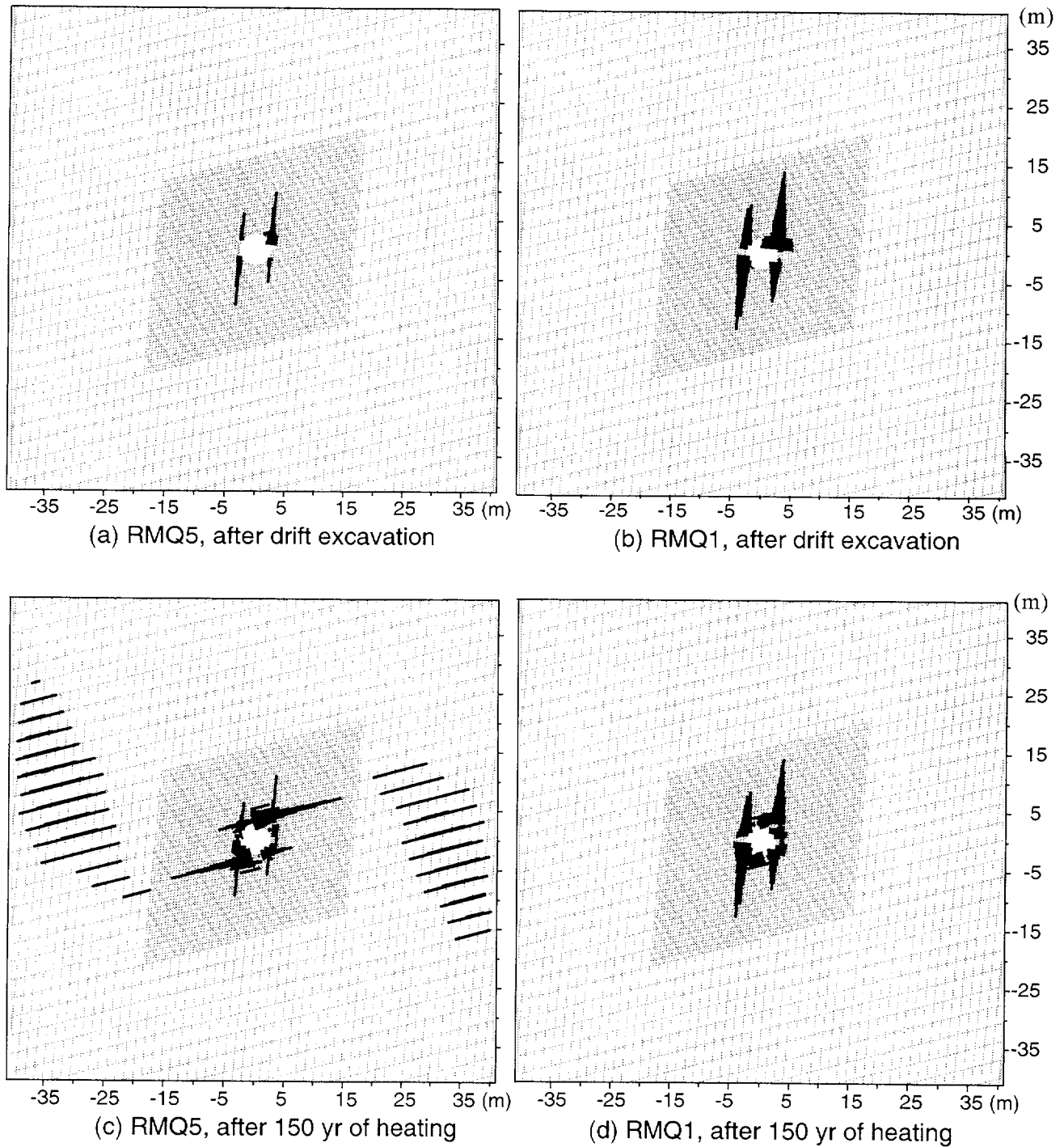


Figure 3-2. Fracture shear displacement for Pattern F. Thickness of dark lines is proportional to fracture shear displacement: (a) RMQ5 rock mass after drift excavation, (b) RMQ1 rock mass after drift excavation, (c) RMQ5 rock mass after 150 yr of thermal load, and (d) RMQ1 rock mass after 150 yr of thermal load

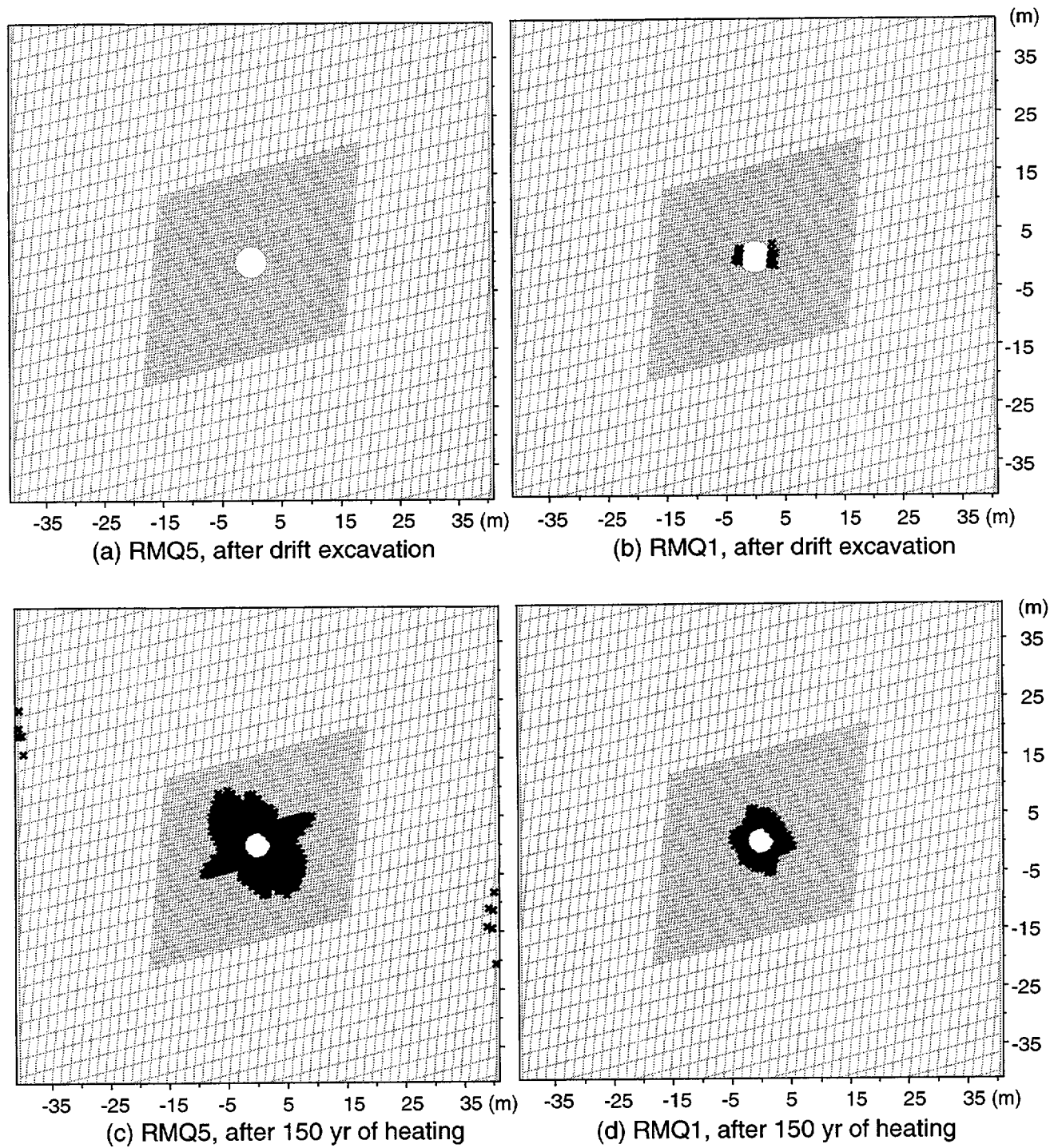


Figure 3-3 Yielding of rock blocks for fracture Pattern F: (a) RMQ5 rock mass after drift excavation, (b) RMQ1 rock mass after drift excavation, (c) RMQ5 rock mass after 150 yr of thermal load, and (d) RMQ1 rock mass after 150 yr of thermal load

Fracture shear displacement increases significantly, particularly in an RMQ5 rock mass, after thermal loading (figures 3-2c and d). Fracture shear displacement increases because superimposing the thermal stress on excavation-induced stress significantly alters the stress state in the repository and surrounding areas. Furthermore, the thermal load changes the orientation of the maximum principal stress from approximately vertical to approximately horizontal near the repository horizon and shifts the location of the concentration of maximum principal stress from the drift sidewalls to the roof and floor areas (Chen et al., 2000a, in press; Ahola et al., 1996; Ofoegbu et al., 2000, in review; Ofoegbu, 2000). This change in stress state favors slip along subhorizontal fractures. Therefore, shear displacement due to thermal loading is mainly along subhorizontal fractures. Such shearing occurs mainly in roof and floor areas instead of sidewalls near the drift. Shearing along subvertical fractures in an RMQ5 rock mass is much more significant than in an RMQ1 rock mass because thermally induced stresses are much higher in an RMQ5 rock mass due to its higher Young's modulus, and thermal stress is directly proportional to rock mass Young's modulus. The fracture shear displacement under thermal load is predominately thermal-stress controlled. Comparison of fracture shear displacement in RMQ1 and RQM5 rock masses before and after thermal loading indicates that, after thermal loading, fracture shear displacement in an RMQ1 rock mass continues to be controlled by structures that exist prior to thermal loading. In an RMQ5 rock mass, on the other hand, fracture shear displacement is predominantly controlled by thermal stresses.

Thermal stresses cause various degrees of yield in rock blocks around the emplacement drift (figures 3-3c and d). In the case of an RMQ1 rock mass, yield of rock blocks after thermal load (figure 3-3d) is superimposed on yield following drift excavation. Yield of rock blocks is more extensive in a higher quality rock mass (RMQ5, figure 3-3c) than in a lower quality rock mass (RMQ1, figure 3-3d). Again, this result is because higher quality rock mass has higher stiffness and, consequently, thermal stress is high enough to meet the failure criterion defined by rock mass strength property values given in table 2-2. Although the strength property values of a lower quality rock mass are less than those of a higher quality rock mass, thermal stresses in the former are also less because of its lower stiffness. Consequently, the zone of rock block yield is not as extensive in an RMQ1 rock mass as it is in an RMQ5 rock mass. These observations on rock block yield show, once again, that the failure in an RMQ5 rock mass is more extensive and controlled by high thermal stresses.

Accordingly, it is inferred that, under the thermal load expected at the proposed YM repository, a higher quality rock mass needs more ground support than a lower quality rock mass. This conclusion is noteworthy because it contradicts the common understanding that a lower quality rock mass needs more ground support. It is, however, not surprising because the common understanding that a lower quality rock mass needs more ground support is derived and should be applied only to ambient conditions or commonly expected conditions in underground mining and tunneling. Consequently, empirical design methodologies that are rooted in conventional mining and tunneling and based on rock mass classifications (e.g., Barton et al., 1974) may be applied only for ground support design following drift excavation and should not be applied to thermal loading conditions without significant modification and verification. Ground support design for the repository should rely on analytical/numerical approaches that use an appropriate combination of models and model parameters. Numerical design approaches and expected ground support performance are discussed in chapter 4. Also, because thermally induced fracture shear displacement mainly occurs along subhorizontal fractures in the roof and floor areas (figure 3-2), drift support design should concentrate on stabilizing these areas, particularly in higher quality rock masses. A lower quality rock mass, on the other hand, may experience instability in sidewall areas following drift excavation. Therefore, different strategies may need to be applied to ground support design in different quality rock masses.

Notable rock mass deformation, particularly fracture shear displacement along subhorizontal fractures, is also observed in inter-drift pillars in an RMQ5 rock mass under thermal load (figures 3-2c and 3-3c). This kind of deformation may not affect drift stability much, but may alter rock mass hydrological properties. This observation is consistent with the evaluation of rock mass permeability change due to TM effects based on inelastic rock mass deformation analyses using a continuum approach (Ofoegbu et al., 2000, in review; Ofoegbu, 2000). Previous study shows that the extent and magnitude of pillar deformation under thermal load largely depend on rock mass thermal expansion coefficient and rock mass Young's modulus (Chen et al., 2000b, in press). In terms of permeability change and channeled fluid flow near the emplacement drift, a higher quality rock mass may experience permeability increase mainly in the horizontal direction, whereas a lower quality rock mass may experience permeability increase mainly in the vertical direction.

Model results presented in this section and in various earlier reports (e.g., Ahola et al., 1996; Chen, 1999; Chen et al., 2000a, in press, 2000b, in press; Nuclear Regulatory Commission, 1999b) show that it is important to use an appropriate combination of stiffness and strength parameters, particularly Young's modulus and friction angles, in drift stability and ground support design analyses. In the case of the proposed YM repository, it may be necessary for DOE to obtain more rock property data, particularly for the lower lithophysal zone where the majority of the repository will be located and for which minimal rock property data are available. These results also indicate that failure of different quality rock masses may be controlled by different mechanisms and different sources of loadings. Specifically, failure in a higher quality rock mass (RMQ5) is controlled by high thermal stress, whereas failure in a lower quality rock mass (RMQ1) may be controlled by structures existing prior to thermal load.

3.1.2 Effect of Fracture Pattern

Comparison of the initial convergence (table 3-1) of the three fracture patterns analyzed in this study indicates that the *local-mine stiffness* is the greatest for Pattern C and the smallest for Pattern E for the same rock mass quality, showing the influence of fracture network on net rock mass quality. Although fracture characteristics are important factors in determining rock mass quality (Hoek and Brown, 1980; Barton et al., 1974); there is, however, no existing procedure that would allow estimation of equivalent mechanical properties for different fracture patterns for modeling purposes, particularly on a drift scale. Furthermore, for the purpose of ground support design, local fracture characteristics within a few drift diameters around the opening may have a significant effect on ground support performance as discussed in section 4.1.2. For these reasons, explicit modeling of fractures using a discontinuum approach and proper interpretation of modeling results from simplified fracture patterns is critical in ground support design. The magnitude of *local-mine stiffness* gives an indication of overall rock mass quality for different fracture patterns used in this study.

Thermally induced drift convergence is much higher in Pattern F than in Pattern C. As indicated in table 2-3, the only difference between these two fracture patterns is that fracture spacing in Pattern F is about twice that of the fracture spacing in Pattern C. If the effect of fractures is factored into overall rock mass quality, Pattern C would have a higher rock mass quality than Pattern F. Consequently, the greater convergence in Pattern F contradicts earlier observations in section 3.1.1.1 that a higher quality rock mass (RMQ5) shows greater thermally induced convergence. This observation indicates that it may not be appropriate to use traditional rock mass classification in analyzing rock mass behavior under thermal load, and fracture network characteristics may need to be included explicitly in a drift-scale model.

Although a regular fracture pattern (Pattern F) was used to illustrate the observations and discussions in section 3.1.1.2, general discussions of the effects of rock mass properties on observed fracture displacement and rock block yielding are applicable to an irregular fracture pattern as well. An irregular fracture pattern (such as Pattern E), however, introduces more instability localized around the drift, particularly in the roof area (figure 3-4), because such an irregular fracture pattern forms more key blocks than a regular fracture pattern. Key blocks are mainly determined by fracture network characteristics (Goodman and Shi, 1985). These key blocks often fall into the drift under gravity shortly after drift excavation. Thermal load does not significantly affect falling of such key blocks. Figure 3-4 shows such key blocks increasing velocity after drift excavation. If the UDEC model ran for a long mechanical simulation time to allow better local equilibrium (without thermal load), these blocks would have fallen before thermal loading was applied. The only reason these blocks show physical detachment in figure 3-4b (after thermal loading) instead of figure 3-4a is much longer mechanical simulation time in figure 3-4b.

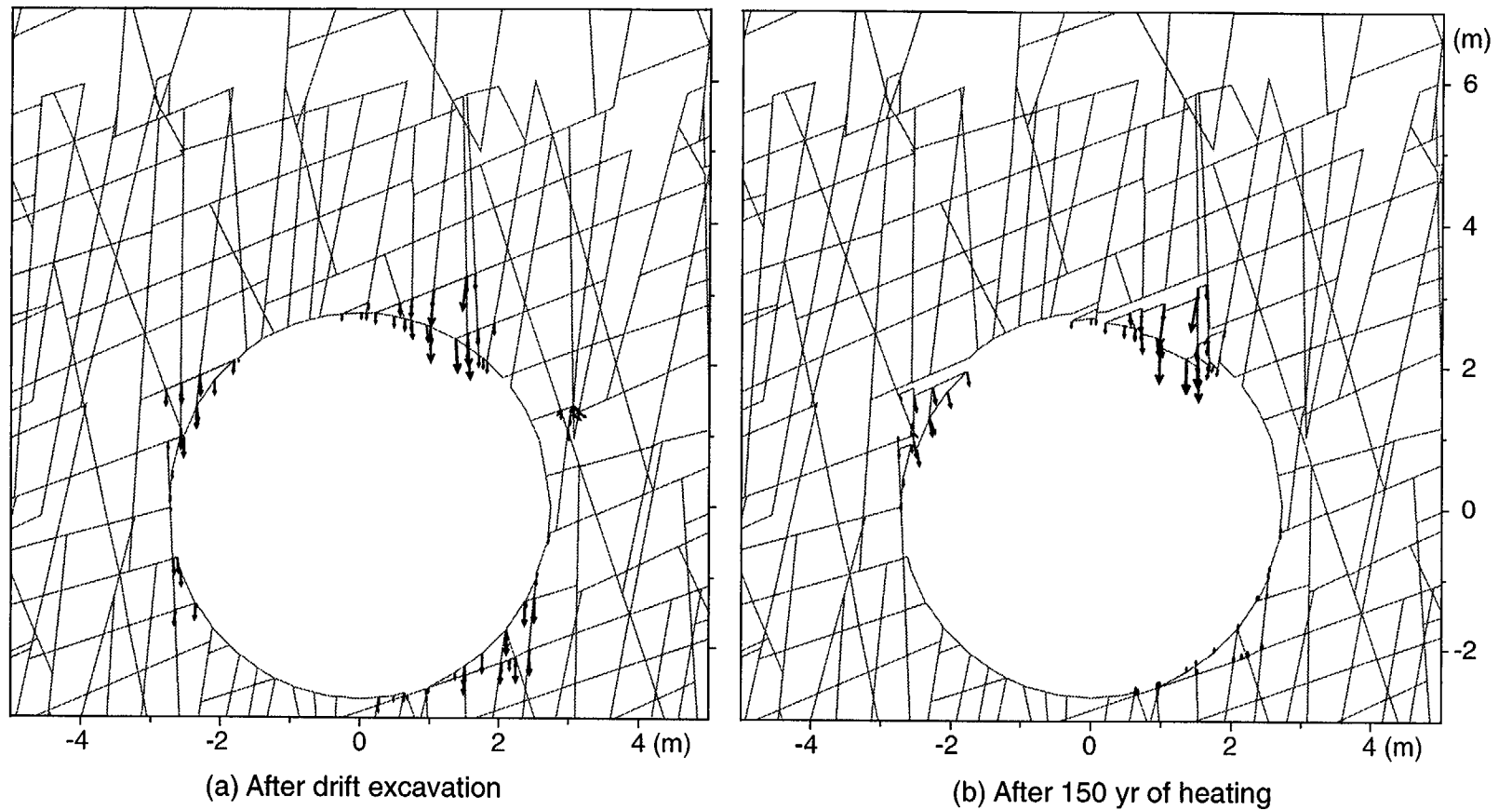


Figure 3-4. Falling key blocks in drift roof area for Pattern E: (a) following excavation, and (b) 150 yr after thermal loading

3.2 DRIFT PERFORMANCE UNDER SEISMIC GROUND MOTION

Drift performance under seismic ground motion at the proposed YM repository has been studied previously (Ahola, 1997; Chen, 1998; Chen et al., 2000a, in press). These earlier studies were based on a drift-scale model with earlier design configurations. Ahola (1997) used a regular fracture pattern and observed that although earthquake ground motion increases fracture shear displacement, yield of rock blocks around emplacement drift, and drift closure in some cases, this yield does not introduce additional drift instability in terms of rockfall. Chen (1998, 1999) used an irregular fracture pattern and found that seismic ground motion can introduce extensive rockfall and collapse of the emplacement drift. Such simulated rockfall, however, largely depends on fracture pattern. The dependence of simulated rockfall on fracture pattern is further demonstrated in this study in that rockfall is not observed with regular fracture patterns (Patterns C and F), whereas a significant amount of falling rock blocks was observed with an irregular fracture pattern (Pattern E).

Besides fracture pattern, rock mass properties also affect seismically induced rockfall. Figure 3-5 shows that simulated rockfall is slightly more extensive in an RMQ1 rock mass than in an RMQ5 rock mass for Pattern E. This difference may be because fracture shear displacement along subvertical fractures, which occurs after drift excavation, facilitated falling of rock blocks under seismic ground motion. Most of the efforts in modeling the effect of input ground motion parameters on drift stability using an unsupported drift have been unsuccessful because of either prolonged computational time or numerical instability. For the few cases that ran successfully, interpreting the results is difficult because there are no quantitative measures and the effects on the distribution of rock block yield and fracture shear displacement are usually small. Consequently, the effects of input ground motion parameters are discussed in section 4.2, where the analyses used a supported drift, and the effect of input ground motion parameters can be measured more quantitatively by comparing loads acting on the ground support system.

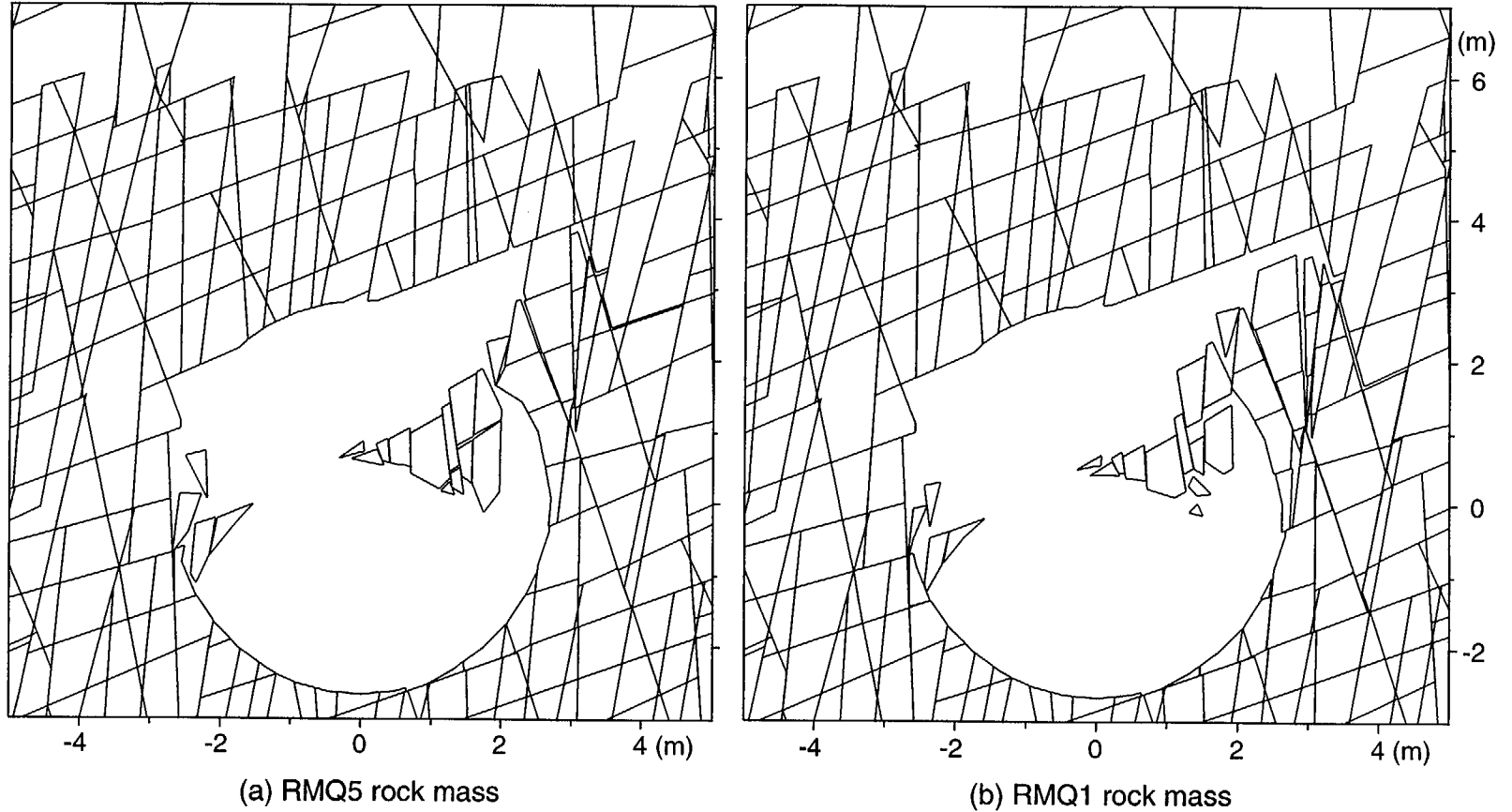


Figure 3-5. Simulated rockfall for Pattern E (using 10-Hz ground motion, with other properties from the basecase; see section 2.5): (a) RMQ5 rock mass, and (b) RMQ1 rock mass

4 GROUND SUPPORT PERFORMANCE

Ground support performance is discussed in this chapter using fully grouted rock bolts and, to a lesser degree, steel sets as examples. Numerical implementation, modeling strategies, and input parameters for ground support are given in section 2.6. The strength parameters for the ground support were chosen to avoid significant failure. The effects of rock mass properties, fracture pattern, and input ground motion parameters on ground support performance are evaluated by examining load acting on ground support and support element failure. Results show that after 150 yr of heating force acting on support system by the surrounding rock is much greater in a high quality rock mass than in a low quality rock mass. This is consistent with observations from chapter 3 that a higher quality rock mass experiences greater deformation than a lower quality rock mass under thermal load.

In conventional mining, the initial convergence (or relaxation) allowed before ground support is installed is important in that it determines the ultimate load on the ground support system. Ideally, initial convergence is kept constant (60 percent of the total convergence) to maintain consistent performance of ground support. In reality, time elapsed before ground support installation can be better controlled than initial convergence. During this initial time period, convergence could be slightly different from location to location, depending on local rock mass mechanical properties and loading conditions. As discussed in section 3.1.1.1, in the case of YM, the initial response of the rock mass to drift excavation is mostly elastic, and ground convergence occurs almost immediately. It is, therefore, even harder to maintain a constant initial convergence ratio. Therefore, in this study, the pseudo mechanical time elapsed before ground support installation was controlled rather than initial convergence, which resulted in a convergence ratio that varies slightly from case to case, mainly among different fracture patterns and, to a lesser degree, between different quality rock masses for the same fracture pattern. As discussed in chapter 3, rock deformation is mainly a result of thermal stresses rather than *in situ* stresses, particularly in a high quality rock mass. Consequently, the slight difference in the initial convergence before ground support is not important to the evaluation of the ultimate performance of ground support.

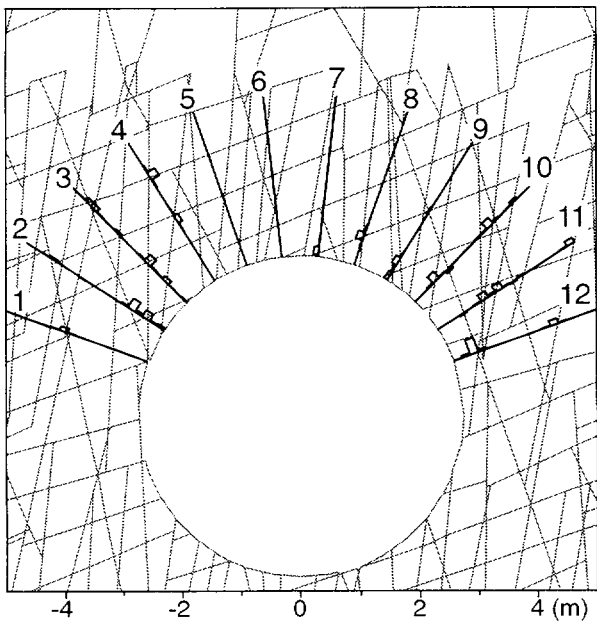
It is anticipated there will be differential thermal expansion between ground support elements and surrounding rock mass. Differential thermal expansion may alter loads acting on and, consequently, performance of ground support. This problem needs to be considered in the design of ground support, particularly rock bolts, for the proposed YM repository. To simplify the problem, this study assumed there is no differential thermal expansion by assigning rock bolts and steel sets a thermal expansion coefficient equal to the rock mass thermal expansion coefficient (section 2.6).

4.1 GROUND SUPPORT PERFORMANCE UNDER *IN SITU* AND THERMAL LOAD

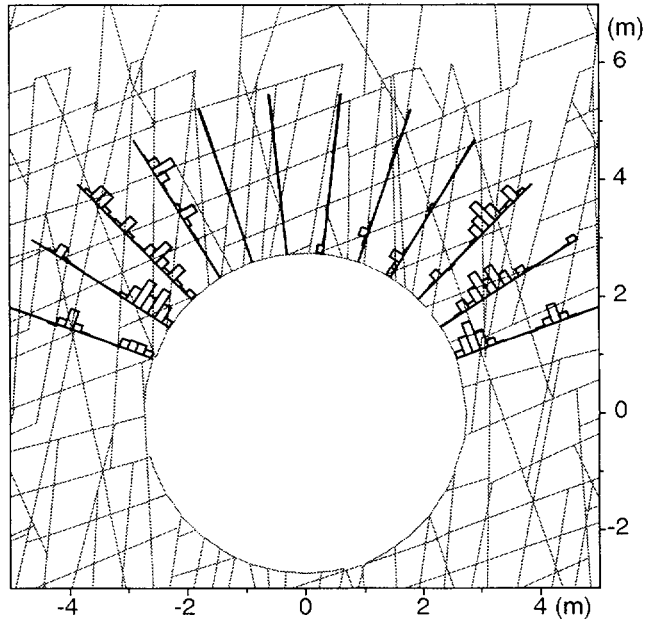
4.1.1 Effect of Rock Mass Properties

4.1.1.1 Rock Bolts

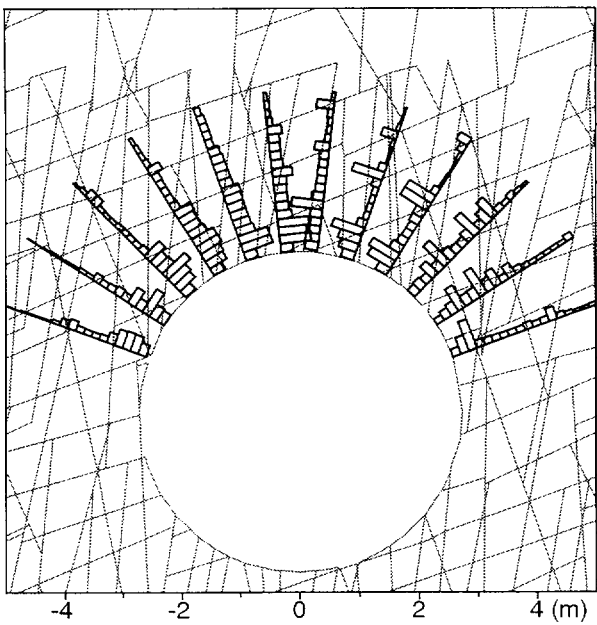
Figure 4-1 compares axial force on rock bolts after drift excavation and after 150 yr of thermal load for RMQ5 and RMQ1 rock masses for Pattern E. Rock bolts are numbered sequentially from left to right to help discussions (figure 4-1a). Thermal load significantly increases axial force in a high quality rock mass and, to a much lesser degree, in a low quality rock mass. In a high quality rock mass, thermal load increases axial force acting on rock bolts by two to three orders of magnitude. Similarly, thermal load significantly increases shear force acting along the rock/grout interface (figure 4-2). Consequently, simulated strain within rock bolt element, axial failure of rock bolts, and shear failure of rock/grout interface are also mainly due to thermal load (figures 4-3, 4-4, and 4-5).



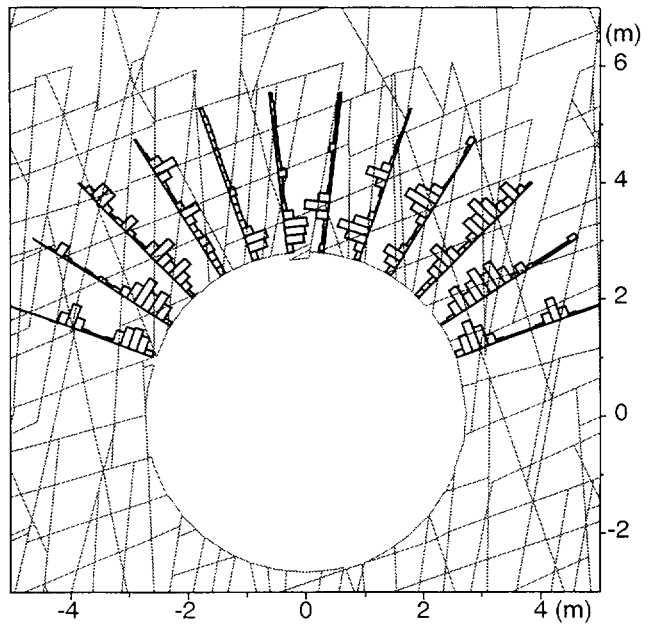
(a) RMQ5, after drift excavation



(b) RMQ1, after drift excavation



(a) RMQ5, after 150 yr of heating



(b) RMQ1, after 150 yr of heating

Figure 4-1. Comparison of axial force on rock bolts for Pattern E: (a) RMQ5 after excavation, (b) RMQ1 after excavation, (c) RMQ5 after 150 yr of thermal load, and (d) RMQ1 after 150 yr of thermal load

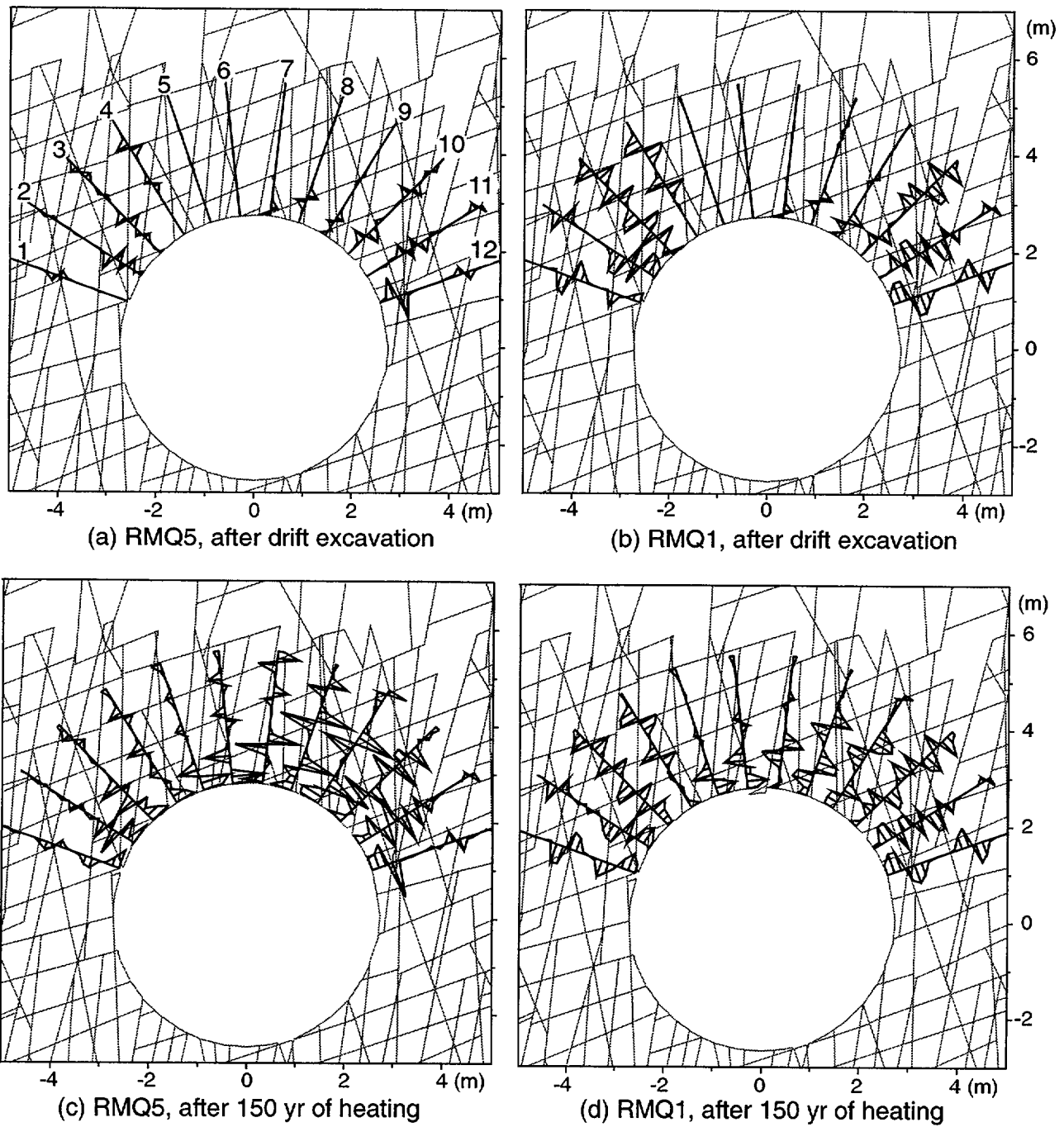


Figure 4-2. Comparison of shear force along rock/grout interface for Pattern E: (a) RMQ5 after excavation, (b) RMQ1 after excavation, (c) RMQ5 after 150 yr of thermal load, and (d) RMQ1 after 150 yr of thermal load

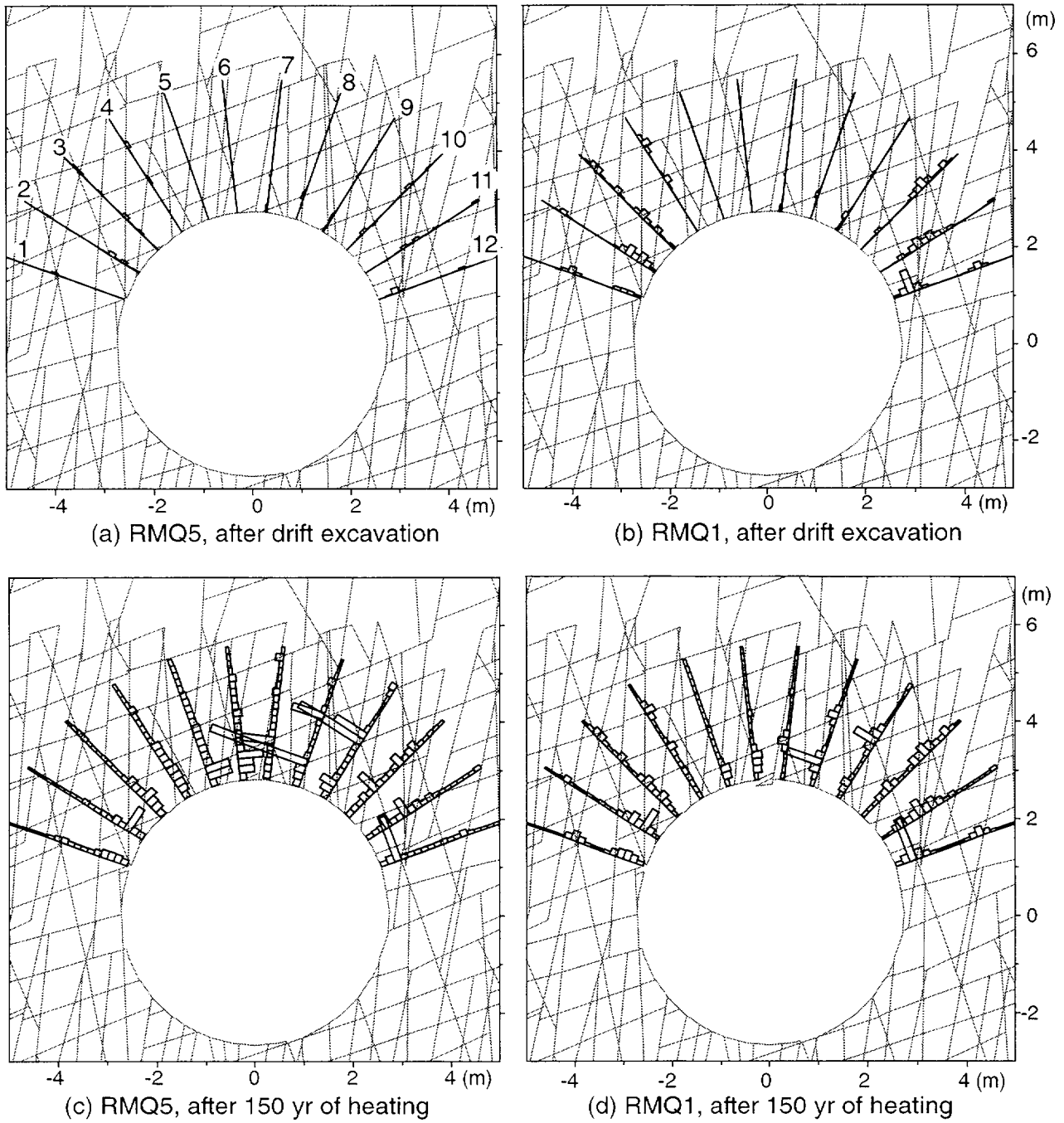
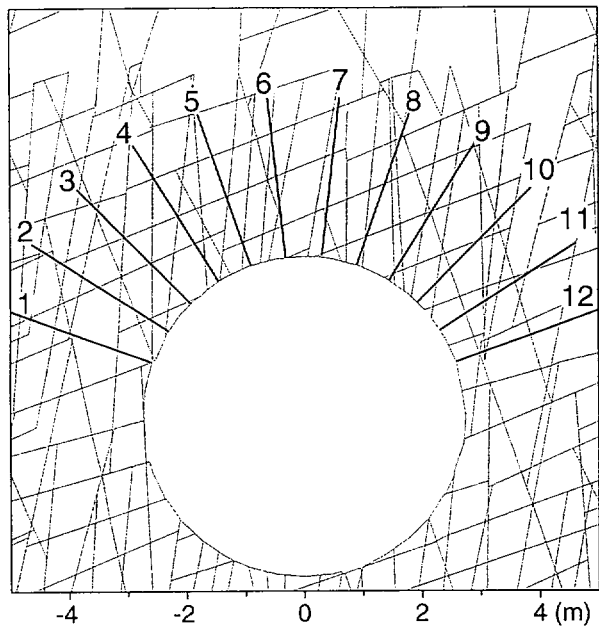
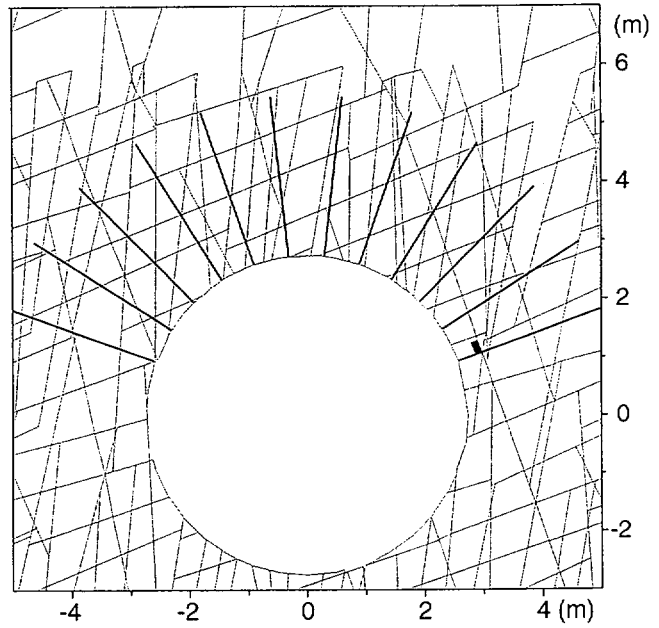


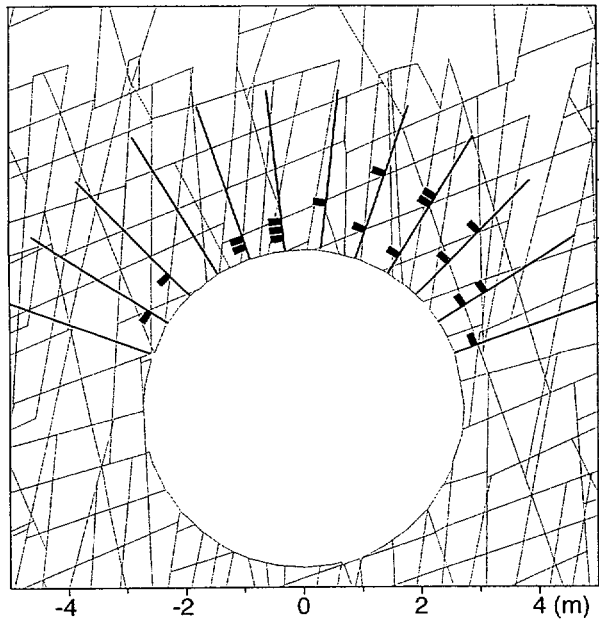
Figure 4-3. Comparison of axial strain in rock bolts for Pattern E: (a) RMQ5 after excavation, (b) RMQ1 after excavation, (c) RMQ5 after 150 yr of thermal loading, and (d) RMQ1 after 150 yr of thermal loading



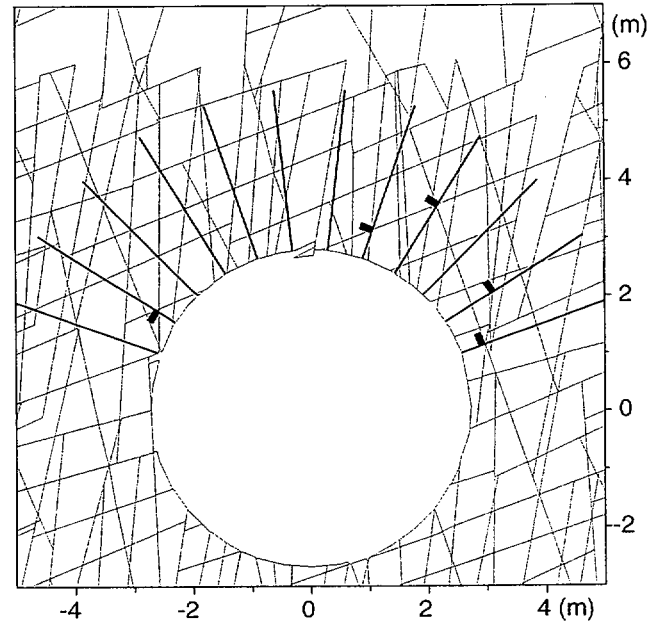
(a) RMQ5, after drift excavation



(b) RMQ1, after drift excavation



(c) RMQ5, after 150 yr of heating



(d) RMQ1, after 150 yr of heating

Figure 4-4. Comparison of axial failure on rock bolts for Pattern E: (a) RMQ5 after excavation, (b) RMQ1 after excavation, (c) RMQ5 after 150 yr of thermal load, and (d) RMQ1 after 150 yr of thermal load

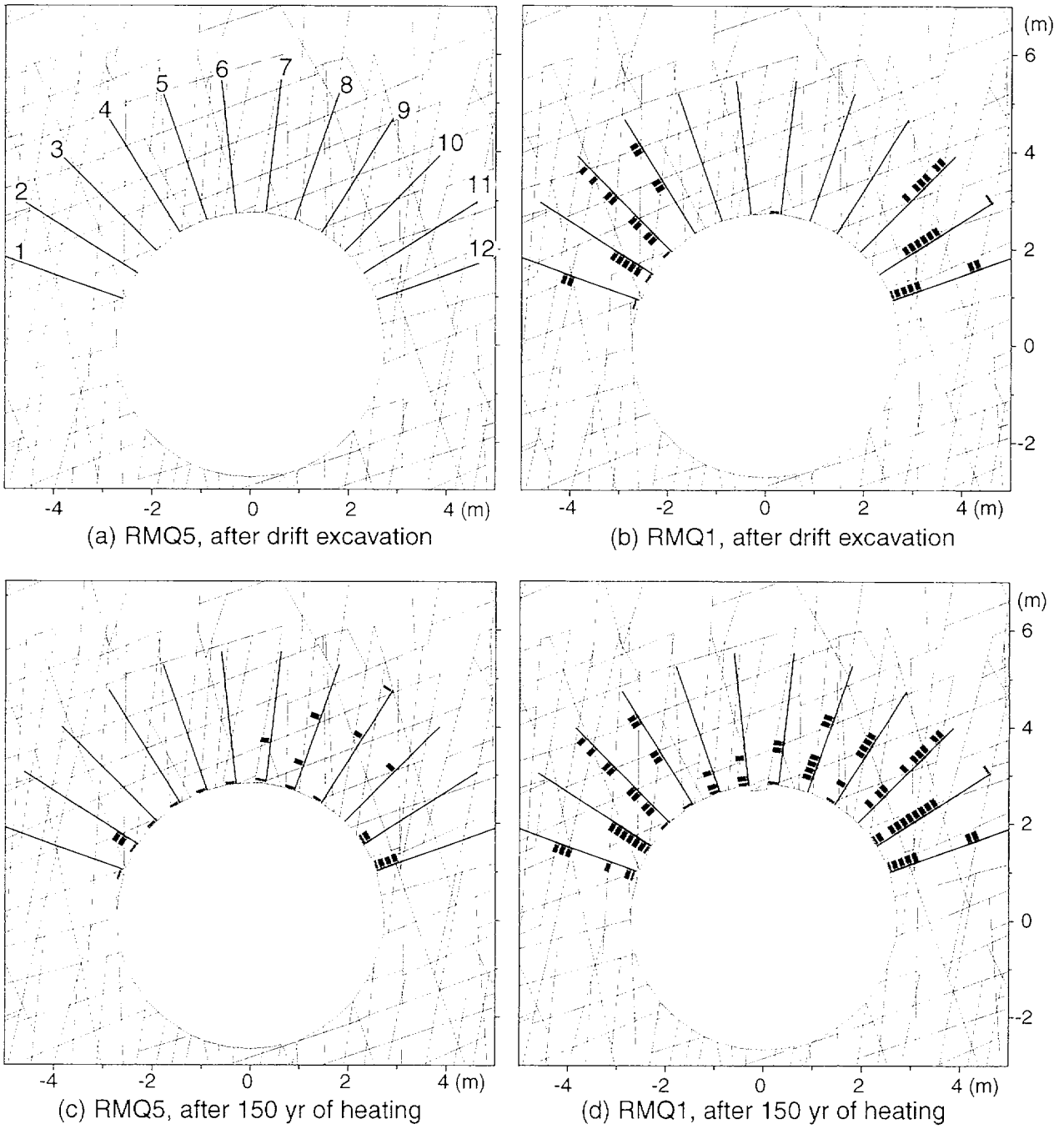


Figure 4-5. Comparison of shear failure along grout/rock interfaces for Pattern E: (a) RMQ5 after excavation, (b) RMQ1 after excavation, (c) RMQ5 after 150 yr of thermal load, and (d) RMQ1 after 150 yr of thermal load

After drift excavation, load acting on support elements (including axial force in rock bolts, axial strain in rock bolt, and shear force along grout/rock interface) is greater in an RMQ1 rock mass than in an RMQ5 rock mass (compare the first and second plots in figures 4-1 through 4-3). The greater load acting on rock bolts in an RMQ1 rock mass indicates that a lower quality rock mass needs stronger ground support, which is consistent with the observation from traditional mining and tunneling that a lower quality rock mass would experience greater deformation than a higher quality rock mass under the same loading conditions. Again, this observation is the foundation on which the empirical design approach for ground support design using rock mass classification is based.

The credibility of this traditional approach, however, was questioned earlier in section 3.1.1.2 based on observations of rock mass deformation around an unsupported drift under thermal load. Figures 4-1 through 4-3 show that after 150 yr of heating loads acting on rock bolts by the surrounding rock mass are greater in an RMQ5 rock mass than in an RMQ1 rock mass (compare plots c and d in figures 4-1 through 4-3). These figures further demonstrate that under thermal load, a higher quality rock mass (RMQ5) needs stronger support than a lower quality rock mass (RMQ1). Again, conventional (or traditional) empirical design concepts for ground support drawn from underground mining and tunneling may not apply to the thermal stress-controlled problems at the proposed YM repository. Consequently numerical/analytical design approaches should be used.

Figures 4-1 through 4-3 also show that following drift excavation forces in support elements are greater along rock bolts located near spring-lines (bolts numbered 1–3 and 10–12) and relatively smaller along those located in the roof area (bolts numbered 5–8). This result is consistent with the earlier observation that, following drift excavation, fracture shear displacements mainly occur along subvertical fractures that bound the sidewall of the emplacement drift (section 3.1.1.2). Such deformation and, consequently, load on rock bolts are controlled by factors that exist prior to thermal load. As thermal stresses increase, however, loads acting on rock bolts located in the roof area become greater and eventually exceed those acting on rock bolts near the spring-line area. This result is consistent with increasing fracture shear displacement along subhorizontal fractures in the roof and floor areas under thermal load, as discussed in section 3.1.1.2. These support element loads and deformations, therefore, are controlled by thermal stresses.

4.1.1.2 Steel Sets

Figure 4-6 compares axial forces on steel sets after drift excavation and after 150 yr of thermal load for RMQ5 and RMQ1 rock masses for Pattern E. Similar to observations made on rock bolts, thermal load increases axial force significantly in a high quality rock mass and, to a lesser degree, in a low quality rock mass. Thermal load increases axial force acting on steel sets (relative to postmining forces) by one order of magnitude in a high quality rock mass and doubles axial force in a lower quality rock mass (compare plots d with b in figure 4-6). Also, the increase in axial forces resulting from thermal load is more significant in the roof and floor areas in both high and low quality rock masses. Similarly, thermal load increases shear force and moment along steel sets significantly (a few orders of magnitude in a higher quality rock mass and a few times in a lower quality rock mass, figures 4-7 and 4-8). Thermal load also increases normal and shear force along rock mass/steel sets interfaces (figures 4-9 and 4-10).

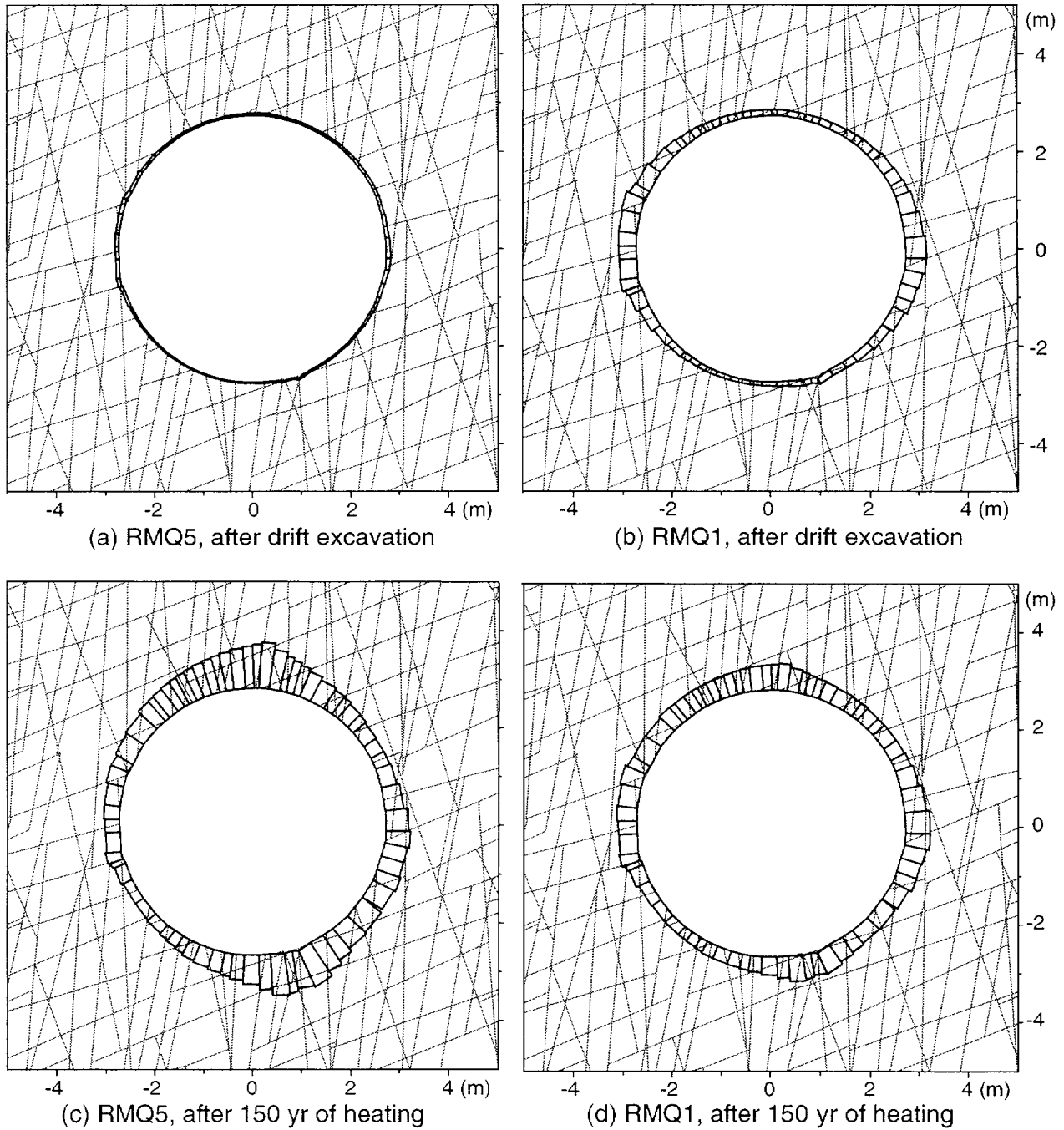


Figure 4-6. Comparison of axial force on steel sets for Pattern E: (a) RMQ5 after excavation, (b) RMQ1 after excavation, (c) RMQ5 after 150 yr of thermal load, and (d) RMQ1 after 150 yrs of thermal load

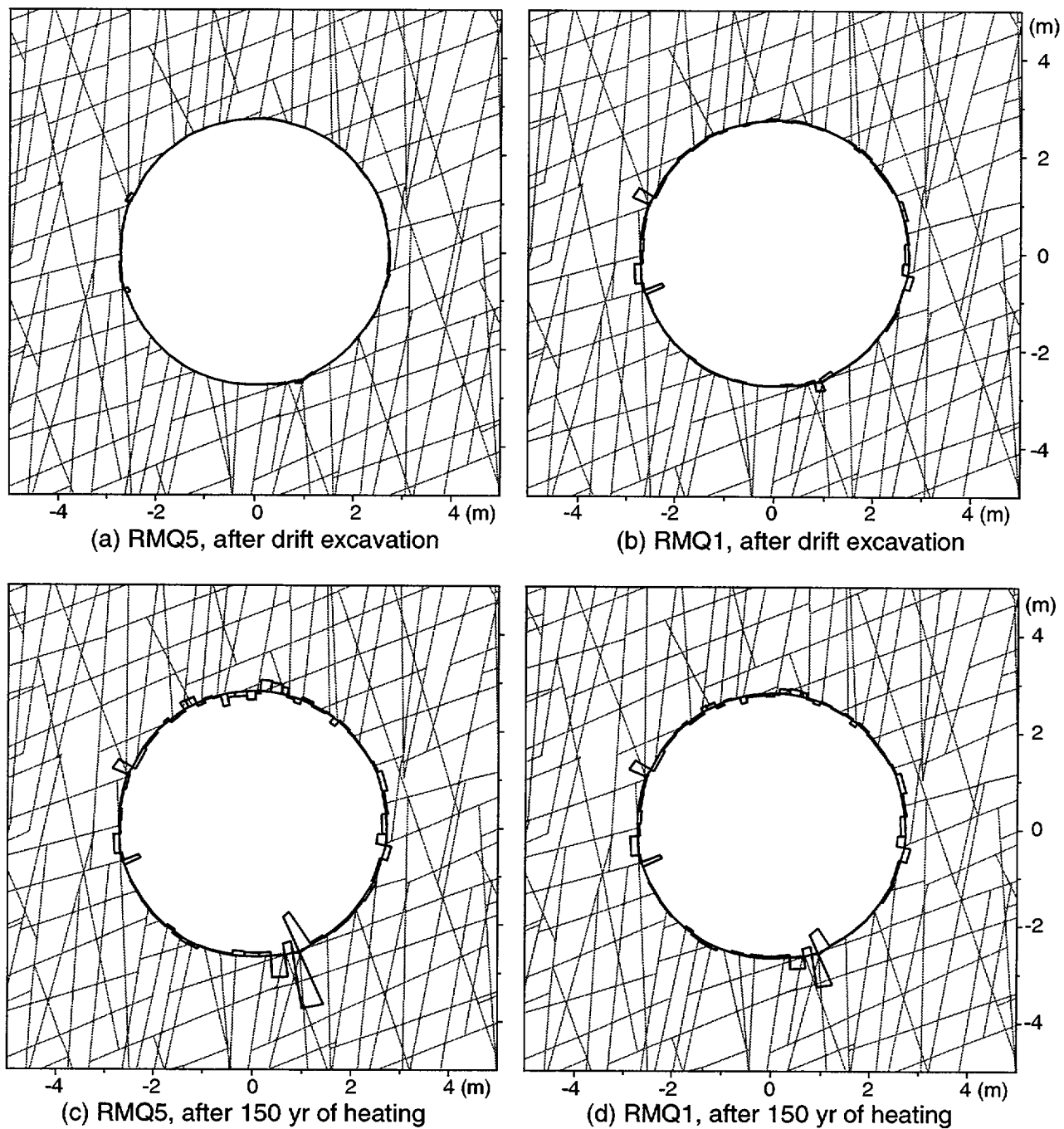
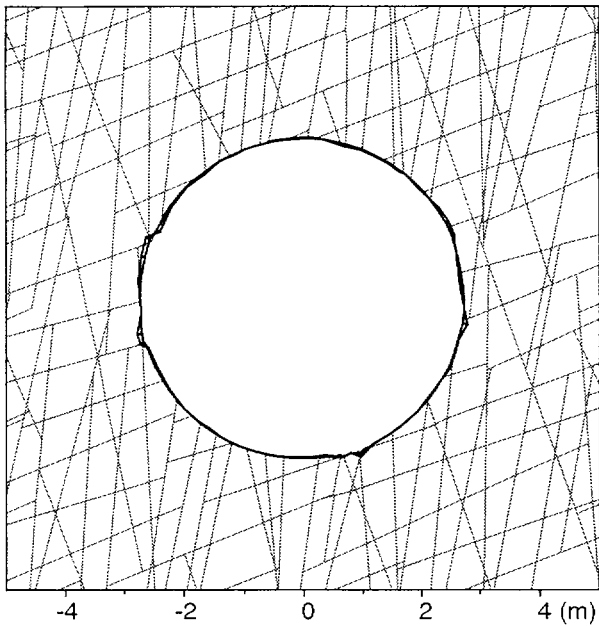
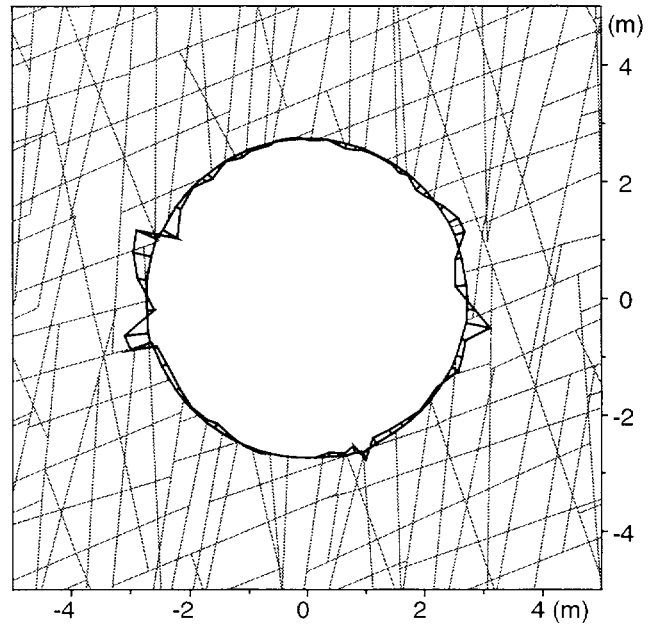


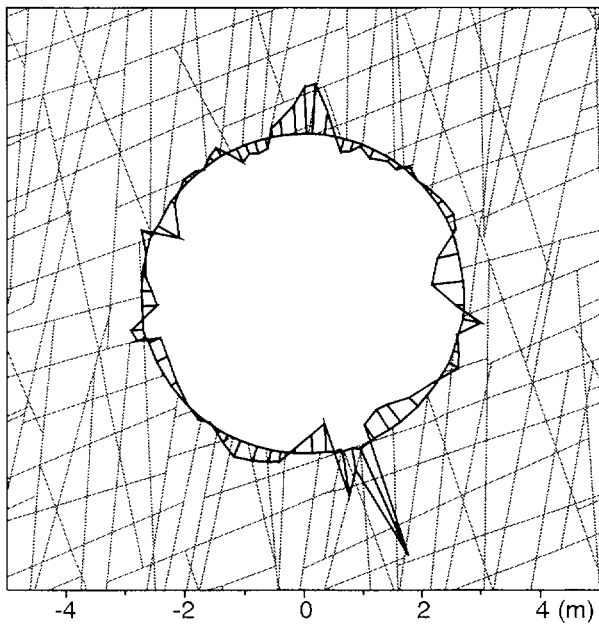
Figure 4-7. Comparison of shear force on steel sets for Pattern E: (a) RMQ5 after excavation, (b) RMQ1 after excavation, (c) RMQ5 after 150 yr of thermal load, and (d) RMQ1 after 150 yr of thermal load



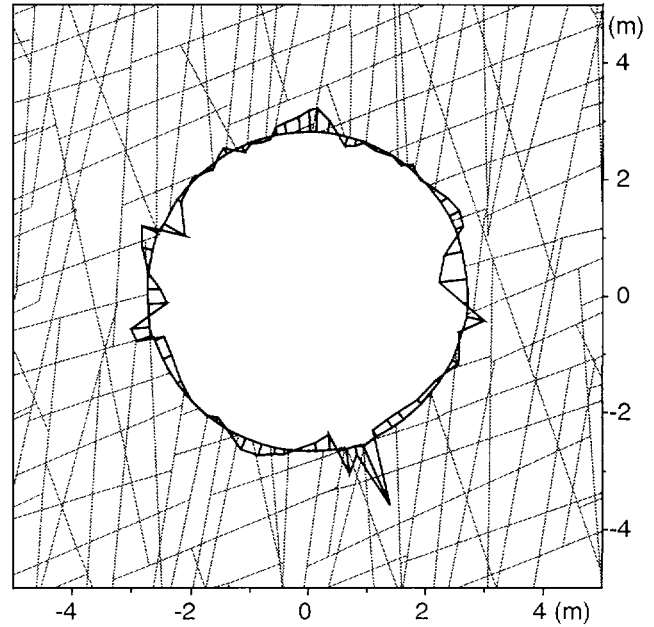
(a) RMQ5, after drift excavation



(b) RMQ1, after drift excavation



(c) RMQ5, after 150 yr of heating



(d) RMQ1, after 150 yr of heating

Figure 4-8. Comparison of moment in steel sets for Pattern E: (a) RMQ5 after excavation, (b) RMQ1 after excavation, (c) RMQ5 after 150 yr of thermal load, and (d) RMQ1 after 150 yr of thermal load

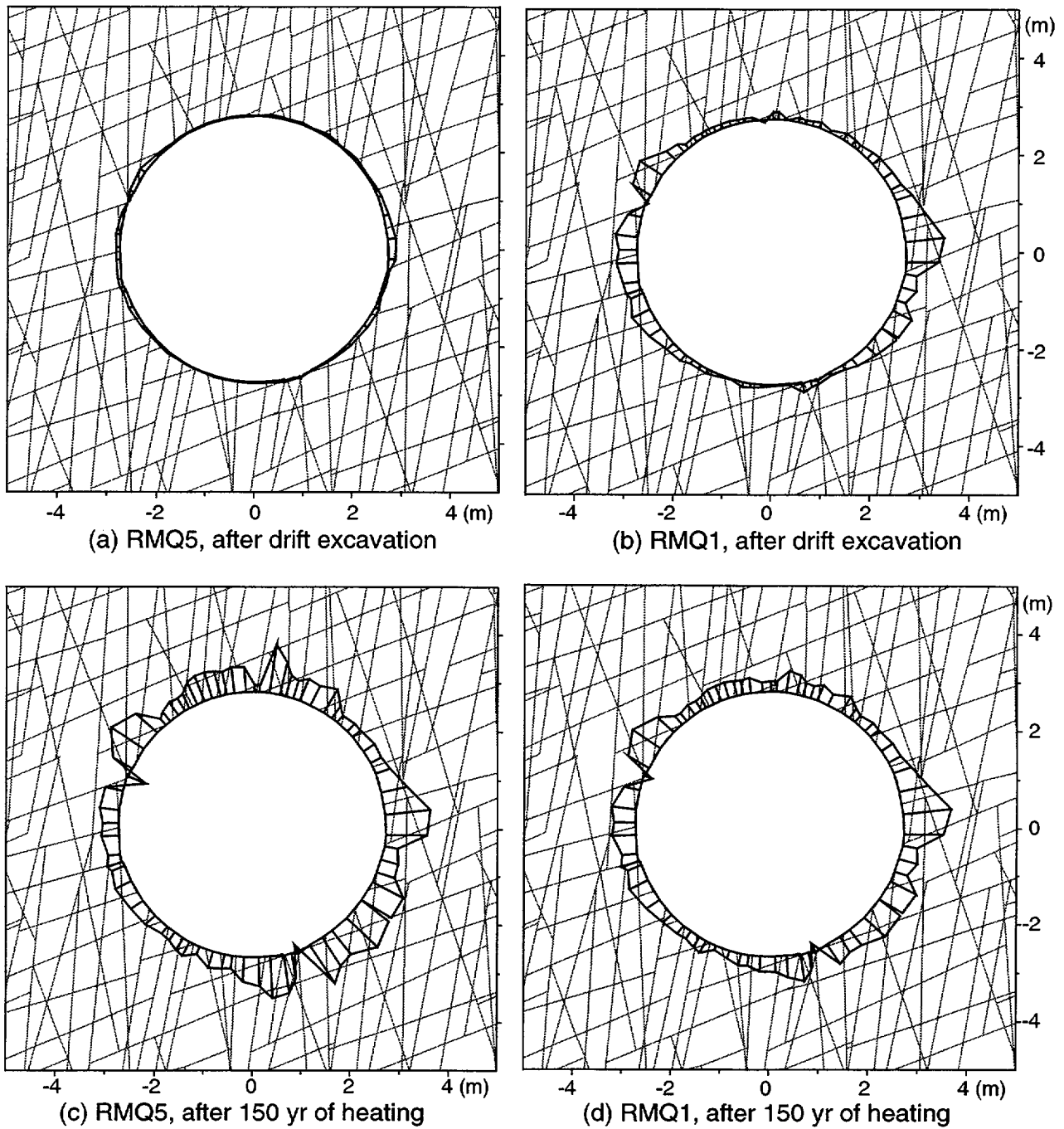


Figure 4-9. Comparison of axial force along rock mass/steel sets interface for Pattern E: (a) RMQ5 after excavation, (b) RMQ1 after excavation, (c) RMQ5 after 150 yr of thermal load, and (d) RMQ1 after 150 yr of thermal load

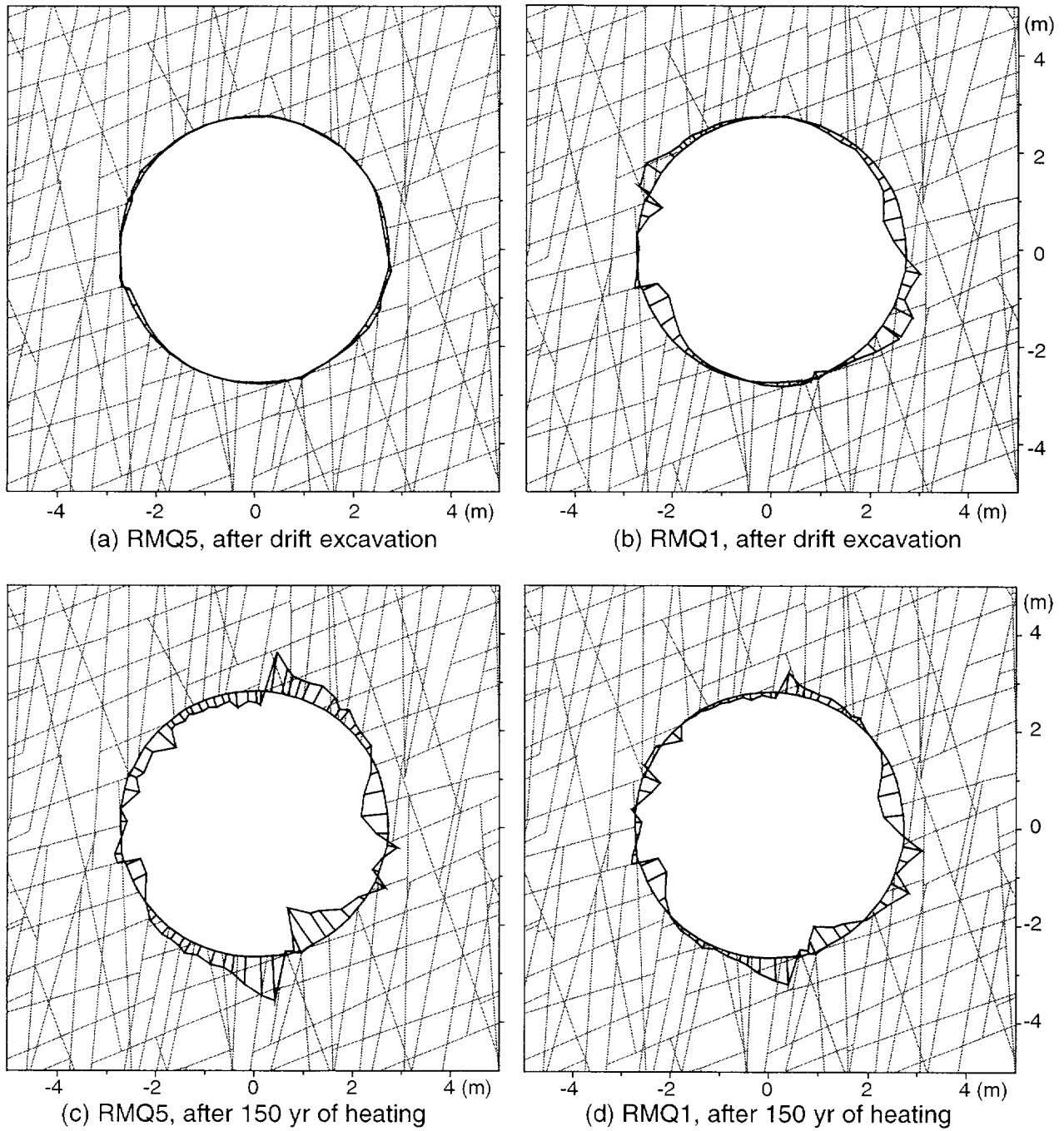


Figure 4-10. Comparison of shear force on steel sets for Pattern E: (a) RMQ5 after excavation, (b) RMQ1 after excavation, (c) RMQ5 after 150 yr of thermal load, and (d) RMQ1 after 150 yr of thermal load

After drift excavation, loads acting on steel sets are greater in an RMQ1 rock mass than in an RMQ5 rock mass (compare the first and second plots in figures 4-6 through 4-10). Greater loads acting on steel sets in an RMQ1 rock mass indicate that a lower quality rock mass needs stronger ground support, which is consistent with the observation from traditional mining and tunneling. The credibility of this traditional approach, however, was questioned earlier in sections 3.1.1.2 based on observations of rock mass deformation around a unsupported drift under thermal load and in section 4.1.1.1 on modeling of rock bolt performance. Figures 4-6 through 4-10 show that after 150 yr of thermal loading loads acting by the surrounding rock mass on steel sets and rock mass/steel sets interfaces are greater in an RMQ5 rock mass than in an RMQ1 rock mass (compare the third and fourth plots in figures 4-6 through 4-10). These figures, once again, demonstrate that, under thermal load, a higher quality rock mass (RMQ5) needs stronger support than a lower quality rock mass (RMQ1), and that conventional (or traditional) empirical design concepts for ground support draw from underground mining and tunneling may not apply to the thermal stress-controlled problems at the proposed YM repository.

4.1.1.3 Effectiveness of Rock Bolts and Steel Sets

Both rock bolts and steel sets are effective tools in controlling rockfall. They are rock mass reinforcement tools. Rock bolts reduce fracture shear displacement where bolts pass through the fractures. Steel sets control drift convergence and rockfall. Neither rock bolts nor steel sets reduce the extent of the yield zone or the distribution of fracture shear displacement beyond the reinforced region around the drift.

4.1.2 EFFECT OF FRACTURE PATTERN

As can be observed in figures 4-1 through 4-3, the locations of peak magnitudes of load acting on rock bolts are controlled by intersecting fractures. In general, the complexity of load distribution along a rock bolt increases as the number of intersecting fractures increases. In other words, loads acting on a rock bolt become increasingly nonuniform as the number of intersecting fractures increases. Loads acting along rock bolts 3, 6, 7, and 10 are compared for the three fracture patterns analyzed in this study in figures 4-11 through 4-13. These figures show that in most cases load and deformation on rock bolts are greater and more irregular in more complicated fracture patterns (Patterns E and F) than in a simpler fracture pattern (Pattern C). The irregularity of load and strain distributions is reflected by the number of peaks on the curves in those figures.

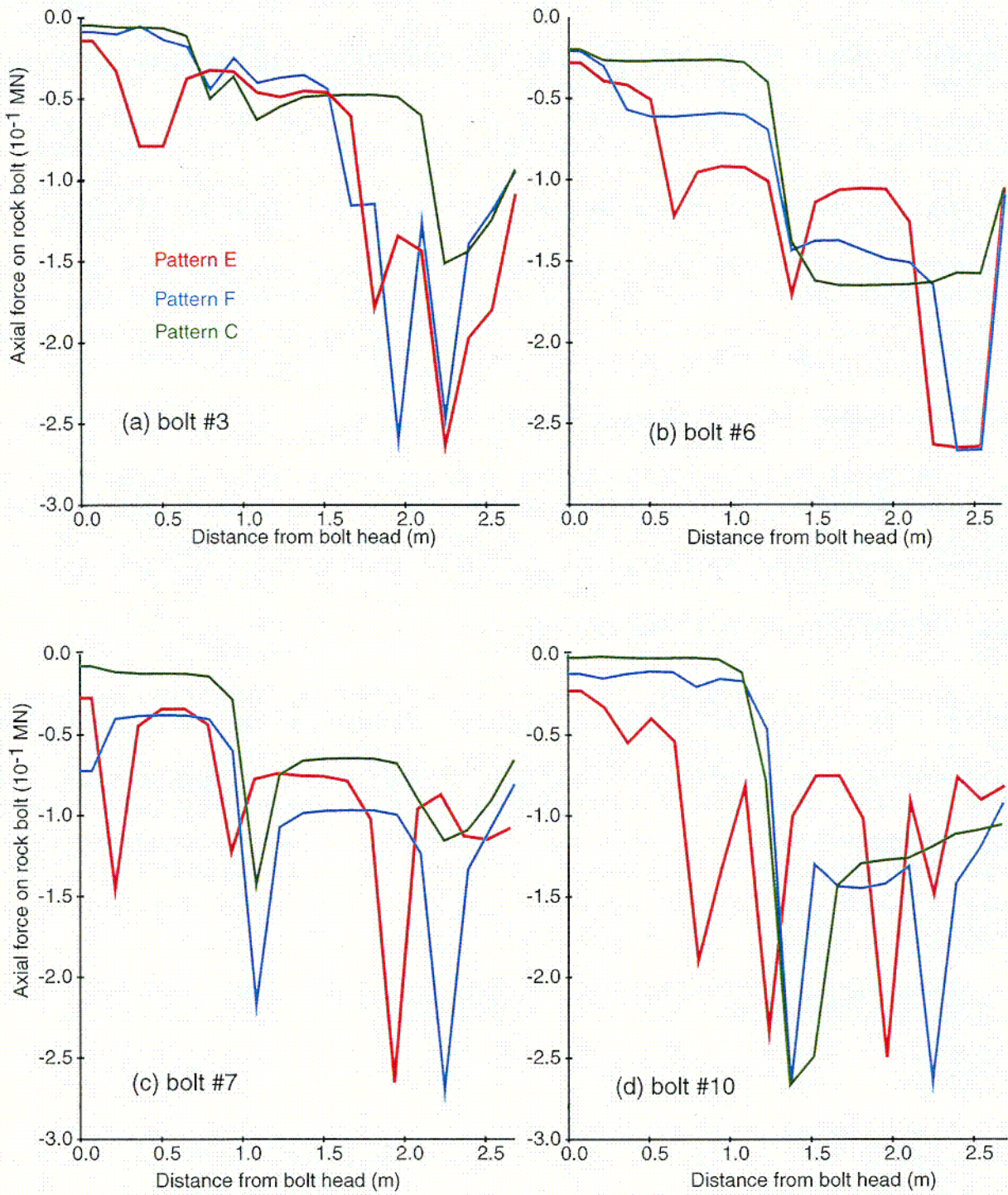


Figure 4-11. Effect of fracture pattern on axial force acting on rock bolts after 150 yr of thermal load in a RMQ5 rock mass. See figure 4-1a for locations of these bolts

C01

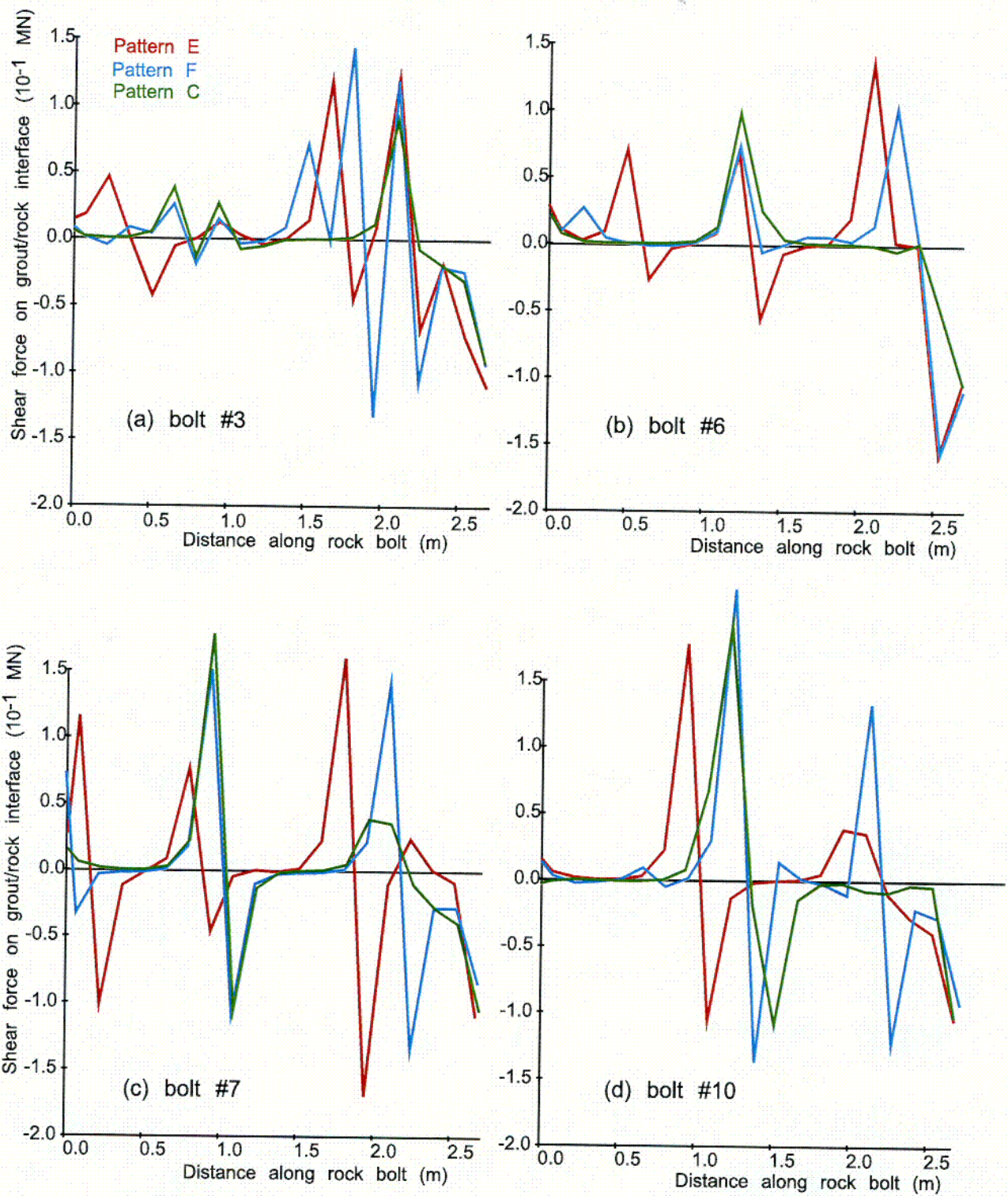


Figure 4-12. Effect of fracture pattern on shear force on grout/rock interface after 150 yr of thermal load in an RMQ5 rock mass. See figure 4-1a for locations of these bolts

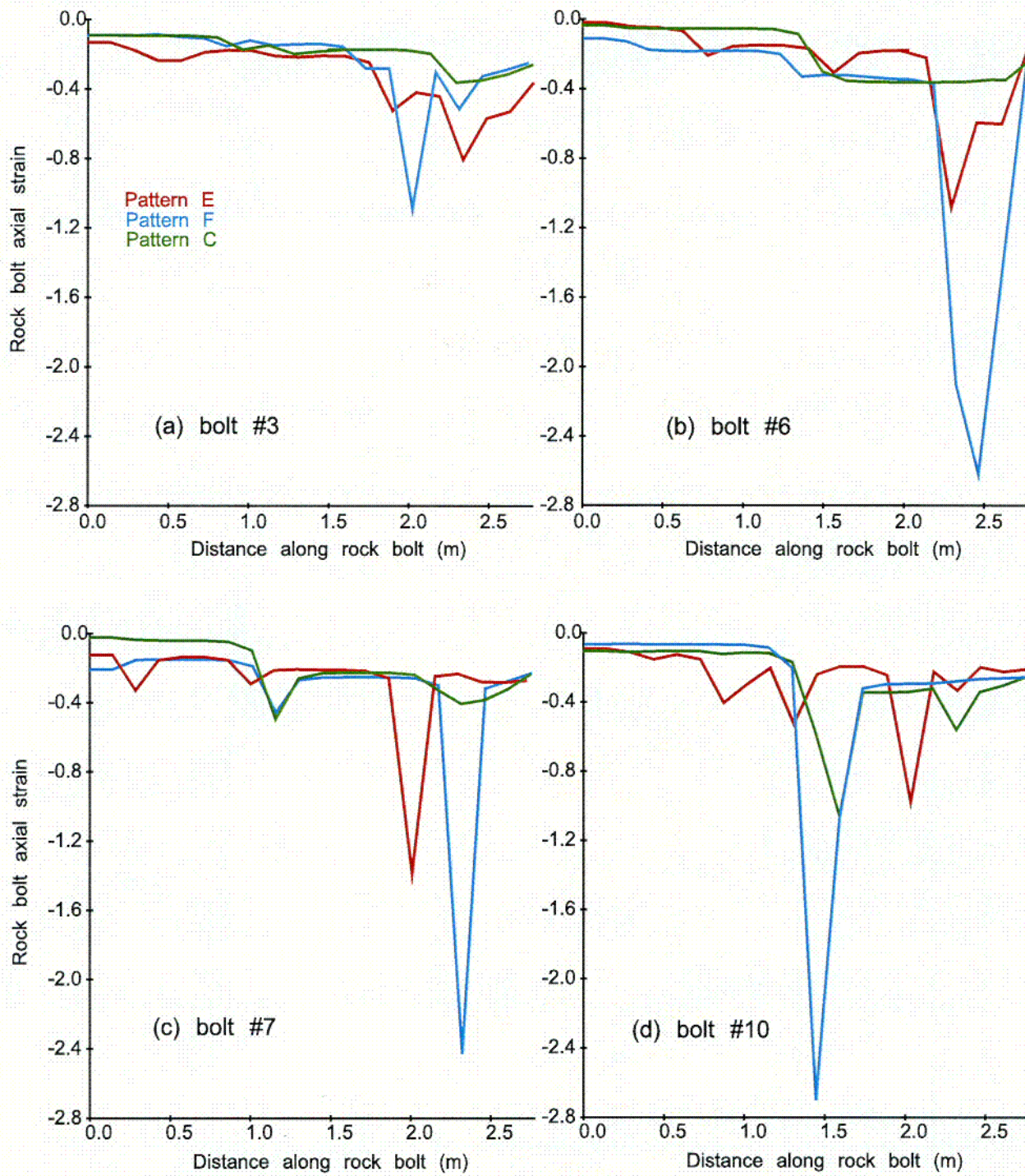


Figure 4-13. Effect of fracture pattern on axial strain on rock bolt after 150 yr of thermal load in an RMQ5 rock mass. See figure 4-1a for locations of these bolts

4.2 GROUND SUPPORT PERFORMANCE UNDER DYNAMIC LOAD

In general, the performance of ground support, measured by loads acting on the support element and support failure, does not appear to be affected by high frequency seismic ground motion (≥ 10 Hz) in either RMQ5 or RMQ1 rock masses. For lower frequency motion (e.g., less than approximately 5 Hz), the performance of ground support is affected to various degrees, depending largely on the frequency. It is, however, unclear how much of the apparent frequency dependence is due to modeling artifacts. Further analyses are needed, preferably using more than one software, more than one form of input ground motion time history (e.g., input directly as ground motion acceleration and velocity), and time-domain analyses supplemented by frequency-domain analyses.

Details of ground support performance under dynamic loading are discussed in the following sections. The potential effects of input ground motion frequency and associated modeling artifacts are emphasized. The potential effects of ground motion amplitude, duration, repeated ground motion events, and input wave form are also discussed. An irregular fracture pattern is used in these discussions instead of a regular fracture pattern because an irregular fracture pattern is more vulnerable to dynamic load than a regular fracture pattern, as discussed in section 3.2. In other words, an emplacement drift in an irregular fracture pattern is less stable than in a regular fracture pattern when subjected to the same ground motion.

4.2.1 Effect of Input Ground Motion Frequency

The effect of input ground motion frequency was studied using frequencies of 10, 5, and 1 Hz on an irregular fracture pattern (Pattern E, table 2-3) for both RQM5 and RMQ1 rock masses. The basecase wave form was used (i.e., a cosine wave with equivalent peak ground acceleration of 0.4 g, as discussed in section 2.3.3) in these analyses.

Figures 4-14 through 4-19 compare the effects of different frequency seismic ground motions on rock bolt performance measured by rock bolt axial force, shear force, and axial strain. Similar effects are seen in axial failure and shear failure as consequences. Rock bolt axial force, shear force, and axial strain after subjecting to 10-Hz seismic ground motion are almost identical to those without seismic ground motion (compare figures 4-1c, 4-2c, and 4-3c with 4-14a, 4-15a, and 4-16a; and compare figures 4-1d, 4-2d, and 4-3d with 4-17a, 4-18a, and 4-19a). A 5-Hz ground motion shows some effects on the distribution and magnitude of axial and shear forces along rock bolts located in the roof area (e.g., bolts 7–9) in an RMQ5 rock mass (compare plots a with b in figures 4-14 through 4-16). The effects are insignificant in an RMQ1 rock mass (figures 4-17 through 4-19). Interestingly, the 1-Hz ground motion shows significant effects on the distribution and magnitude of rock bolt axial force, shear force, and axial strain in an RMQ5 rock mass (compare plots c with a and b in figures 4-14 through 4-16). The thermal load increases axial strain by more than five times in some rock bolts (e.g., bolts located on the right hand side of the drift, figure 4-16c). This pronounced effect is accompanied by extensive failure of rock bolts and severe deformation of the drift and surrounding rock mass (see plots c in figures 4-14 through 4-16). The effect is less significant in an RMQ1 rock mass (see figures 4-17 through 4-19).

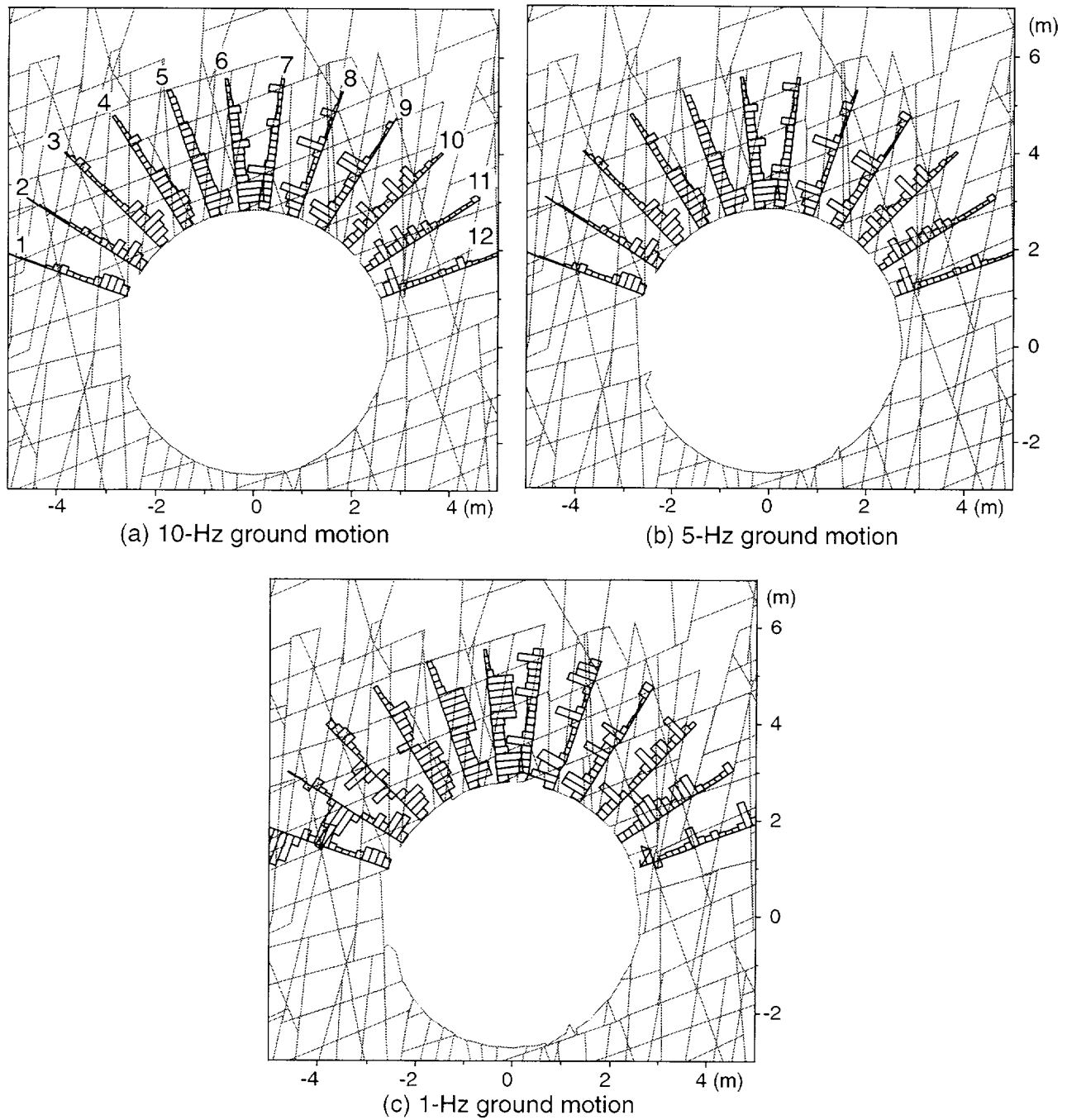


Figure 4-14. Axial force in rock bolts after 150 yr of thermal load and a ground motion event with various input frequencies for Pattern E in an RMQ5 rock mass: (a) 10-Hz ground motion, (b) 5-Hz ground motion, and (c) 1-Hz ground motion

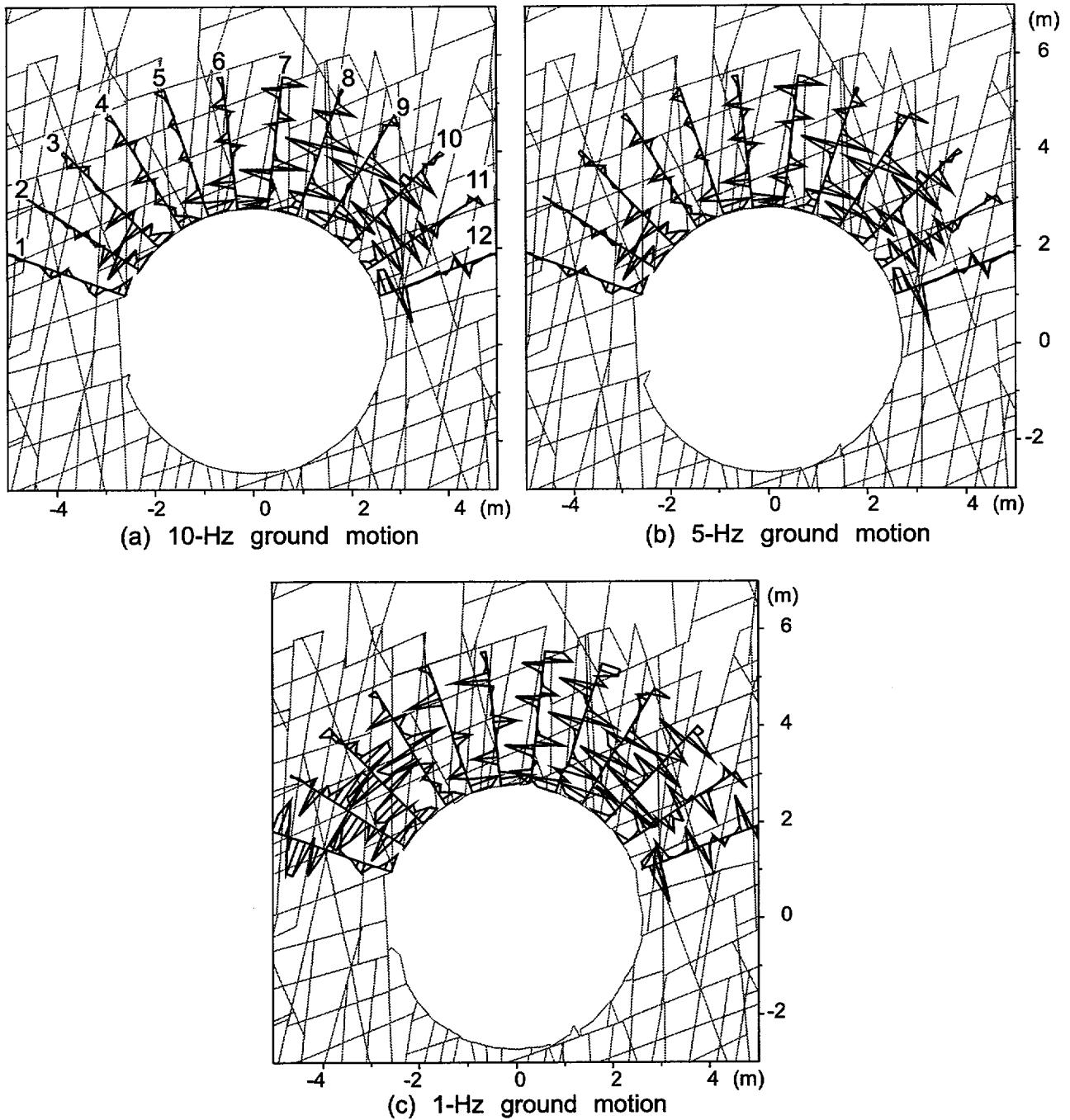


Figure 4-15. Shear force on grout/rock interface after 150 yr of thermal load and a ground motion event with various input frequencies for Pattern E in an RMQ5 rock mass: (a) 10-Hz ground motion, (b) 5-Hz ground motion, and (c) 1-Hz ground motion

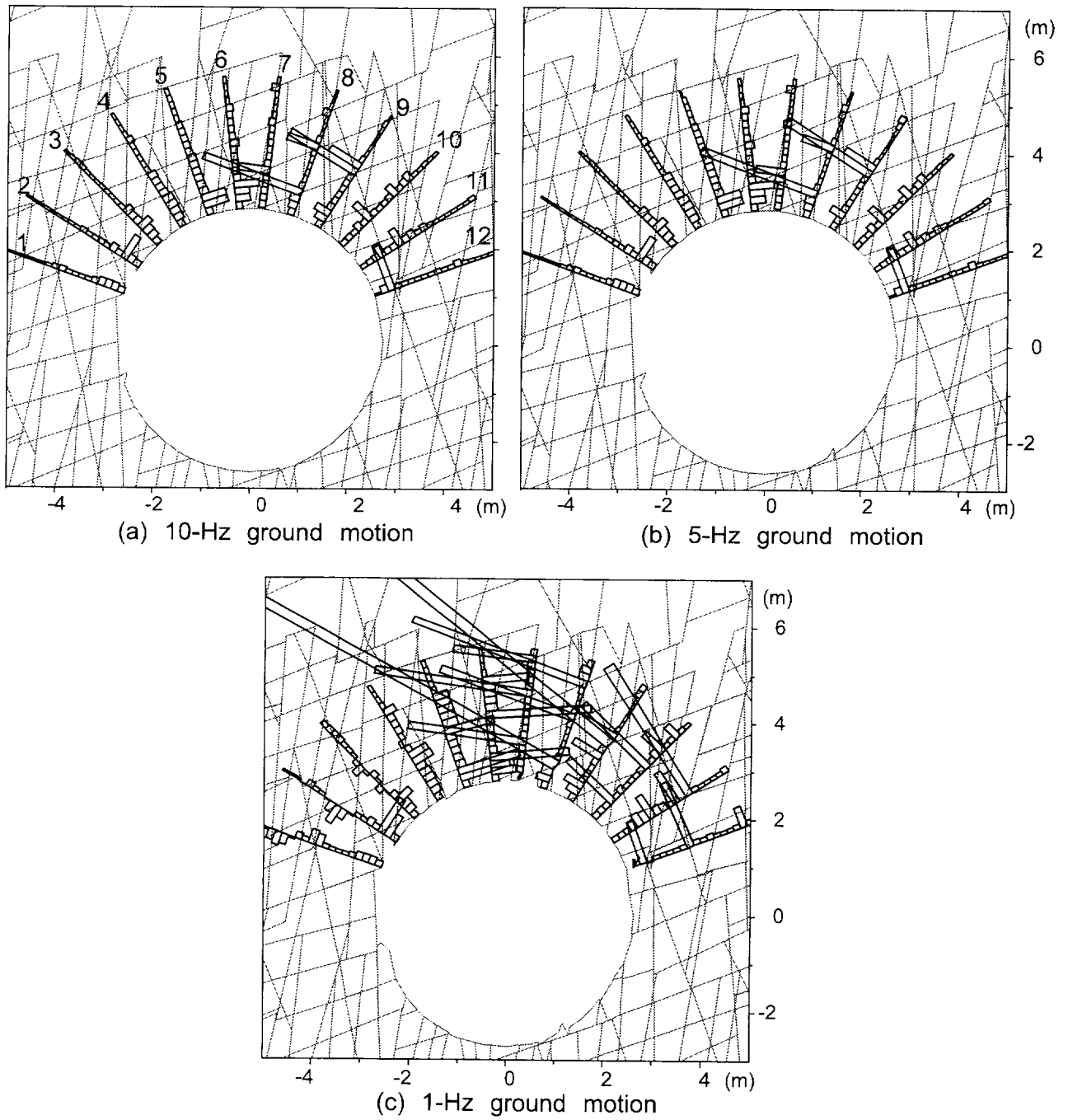


Figure 4-16. Rock bolt axial strain after 150 yr of thermal load and a ground motion event with various input frequencies for Pattern E in an RMQ5 rock mass. a. 10-Hz ground motion, (b) 5-Hz ground motion, and (c) 1-Hz ground motion

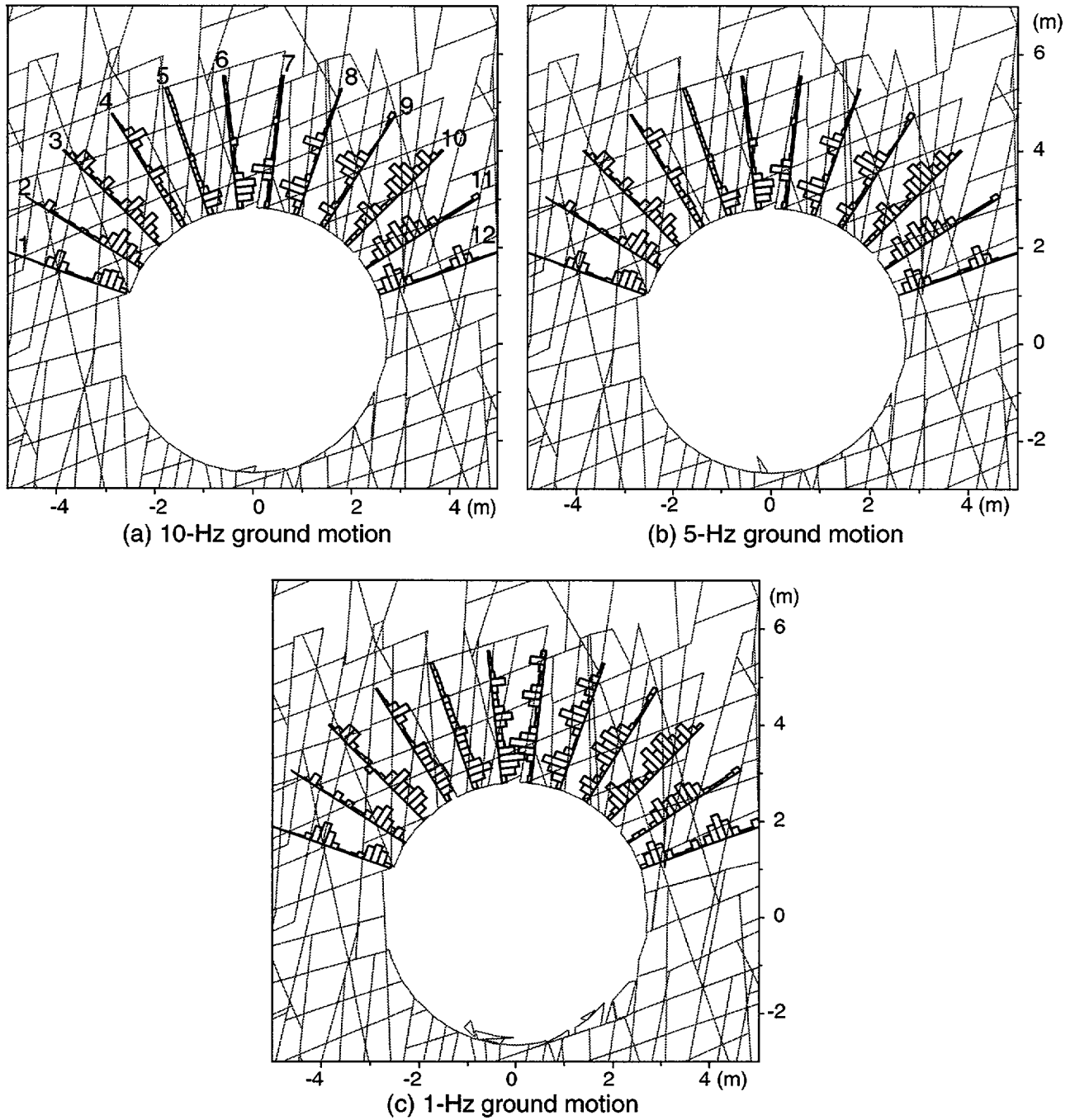


Figure 4-17. Axial force in rock bolts after 150 yr of thermal load and a ground motion event with various input frequencies for Pattern E in an RMQ1 rock mass: (a) 10-Hz ground motion, (b) 5-Hz ground motion, and (c) 1-Hz ground motion

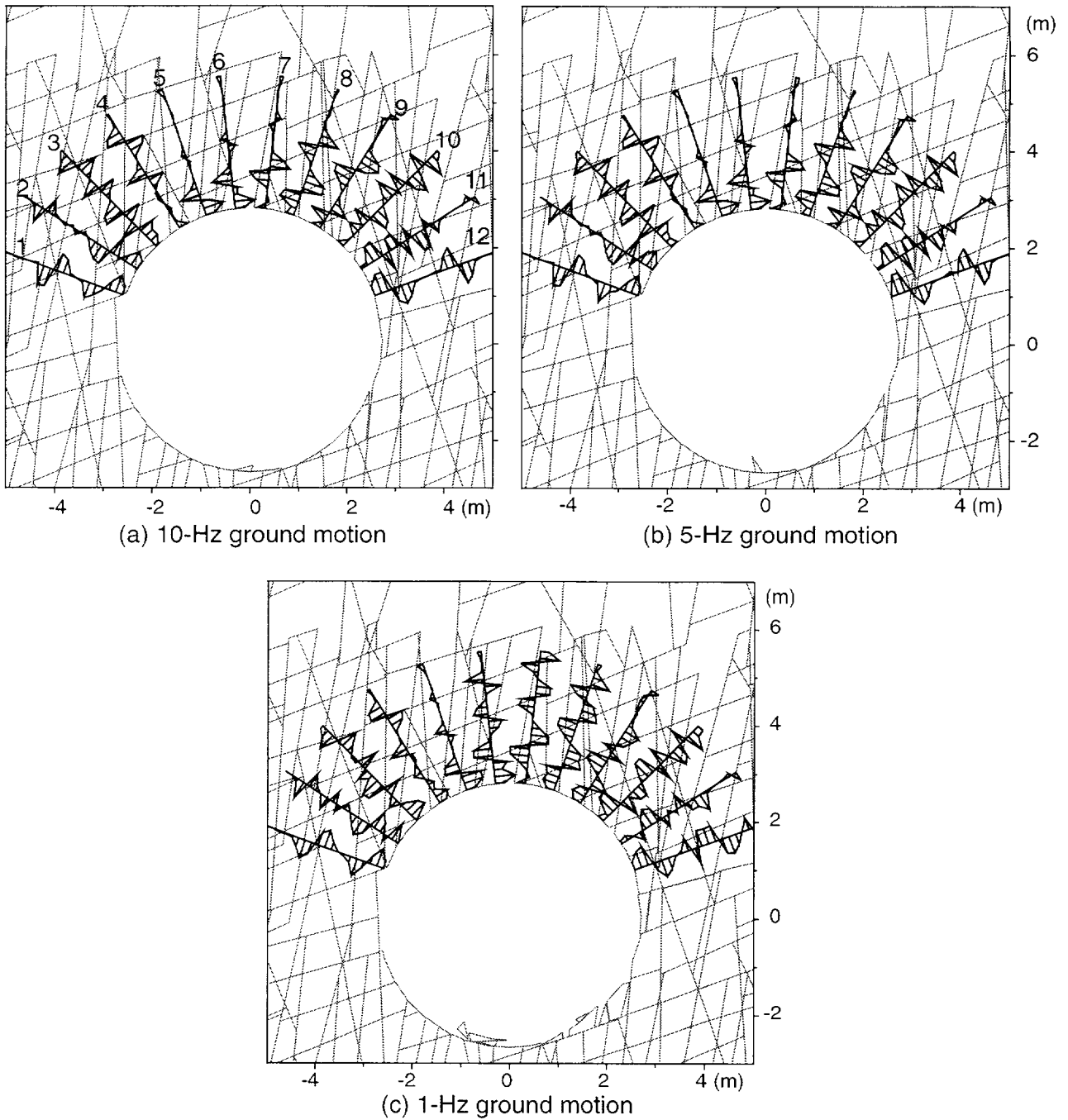


Figure 4-18. Shear force on grout/rock interface after 150 yr of thermal load and a ground motion event with various input frequencies for Pattern E in an RMQ1 rock mass: (a) 10-Hz ground motion, (b) 5-Hz ground motion, and (c) 1-Hz ground motion

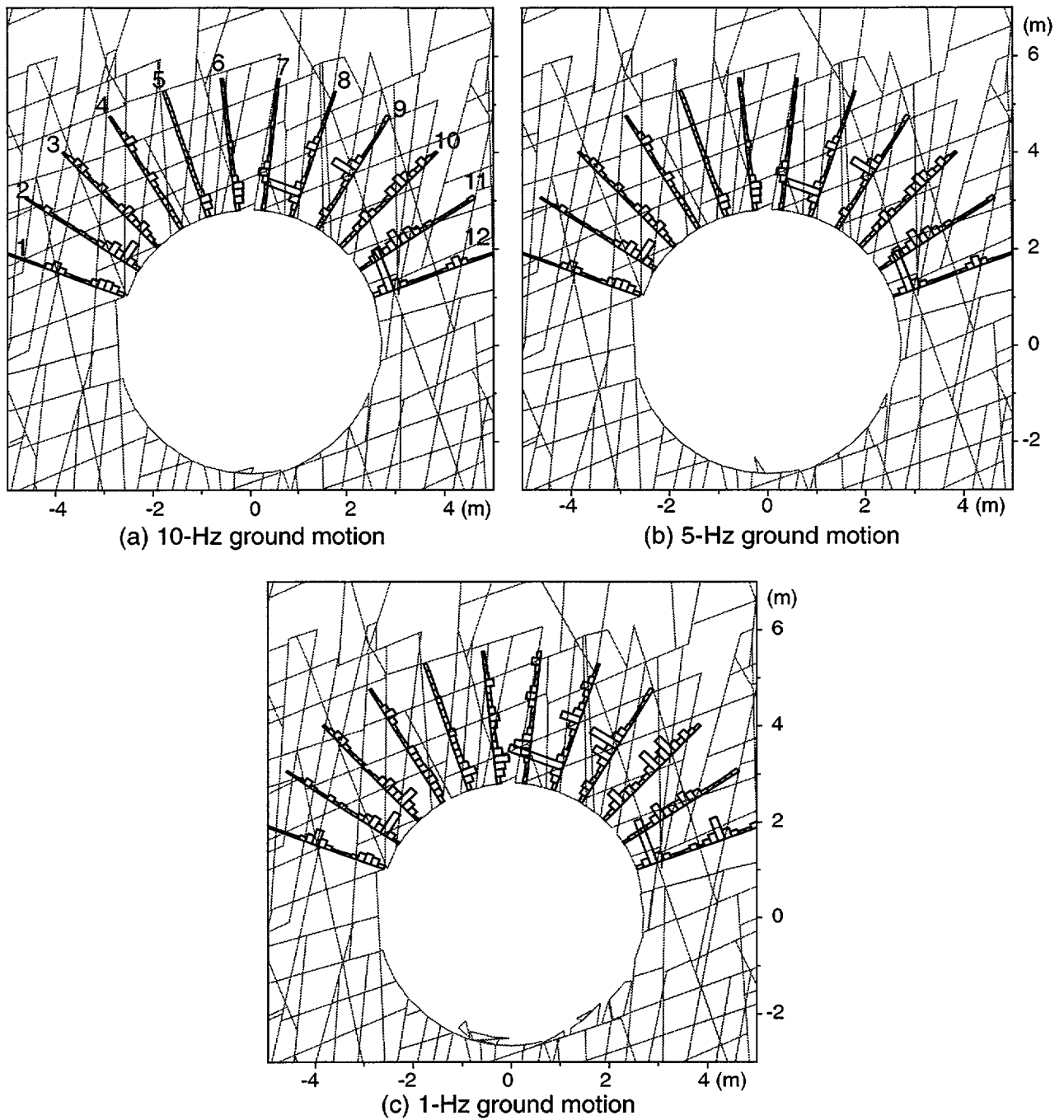


Figure 4-19. Rock bolt axial strain after 150 yr of thermal load and a ground motion event with various input frequencies for Pattern E in an RMQ1 rock mass: (a) 10-Hz ground motion, (b) 5-Hz ground motion, and (c) 1-Hz ground motion

4.2.2 Effect of Ground Motion Amplitude, Duration, and Repeated Ground Motions

The effects of input ground motion amplitude, duration, and repeated ground motions were evaluated using an emplacement drift within an irregular fracture pattern (Pattern E, table 2-3) and an RMQ5 rock mass. The model was subjected to a 5-Hz ground motion, assuming a cosine wave. The variation cases included doubled ground motion amplitude (peak acceleration from 0.4 g to 0.8 g), increased duration of strong motion (simulation time from 1 to 4 s), and repeated ground motions (the model was subjected to a 0.4 g ground motion twice).

Figures 4-20 through 4-22 compare rock bolt axial force, shear force, and axial strain for various cases. Results for the basecase ground motion (i.e., peak ground acceleration of 0.4 g, strong motion duration of 1 s simulation time, and a single ground motion event) are presented in the first plot (plot a) in these figures for comparison. Increasing the amplitude of ground motion from 0.4 g to 0.8 g slightly alters the distribution of load and strain in rock bolts and increases the magnitude of load and strain in rock bolts located in the roof and right spring-line areas (e.g., bolts 7–10, compare plots b with a in figures 4-19 through 4-22). This effect, however, does not introduce additional failure in the ground support and is, overall, not significant when compared to the effect of input ground motion frequency when the frequencies are lower than approximately 5 Hz.

Increasing the duration of strong motion from 1 to 4 s alters the distribution and increases the magnitude of the maximum load and strain in rock bolts located in the roof and near right spring-line area (compare plots c with a in figures 4-19 through 4-22). This effect is more significant than doubling ground motion amplitude and introduces additional bolt axial and grout shear failure in some rock bolts. The effect, however, is less significant than changing the frequency of the input ground motion from 5 Hz to 1 Hz.

A second ground motion event of the same duration, amplitude, and frequency was simulated after bringing the model to equilibrium following the first ground motion event to evaluate the effect of repeated ground motion events. Comparison of plots d with a in figures 4-19 through 4-22 shows that the effect of the second ground motion is insignificant. The only possible exception is near the drift end of bolt 2, where the second ground motion appears to have increased load on one node. It is a localized effect and may actually represent a rock block falling between bolts 1 and 2 after enough cycling in UDEC, not due to the second ground motion event. These observations on the effect of repeated ground motion events are different from the observations of earlier studies based on laboratory and *in situ* testing (Hsiung et al., 1992; 1999; Kana et al., 1995). These earlier studies found that multiple seismic events are likely to increase drift instability and weaken rock masses through accumulation of permanent deformation. The apparent discrepancy could be because the simulation time in UDEC modeling was extremely short and only two repeated ground motion events were examined.

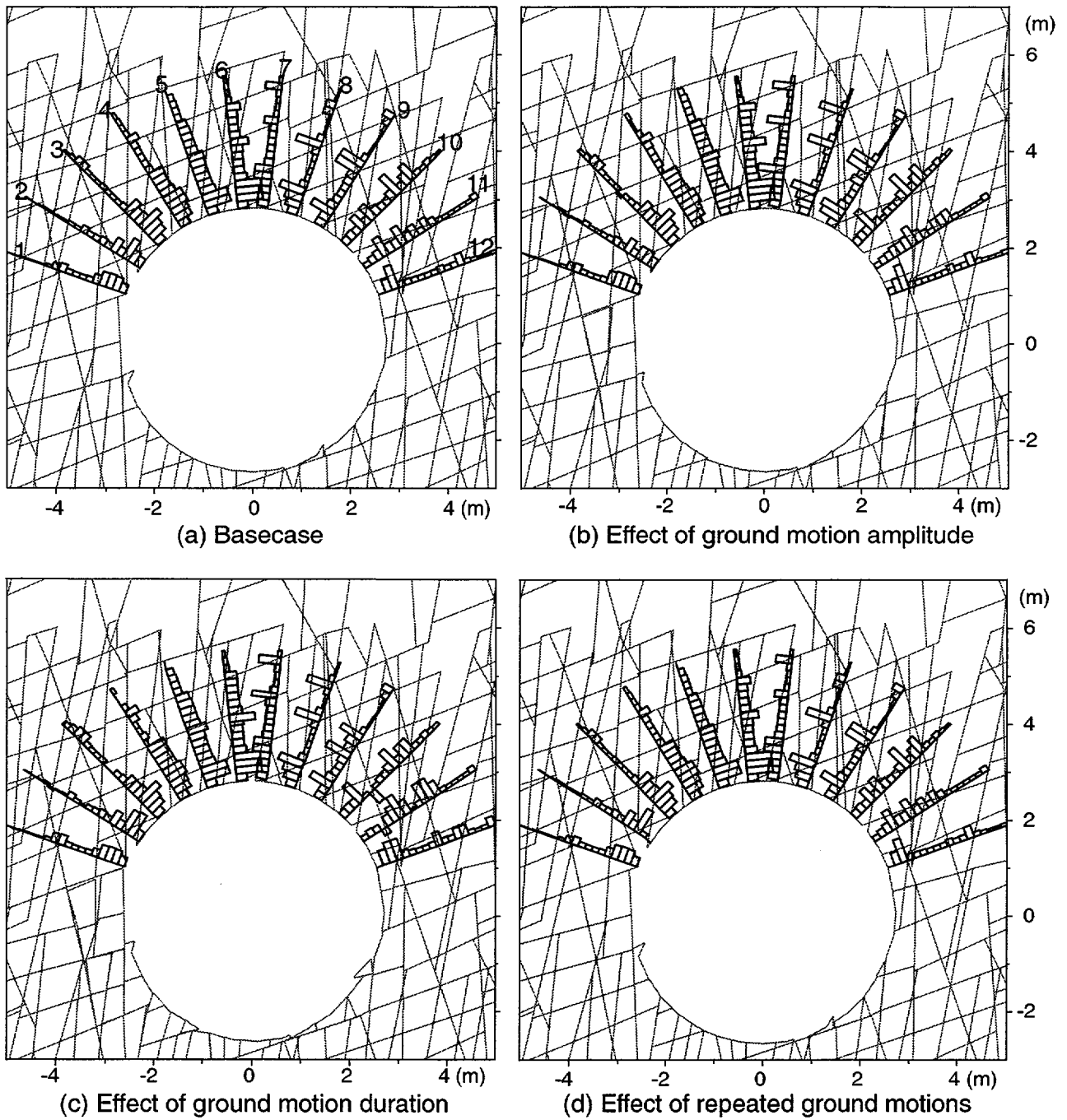


Figure 4-20. Axial force along rock bolts subjected to 150 yr of thermal load and 5-Hz ground motion for Pattern E in an RMQ5 rock mass: (a) Basecase, (b) effect of ground motion amplitude, (c) effect of duration, and (d) effect of repeated ground motions

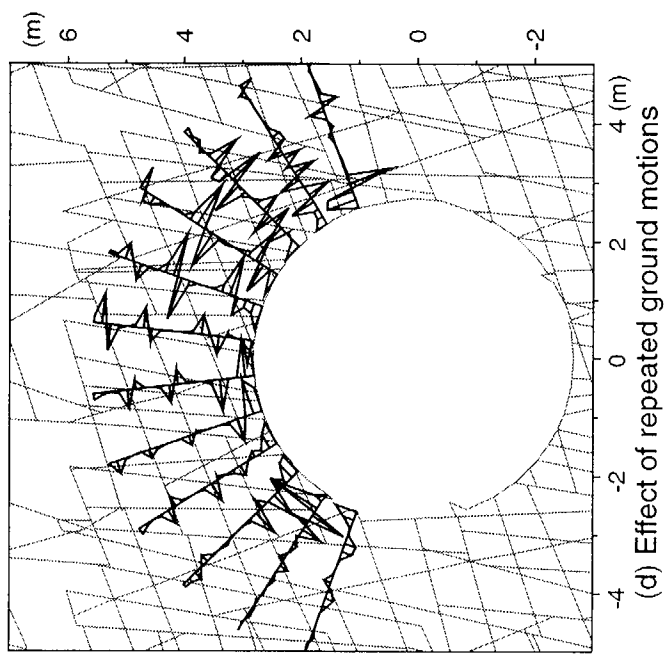
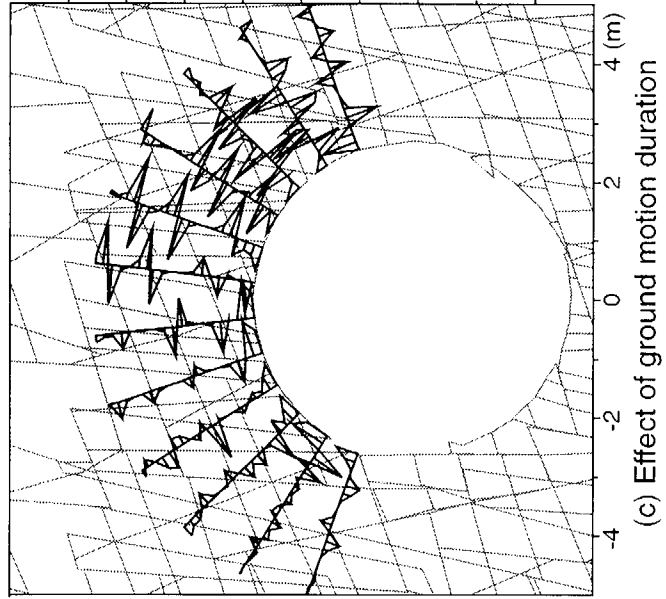
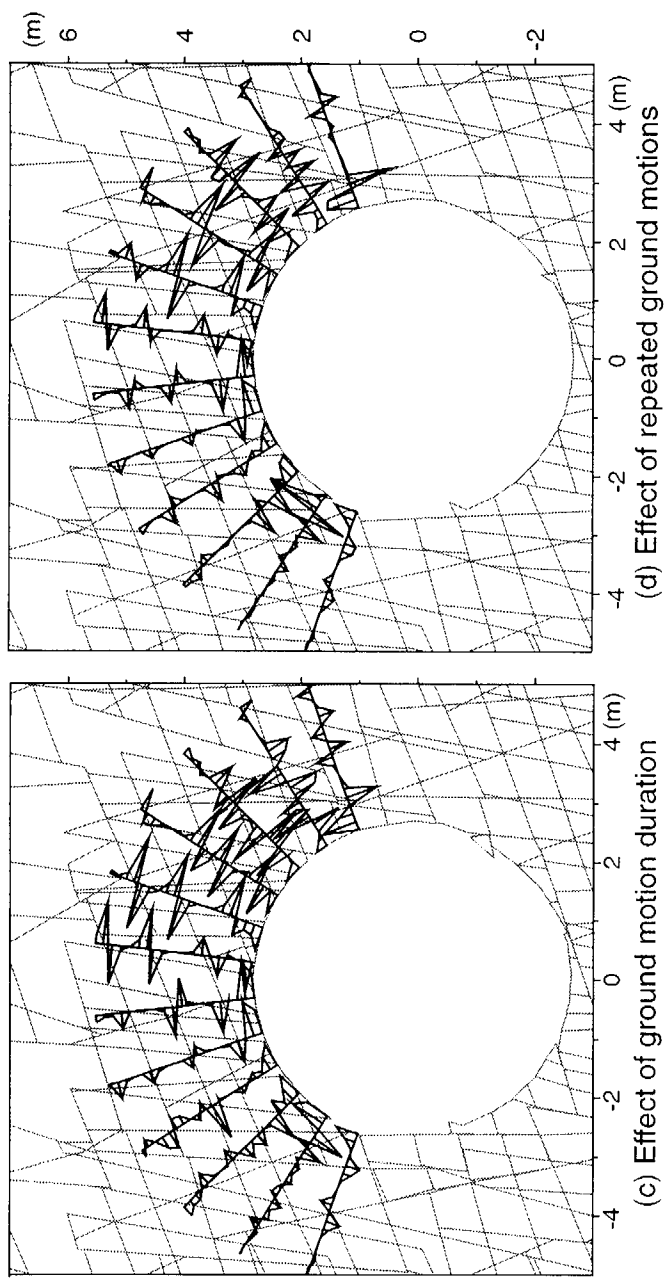
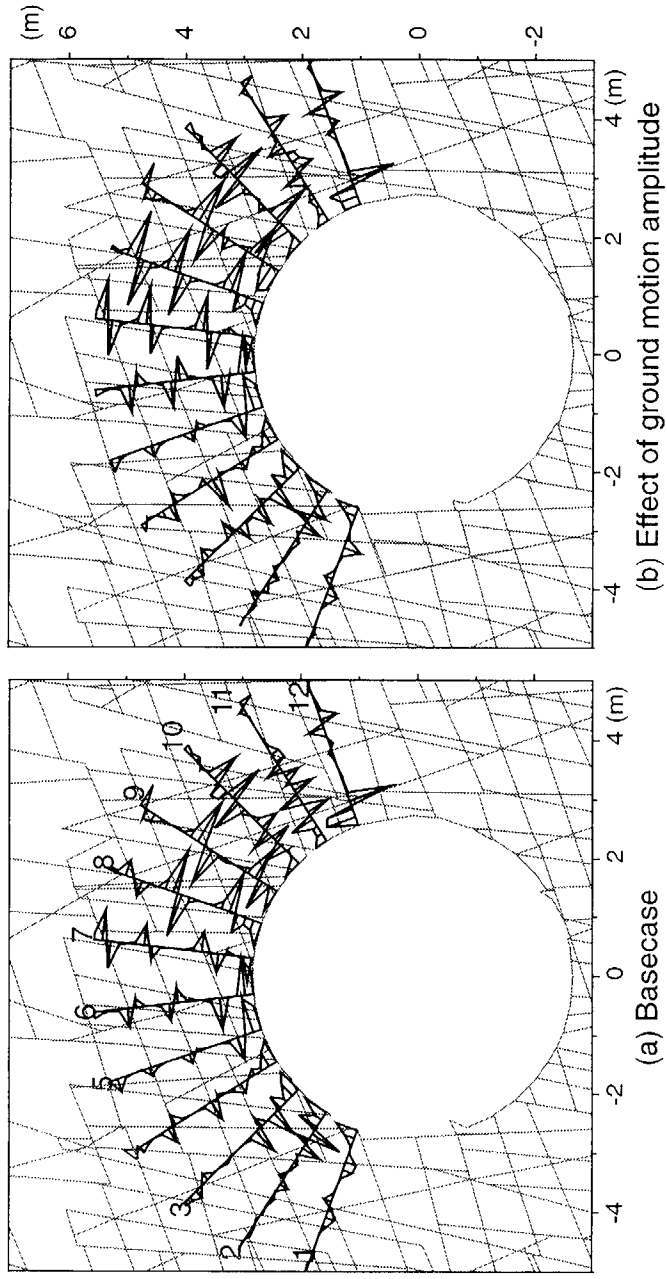


Figure 4-21. Shear force on grout/rock interface after subjecting to 150 yr of thermal load and 5-Hz ground motion for Pattern E in an RMQ5 rock mass: (a) Basecase, (b) effect of ground motion amplitude, (c) effect of duration, and (d) effect of repeated ground motions

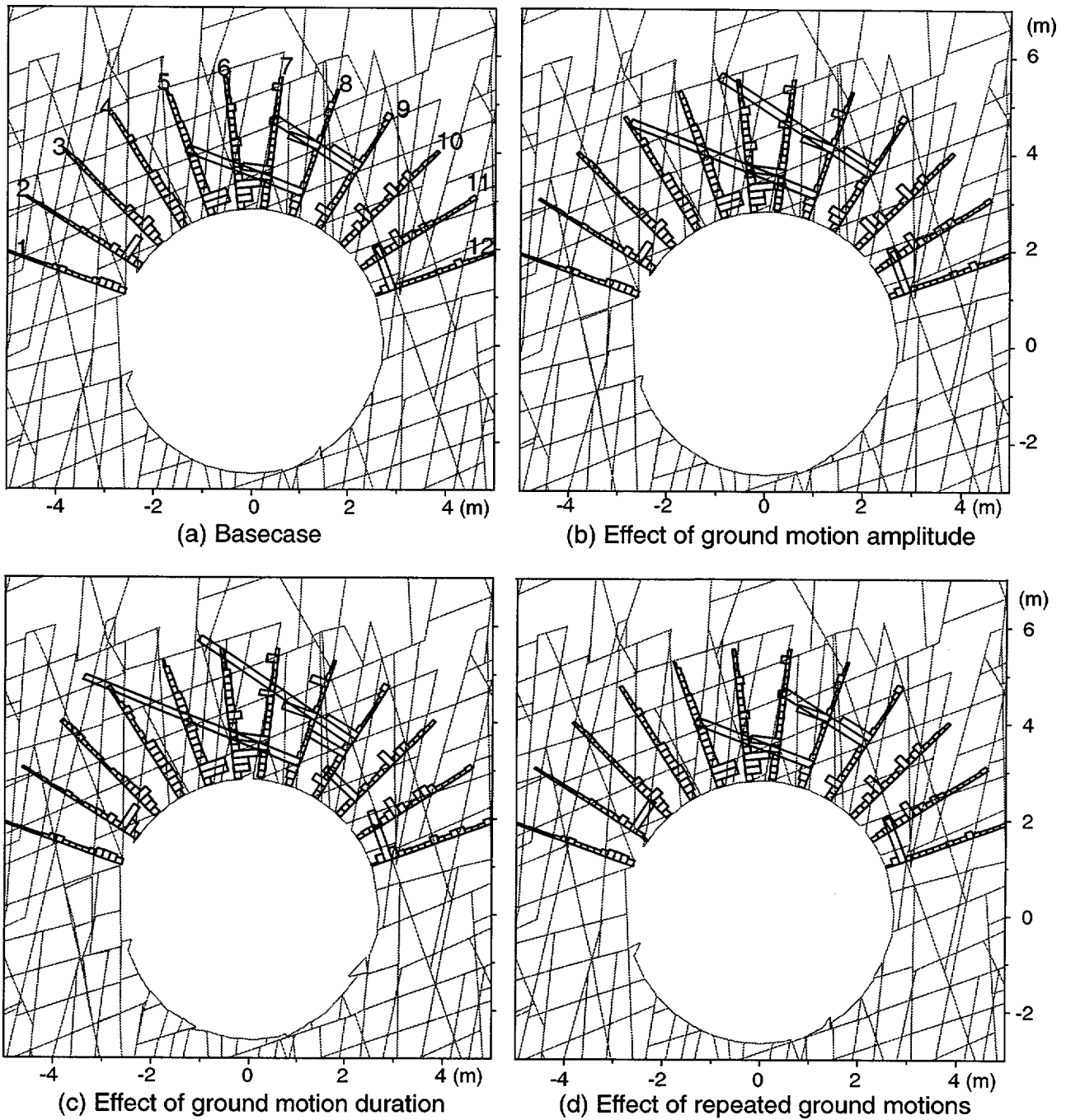


Figure 4-22. Axial strain of rock bolts after subjecting to 150 yr of thermal load and 5-Hz ground motion for Pattern E in an RMQ5 rock mass: (a) Basecase, (b) effect of ground motion amplitude, (c) effect of duration, and (d) effect of repeated ground motions

4.2.3 Effect of Design Ground Motion Time History

An attempt was made to evaluate the effect of design ground motion time history using the preliminary design velocity time histories developed by the DOE as given in figure 2-3. The UDEC model was run for the complete 80 s time history only on simple fracture patterns. For complicated fracture pattern (e.g., Pattern E), only about the first 5 s of the strong motion was completed. After that, the UDEC model encountered problems such as numerical instability, exceeding memory limit, and too small time steps. Modeling results from simple fracture patterns and an RMQ5 rock mass do not show significant effects on either drift stability or ground support performance.

4.2.4 General Discussion on Dynamic Modeling Using Universal Distinct Element Code

Dynamic modeling using UDEC is difficult and, in some cases, impractical because it is time consuming. Preliminary modeling results presented in this report and in previous studies show that dynamic load has various degrees of influence on drift stability and ground support performance. The extent of such effects depends on many factors, including fracture pattern, input ground motion parameters (particularly frequency), and, to a lesser degree, rock mass properties. These effects need to be evaluated in drift stability and ground support design analyses for both preclosure design and postclosure performance evaluation. DOE proposed using UDEC and Fast Lagrangian Analysis of Continua (FLAC) to conduct its seismic design analyses.¹ UDEC and FLAC treat dynamic input in a similar fashion. Based on experience to date, the author of this report is skeptical about the capability of these numerical tools. The problems with UDEC dynamic modeling must be resolved before it can be reliably used for ground support design.

- (i) The form of input ground motion that UDEC accepts is limited to stress history, which is converted from velocity history based on rock mass properties. A stress history may not be appropriate for a highly prestressed model. If input acceleration is to be used rather than velocity, the acceleration needs to be converted to velocity; frequency has a large effect on this conversion. A factor of 10 difference was observed in input stress amplitudes between frequency 1- and 10-Hz ground motions, as indicated in table 2-2. These conversions make it difficult to interpret modeling results and distinguish true frequency effects from modeling artifacts.
- (ii) Drift stability under dynamic load depends largely on simulated fracture pattern. When the fracture patterns are simplified, almost no response can be observed. For more complicated fracture patterns, however, there are problems such as numerical instability. A complicated fracture pattern also increases the size of the problem and often makes it impractical to do sensitivity analyses or to use a time history longer than a few seconds.
- (iii) A time history is only a particular case in a spectrum of ground motions. It may be necessary in ground support design to conduct frequency-domain analyses. UDEC is not currently capable of such analyses.
- (iv) A geological model may respond differently to different forms of dynamic input. The differences in model responses to velocity, stress, or acceleration inputs need to be examined, and UDEC is not currently capable of such examinations.

¹ Presentation: Modeling of TM Behavior. DOE/NRC Appendix 7 meeting on ground control, November 1, 1999. Yiming Sun.

Also, the author of this report is not aware of any other existing numerical tools that are based on a discontinuum modeling approach and could be better suited for dynamic design for the proposed YM repository. A practical solution to the lack of appropriate discontinuum tools may be found by supplementing UDEC analyses with analyses using well established continuum numerical software that has the capability of modeling seismic ground motion in more than one form and in both frequency and time domains.

5 CONCLUSIONS

Results obtained from this study directly contribute to resolution of the preclosure design aspects of the Repository Design and Thermal-Mechanical Effects Key Technical Issue (Nuclear Regulatory Commission, 1999b). Knowledge gained and results from this study have been helpful in developing acceptance criteria and review methods for repository subsurface design in the Yucca Mountain Review Plan¹ (YMRP) and in evaluating the DOE design approaches for subsurface facilities, particularly for ground support.² For example, based on results from this study, an acceptance criterion was developed in YMRP for the design of ground support system that requires the design of ground support be based on appropriate design methodologies and interpretations of modeling results.¹ Fracture displacement results also contribute to evaluating thermal-mechanical effects on rock mass permeability changes (Ofoegbu et al., 2000, in review), which may bear on postclosure repository performance. The following conclusions were reached based on this study.

- Superimposing thermal stresses on excavation-induced stresses significantly alters the stress state in the repository and surrounding areas. Thermal load changes the orientation of the maximum principal stress from approximately vertical to approximately horizontal near the repository horizon and shifts the location of the concentration of maximum principal stress from the drift sidewalls to the roof and floor areas.
- Thermally induced deformation is greater in a higher quality rock mass than in a lower quality rock mass based on observations of drift closure, the distribution and magnitude of fracture shear displacement, and the extent of rock block yield. This observation contradicts the common understanding that a lower quality rock mass would experience greater deformation than a higher quality rock mass under the same loading conditions. This common understanding, however, is based on experiences and observations from underground tunneling and mining under ambient conditions rather than heated conditions.
- Fracture shear displacement following drift excavation is mainly along subvertical fractures and is limited to those subvertical fractures that bound the sidewalls of the emplacement drift. Such deformation is controlled by factors such as existing fractures, depth of the drift, drift geometry and dimension, and density of overburden rocks. It is a structure-controlled phenomenon and the deformation is greater in a lower quality rock mass than in a higher quality rock mass.
- Fracture shear displacement induced by thermal load is mainly along subhorizontal fractures and occurs in the roof and floor areas. Such deformation is controlled by high thermal stresses and is much greater in a higher quality rock mass. It is a stress-controlled phenomenon resulting from thermal stress being much higher in a higher quality rock mass than in a lower quality rock mass because of the higher Young's modulus in a higher quality rock mass.

¹Nuclear Regulatory Commission, Office of Nuclear Material Safety and Safeguards-Draft. Yucca Mountain Review Plan Revision 0. 2000. In preparation.

²Nuclear Regulatory Commission, Issue Resolution Status Report, Key Technical Issue: Repository Design and Thermal-Mechanical Effects. Revision 3. 2000. In preparation.

- Accordingly, under the thermal load expected at the proposed YM repository, a higher quality rock mass would need more ground support than a lower quality rock mass. Because thermally induced rock deformation mainly occurs in the roof and floor areas, ground support design should concentrate on stabilizing these areas. Experience on ground support design gained from the ESF and conventional underground mining and tunneling may not be applicable to ground support design under thermal load, particularly not for higher quality rock masses.
- Notable rock mass deformation, particularly fracture shear displacement along subhorizontal fractures, is observed in interdrift pillars in a higher quality rock mass after thermal load. Although this kind of deformation may not directly affect drift stability, it may alter rock mass hydrological properties and change fluid flow characteristics. A slight increase in the rock mass thermal expansion coefficient could significantly increase the extent and magnitude of such deformation.
- Although a higher quality rock mass shows greater deformation under thermal load, a numerical model with more fractures (logically should have lower quality) exhibits more extensive deformation. Consequently, it may not be appropriate to simply factor the effect of fractures into overall rock mass quality in design of drifts and ground support using a numerical approach. Some fractures need to be explicitly modeled, and modeling results need to be appropriately interpreted.
- Under seismic ground motion, an emplacement drift in a lower quality rock mass appears to be less stable and show more extensive simulated rockfall.
- Thermal load increases the loads acting on ground support (both rock bolts and steel sets) in both a lower quality rock mass and a higher quality rock mass. The increase in loads acting on the ground support system, however, is much more significant in a higher quality rock mass. This increase is consistent with observations on rock mass deformation in previous conclusions.
- Fracture patterns affect the distribution and magnitude of loads acting on ground supports. For example, the locations of peak magnitudes of load acting along rock bolts are well correlated with intersecting fractures. In general, the complexity of load distribution in ground support systems increases as the number of intersecting fractures increases. The more complicated the fracture pattern, the less uniform the loads on ground supports.
- In general, the performance of a ground support system, measured by ground support loads and failure, does not appear to be affected by high-frequency motion (e.g., 10 Hz), regardless of rock mass quality. At lower frequency ground motion (e.g., less than about 5 Hz), however, ground support performance is affected by ground motion to various degrees, depending largely on frequency level. The effect of frequency is, however, complicated by the fact that a model may respond differently to an acceleration excitation than to a velocity excitation. Also, it should be noted that observed frequency effects are based on short simulation time. Further work is necessary to consider frequency effects using different forms of excitations (i.e., displacement, velocity, and acceleration) in both time domain and frequency domain. Until further analyses are conducted, it is difficult to distinguish whether such effects are caused by frequency, different forms of input excitation, or modeling artifacts.

- Other input ground motion parameters (including duration, amplitude, and repeated ground motion events) have effects on ground support performance. These effects are insignificant, however, compared to the potential frequency and wave form effects and usually do not lead to additional ground support failure.

6 REFERENCES

- Ahola, M.P. *A Parametric Study of Drift Stability in Jointed Rock Mass. Phase II: Discrete Element Dynamic Analysis of Unbackfilled Drifts*. CNWRA 97-007. San Antonio, TX: Center for Nuclear Waste Regulatory Analyses. 1997.
- Ahola, M.P., R. Chen, H. Karimi, S.M. Hsiung, and A.H. Chowdhury. *A Parametric Study of Drift Stability in Jointed Rock Mass. Phase I: Discrete Element Thermal-Mechanical Analysis of Unbackfilled Drifts*. CNWRA 96-009. San Antonio, TX: Center for Nuclear Waste Regulatory Analyses. 1996.
- Anna, L.O. *Preliminary Three-Dimensional Discrete Fracture Model of Topopah Spring Tuff in the Exploratory Studies Facility, Yucca Mountain Area, Nye County, Nevada*. U.S. Geological Survey Open-File Report 97-834. 1998.
- Barton, N., R. Lien, and J. Lunde. Engineering classification of rock masses for design of tunnel support. *Rock Mechanics* 6(4):189–236. 1974.
- Barton, N., S. Bandis, and K. Bakhtzer. Strength, deformation and conductivity coupling of rock joints. *International Journal of Rock Mechanics and Mining Sciences and Geomechanics Abstracts*. 22(3): 121–140. 1985.
- Barrett, L.H. *Basis for Department of Energy Design Selection*. September 10. DOE (1998b). 1999. Letter to J.L. Cohory. U.S. Department of Energy. Washington, DC: U.S. Department of Energy. (September 10). 1999.
- Brechtel, C.E., M. Lin, E. Martin, and D.S. Kessel. *Geotechnical Characterization of the North Ramp of the Exploratory Studies Facility*. SAND95–0488/1. Albuquerque, NM: Sandia National Laboratories. 1995.
- Chen, R. *Analyses of Drift Instability and Rockfall Due to Earthquake Ground Motion at Yucca Mountain, Nevada: Progress Report*. San Antonio, TX: Center for Nuclear Waste Regulatory Analyses. 1998.
- Chen, R. Analyses of drift stability and rockfall due to earthquake ground motion at Yucca Mountain, Nevada. *Proceedings of the 37th U.S. Rock Mechanics Symposium, Rock Mechanics for Industry, June 6–9, 1999, Vail, Colorado*. B. Amadei, R.L. Kranz, G.A. Scott, and P.H. Smeallie, eds. Rotterdam, Netherlands: A.H. Balkema. 759–766: 1999.
- Chen, R., M.P. Ahola, S.M. Hsiung, and A.H. Chowdhury. Thermal-mechanical stability of emplacement drifts for a proposed nuclear waste repository at Yucca Mountain. *Environmental Geotechnology 1&2. Proceedings of the 4th International Symposium on Environmental Geotechnology and Global Sustainable Development, August 9–12, 1998, Boston, Massachusetts*. In press. 2000a.

- Chen, R., G.I. Ofoegbu, and S. Hsiung. Modeling drift stability in fractured rock mass at Yucca Mountain, Nevada—discontinuum approach. *Proceedings, 4th North American Rock Mechanics Symposium, Seattle, Washington, July 30-August 2*. H.I. Inyong and V.O. Ogunro eds. In press. 2000b.
- Civilian Radioactive Waste Management System Management and Operating Contractor. *ESF Ground Support Design Analysis*. BABEE0000-01717-0200-00002. Revision 00. Las Vegas, NV. 1995.
- Civilian Radioactive Waste Management System Management and Operating Contractor. *Yucca Mountain Site Geotechnical Report*. B00000000-01717-5705-00043 Revision 01. Las Vegas, NV: Civilian Radioactive Waste Management System Management and Operating Contractor. 1997a.
- Civilian Radioactive Waste Management System Management and Operating Contractor. *Confirmation of Empirical Design Methodologies*. BABEE0000-01717-5705-00002 Revision 00. Las Vegas, NV: Civilian Radioactive Waste Management System Management and Operating Contractor. 1997b.
- Civilian Radioactive Waste Management System Management and Operating Contractor. *Repository Thermal Loading Management Analysis*. B00000000-01717-0200-00135. Revision 00. Las Vegas NV: Civilian Radioactive Waste Management Systems Management and Operating Contractor. 1997c.
- Civilian Radioactive Waste Management System Management and Operating Contractor. *Repository Ground Support Analysis for Viability Assessment*. BCAA00000-01717-0200-00004. Revision 01. Las Vegas, NV: Civilian Radioactive Waste Management System Management and Operating Contractor. 1998.
- Civilian Radioactive Waste Management System Management and Operating Contractor. *Fracture Data from the Exploratory Studies Facility*. EBS-SSR-993001. MOL. 19991011.0070. Las Vegas, NV: Civilian Radioactive Waste Management System Management and Operating Contractor. 1999a.
- Civilian Radioactive Waste Management System Management and Operating Contractor. *Drift Degradation Analysis*. ANL-EBS-MD-000027. Revision 00. Las Vegas, NV: Civilian Radioactive Waste Management System Management and Operating Contractor. 1999b.
- Goodman, R.E., and G. Shi. *Block Theory And Its Application to Rock Engineering*. Englewood Cliffs, NJ: Prentice-Hall, Inc. 1985.
- Hsiung, S.M., W. Blake, A.H. Chowdhury, and T.J. Williams. Effect of mining-induced seismic events on a deep underground mine. *Pure and Applied Geophysics*. 139 (3-4): 1992.
- Hsiung, S.M., D.D. Kana, M.P. Ahola, A.H. Chowdhury, and A. Ghosh. *Laboratory Characterization of Rock Joints*. NUREG/CR-6178, CNWRA 93-013. Washington, DC: Nuclear Regulatory Commission. 1993.
- Hsiung, S.M., D.J. Fox, and A.H. Chowdhury. Effects of repetitive seismic loads on underground excavations in jointed rock mass. *7th International Conference on Radioactive Waste Management and Environmental Remediation, September 25-28, Nagoya, Japan*: ASME International. 1999.

- Hoek, E., and E.T. Brown. *Underground Excavations in Rock*. London, England: The Institute of Mining and Metallurgy. 1980.
- Itasca Consulting Group, Inc. *UDEC—Universal Distinct Element Code, Version 3.1*. Minneapolis, MN. 2000.
- Kana, D.D., S.M. Hsiung, and A.H. Chowdhury. A scale model study of seismic response of an underground opening in jointed rock. *Proceedings of the Thirty-Fifth U.S. Symposium on Rock Mechanics, Reno, Nevada*. 1995.
- Lin, M., M.P. Hardy, and S.J. Bauer. *Fracture Analysis and Rock Quality Designation Estimation for the Yucca Mountain Site Characterization Project*. SAND92-0449. Albuquerque, NM: Sandia National Laboratories. 1993.
- Nuclear Regulatory Commission. *Issue Resolution Status Report, Key Technical Issue: Structural Deformation and Seismicity*. Revision 2. Washington, DC: Nuclear Regulatory Commission, Division of Waste Management. Office of Nuclear Material Safety and Safeguards. 1999a.
- Nuclear Regulatory Commission. *Issue Resolution Status Report, Key Technical Issue: Repository Design and Thermal-Mechanical Effects*. Revision 2. Washington, DC: Nuclear Regulatory Commission., Division of Waste Management. Office of Nuclear Material Safety and Safeguards. 1999b.
- Ofoegbu, G.I. *Thermal-Mechanical Effects on Long-Term Hydrological Properties at the Proposed Yucca Mountain Nuclear Waste Repository*. CNWRA2000-03. San Antonio, TX: Center for Nuclear Waste Regulatory Analyses. 2000.
- Ofoegbu, G. I., S. Painter, R. Chen, R. W. Fedors, and D.H. Ferrill. Geomechanical and Thermal Effects on Moisture Flow at the Proposed Yucca Mountain Nuclear Waste Repository. *Nuclear Technology*. In Review. 2000.
- Risk Engineering, Inc. *Seismic Design Basis Inputs for a High-Level Waste Repository at Yucca Mountain, Nevada*. B00000000-01727-5700-0018. Revision 0. Boulder, CO: Risk Engineering. 1998.
- Sweetkind, D.S., and S.C. Williams-Stroud. *Characteristics of Fractures at Yucca Mountain, Nevada: Synthesis Report*. Administrative Report. Denver, CO: U.S. Geological Survey. 1996.
- TRW Environmental Safety Systems, Inc. *License Application Design Selection Report*. B00000000-01717-4600-00123. Revision 01. 1999.
- U.S. Department of Energy. *Preclosure Seismic Design Methodology for a Geologic Repository at Yucca Mountain*. YMP/TR-003-NP. Las Vegas, NV: U.S. Department of Energy, Office of Civilian Radioactive Waste Management. 1997.

- Wernicke, B.P. Cenozoic extensional tectonics of the Western Cordillera. *The Cordilleran Orogen: Conterminous U.S.: The Geology of North America*. Volume G-3. B.C. Burchfiel, P.W. Lipman, and M.C. Zoback, eds. Boulder, CO: Geological Society of America: 553–581. 1992.
- Wong, I.G., and J.C. Stepp. *Probabilistic Seismic Hazard Analyses for Fault Displacement and Vibratory Ground Motion at Yucca Mountain, Nevada*. Final Report. Oakland, CA: 1998.
- Williams Form Engineering Corporation. *Rock Anchor Systems No. 392*. Los Angeles, CA: 1992.

CNWRA 2000-04

DRIFT STABILITY AND GROUND SUPPORT PERFORMANCE UNDER THERMAL AND
DYNAMIC LOAD IN FRACTURED ROCK MASS AT YUCCA MOUNTAIN, NEVADA

